January 2010

Synthetic ion transporters: new analytical approaches for the investigation of ion binding and transport

Ionut Carasel
Washington University in St. Louis

WASHINGTON UNIVERSITY

Department of Chemistry

Dissertation Examination Committee:
George W. Gokel, co-Chair
Kevin Moeller, co-Chair
Aaron DiAntonio
John Bleeke
Joshua Maurer
Liviu Mirica

Synthetic ion transporters: new analytical approaches for the investigation of ion binding and transport

By

Ionut Alexandru Carasel

A dissertation presented to the
Graduate School of Arts and Sciences
of Washington University in
partial fulfillment of the
requirements for the degree
of Doctor of Philosophy

August 2010

Saint Louis, Missouri

ABSTRACT OF THE DISSERTATION

Synthetic ion transporters: new analytical approaches for the investigation of ion binding and transport

by

Ionut Alexandru Carasel

Doctor of Philosophy in Chemistry
Washington University in St. Louis, 2010
Dr. George W. Gokel, co-Chair
Dr. Kevin Moeller, co-Chair

The work reported in this dissertation focuses on synthetic ion transporters (SATs). SATs have a relatively simple chemical structure but they aggregate, self-assemble and insert in biological membranes much in the same way as their much more complex naturally occurring analogs. This makes SATs valuable tools for the investigation of these supramolecular and membrane related processes with the final goal of developing new therapeutical agents useful in the treatment of conditions stemming from ionic imbalances.

Two families of synthetic anion transporters are studied in this dissertation: pyrogallol[4]arene derivatives and dianilides of isophthalic and dipicolininc acids. Experiments aimed at investigating their solution behavior, anion binding properties and the strength of the interactions present in the host•anion adducts employed analytical techniques such as high performance liquid chromatography, electrospray mass spectrometry, UV-vis and NMR spectroscopy. Insights derived from these experiments were instrumental to our understanding of the stability and transport mechanisms pertaining to these two families of compounds.

Acknowledgements

A great number of people contributed to my professional development and success as a graduate student. First and foremost I would like to thank my research advisor Professor George W. Gokel. Without his constant support and guidance none of the work presented in this dissertation would have been possible.

I would like to extend my gratitude to Professor Kevin D. Moeller and Professor Joshua Maurer for being members in my research advisory committee. Their help and input throughout my graduate carrier has been invaluable. Also I would like to thank Professors John Bleeke, Liviu Mirica and Aaron DiAntonio for their time and advice and for accepting to be members in my dissertation examination committee.

Special recognition should be awarded to Professor Rudolph K. Winter and Joseph Kramer from the Chemistry Department at University of Missouri St Louis. The work presented in chapters four and five of this dissertation is a result of our collaborative work and could not have been performed without their assistance.

In my tenure in the Gokel laboratory I was fortunate enough to meet many gifted postdoctoral assistants and graduate students: Dr. Robert Pajewski, Jola Pajewska, Dr. Riccardo Ferdani, Dr. Wei Wang, Dr. Lei You, Dr. Ruiqiong Li, Dr. Elizabeth Elliot, Dr. Brock Levin, Dr. Natalie Barkey, Dr. Oleg Kulikov, Carl Yamnitz, Megan Daschbach, Saeedeh Negin, Jason Atkins and Mohit Patel. Working side by side with them helped me grow and mature as a scientist.

I would like to acknowledge Ema Voinescu, Cristian Jitianu, Bogdan Dinca, Mugur Kacso, Jennifer Bergstrom, Alina Handorean, Matt van Duzor, Stefan Bennewitz,

Donnie Smith, Matt Lenze, Aileen Bongat, Colin White, Heather Helm and Leo Seballos for their help and friendship.

Finally, I would like to thank my parents, my sister and all the members of my family for their love, encouragement and unwavering support.

Table of Contents

List of Figures

Chapter 1

Chapter 2

Chapter 3

Chapter 4

Chapter 5

Chapter 6

List of Tables

Chapter 1. Introduction: Biological membranes and ion channels

Biological membranes

Living organisms have as their basic building block the cell.[1] Throughout evolution a large number of various cell types have differentiated, diversity that came as a response to the broad range of functions that the cells were called upon to fulfill. In Figure 1.1 a cartoon representation of an eukaryotic cell is shown.

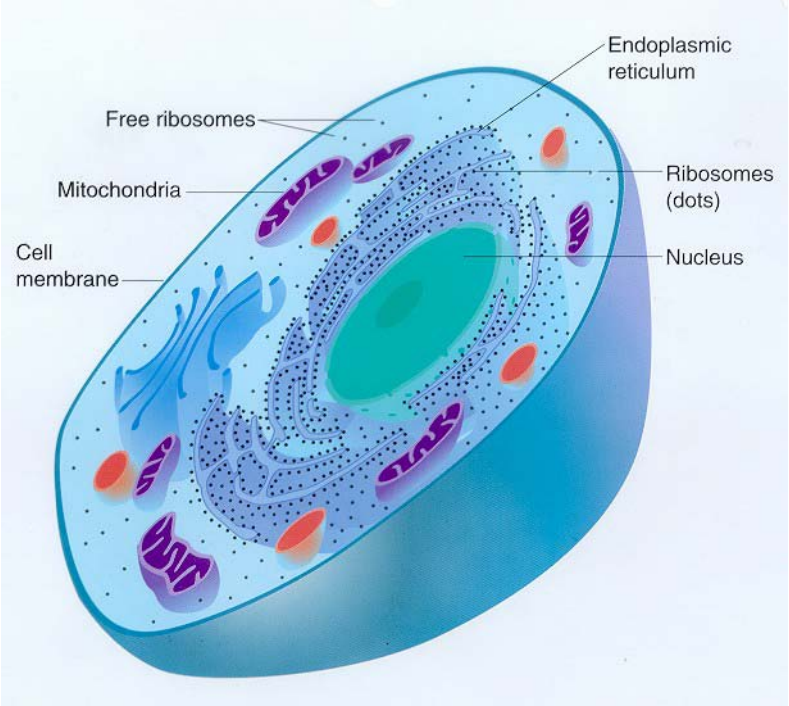

Figure 1.1 Cartoon representation of an eukaryotic cell

Despite the broad range of functions that cells accomplish, the main components of a cell remain largely unchanged. At the outside of the cell we have a membrane, that isolates the inside components from the outside environment. The intracellular components are ribosomes (responsible for the synthesis of proteins), mitochondria (involved in the generation of cellular energy), endoplasmatic reticulum (with a role in

the synthesis of proteins and lipids) and the nucleus (where the genetic information is stored).

The barrier role[2] that the cellular membrane has is a very important one. The cell could not survive or even be defined as an entity without the outside membrane. The composition of the membrane is very complex, but the main constituent is represented by phospholipids.[3] An example of a phopsholipid molecule is presented in Figure 1.2, using 1,2-Dioleoyl-*sn*-glycero-3-phosphocholine (DOPC).

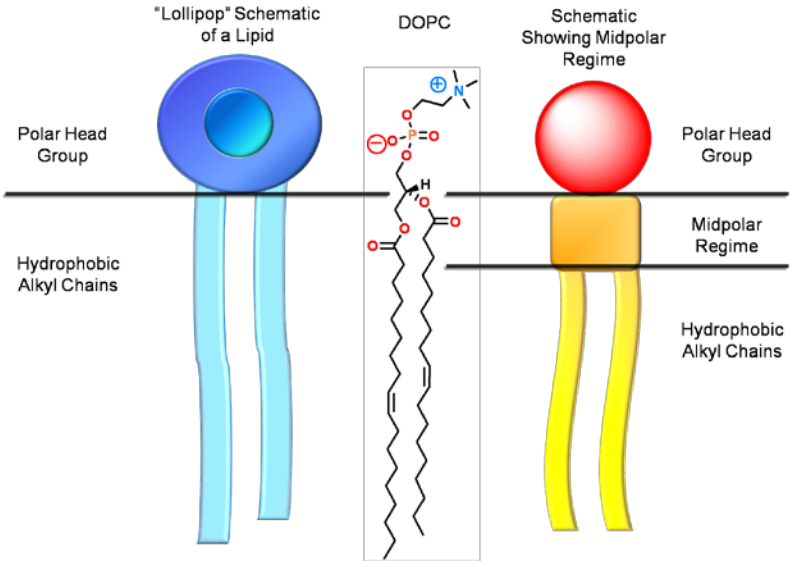

Figure1.2 Structure of a phospholipid, DOPC.

As Figure 1.2 shows phospholipids have three main regions based on the polarity of the moieties that are present in the structure. The polar head group is comprised of the phosphate and the choline, having two electric charges. The region of intermediate polarity is formed of the ester groups while the long hydrocarbon chains form the region of low polarity.

When a multitude of phospholipids come together and form the cellular membrane they arrange themselves based on the relative polarity and give rise to a bilayer structure. The result of a calculation for such a structure is presented in Figure 1.3.

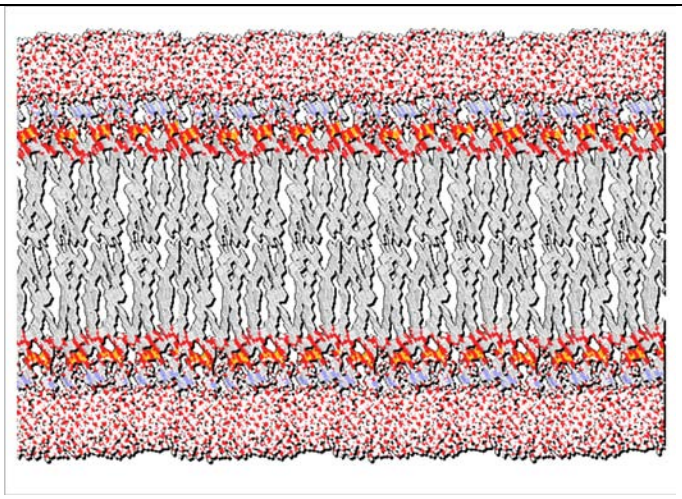

Figure 1.3 Calculated structure of a phospholipid bilayer

The polar head groups reside on the exterior of the bilayer in direct contact with the aqueous external environment while the long hydrocarbon chains are placed at the core of the membrane.

Membrane permeability

The phospholipid arrangement shown in Figure 1.3 provides very good insulation properties for the membrane, ensuring that there are no leaks in or out of the cell. In fact, there are only a few molecules that can freely diffuse through the phospholipid bilayer (Figure 1.4). Small gaseous molecules like O_2, N_2 or NO or small lipid soluble molecules like fatty acids or steroid hormones can freely diffuse through the membrane. Limited

permeability exists for small polar molecules like water, urea or glycerol that can to a certain point penetrate the phospholipid bilayer. Larger molecules like proteins, nucleic acids, charged species like cations and anions (Na^+, K^+, Ca^{2+}, Cl^-), amino acids cannot pass through the phospholipid bilayer.

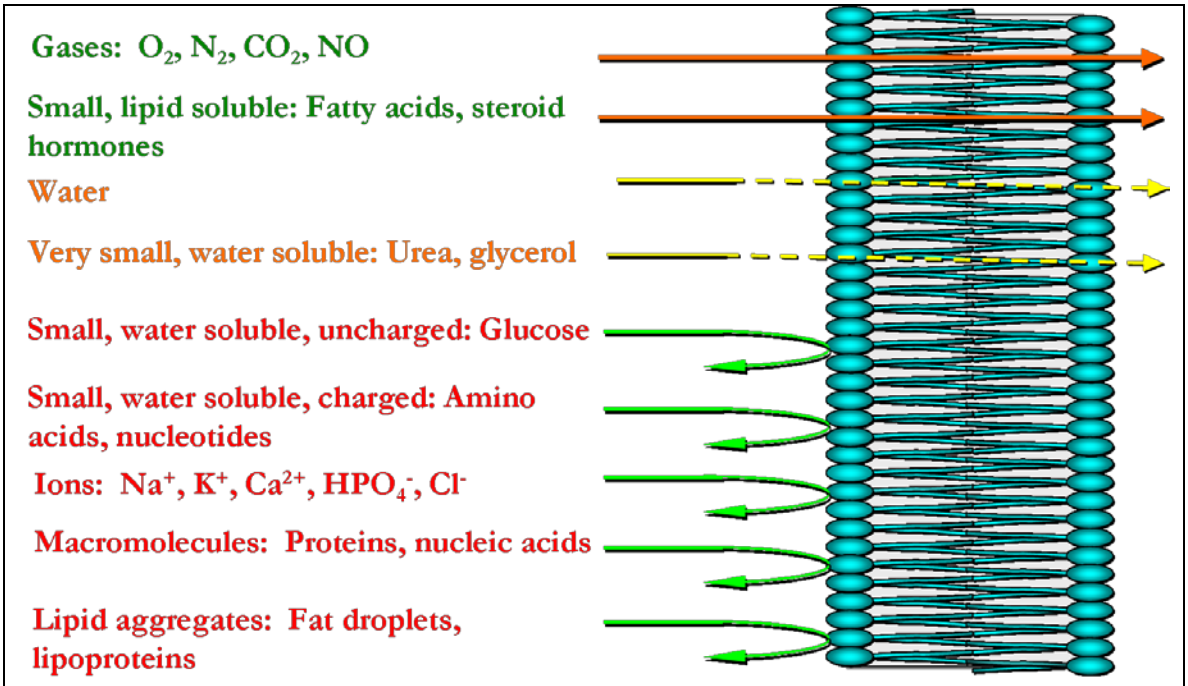

Figure 1.4 Membrane permeability

Most, if not all of the components mentioned as being unable to permeate the membrane are important for the survival and well being of the cell. The transport of these molecules is accomplished with the help of the proteins that are embedded in the membrane and which ensure that the necessary nutrients are available to the cell.

Cellular membrane complexity

The presence of membrane proteins paints a more realistic picture of the structure of the membrane. It is not just a phospholipid bilayer; it contains a large number of

surface or transmembranar proteins. A cartoon representation of such a phospholipid membrane is presented in figure 1.5.

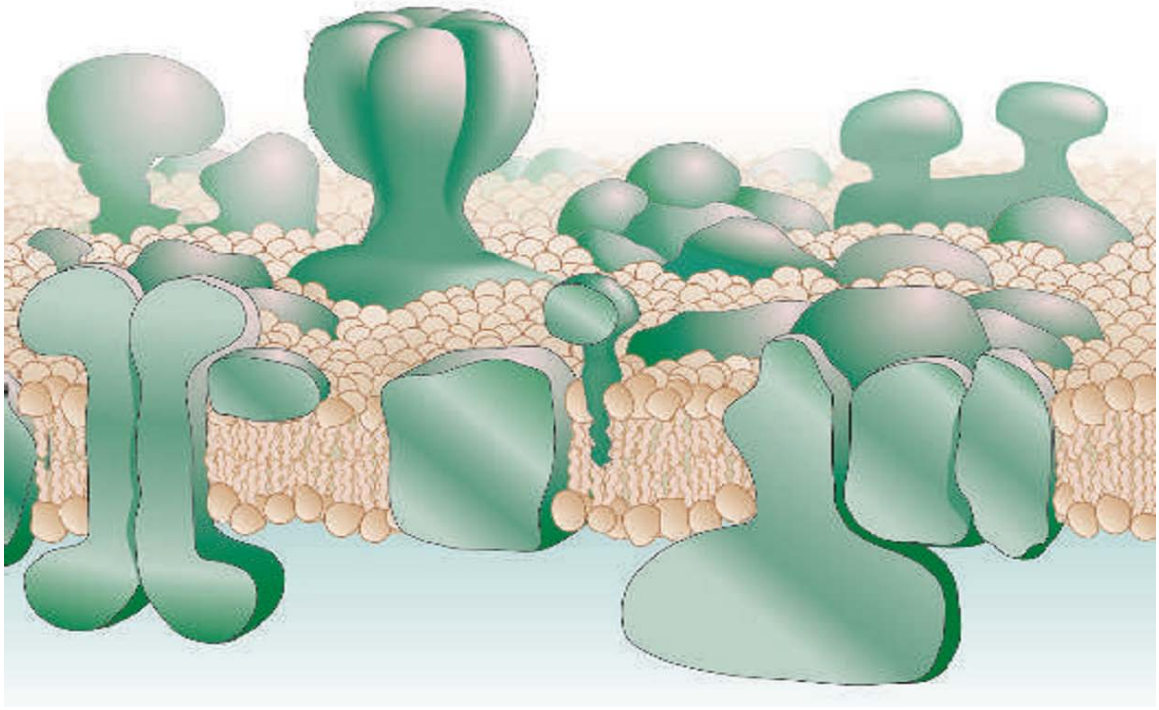

Figure1.5 Cartoon representation of the phospholipid bilayer with embedded proteins

Membrane proteins can transport compounds across the membrane via two types of mechanisms: channel or carrier[4].

Naturally occurring channels and carriers

The two transport mechanisms (carrier and channel) are depicted in cartoon form in Figure 1.6.

A carrier is usually a smaller molecule that captures the host on one side of the membrane, diffuses to the other side of the bilayer where it releases the guest.

A protein acting as a channel forms a pore through the membrane allowing for the otherwise too polar or too big molecules to pass and enter the cell. The channels are generally very large proteins containing hundreds of amino acids.

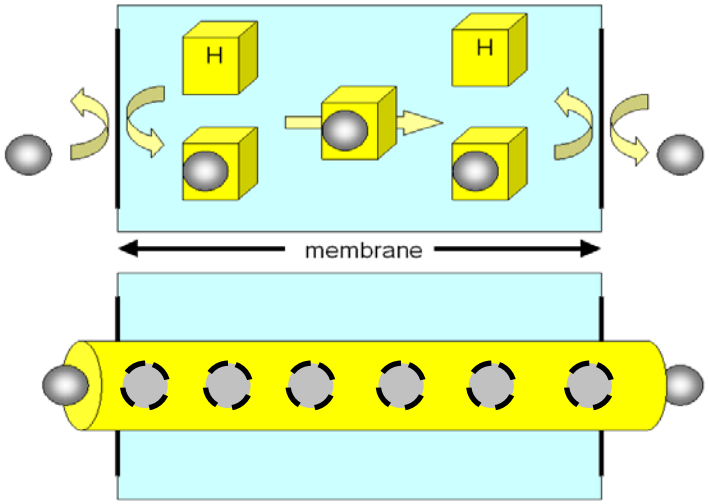

Figure 1.6 Carrier (top panel) and channel (lower panel) transport mechanisms.

To exemplify the complexity of naturally occurring channels, the structure of a Cl^- transporter from *S. typhimurium* is presented in Figure 1.7. It has two subunits (highlighted in red and blue in Figure 1.7.) each containing a large number of amino acids.

Figure 1.7 Ribbon representation of the *S. thyphimurium* Cl^- transporter. A Cl^- ion in the selectivity filter is represented as a green sphere.

The study of these molecules has always been hindered by their complexity. Hence the incentive for chemists and biochemists to design and study smaller model molecules that retain the ion transport activity but at the same time allow for easier synthesis, manipulation and study.

Previous reports of synthetic ion transporters

Due to the macrocyle's ability to complex various ions, structures such as crown ethers,[5] calixarenes,[6] and cyclodextrins[7] have been attractive for scientists desiring to design new ion channels. As exemplified below, these structures have been widely utilized by various groups.

One of the first reported synthetic ion channels was the one published by Tabushi and coworkers in 1982.[8] Since then quite a large number of structures have been designed, analyzed and studied in the growing field of ion channels.

The Tabushi channel was based on a β-cyclodextrin (Figure 1.8A).[8] The channel character was confirmed by monitoring the transport of copper and cobalt ions. As far as the transport mechanism it was speculated that two molecules come together in a "tail to tail" arrangement, thus forming a pore that allowed the ions to pass.

Another design that bears a number of structural similarities with Tabushi's compound is the one reported by Gin and coworkers. In this case the cyclodextrin was functionalized with long polietheric tails, that were intended to span the phospholipid bilayer and thus reducing the number of molecules required for transport to one (Figure 1.8B).[9] Data reported shows that this structure is an anion selective transporter.

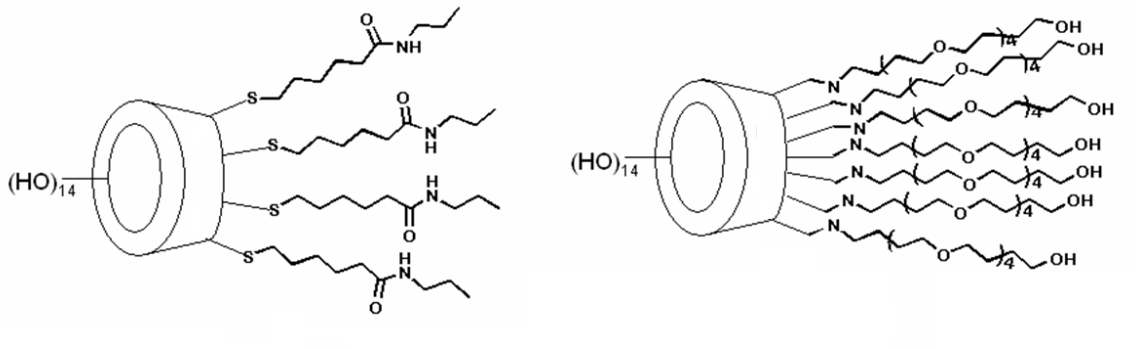

Figure 1.8 A) Tabushi channel. B) Gin's cyclodextrin channel

Davis and coworkers reported an active channel based on a different conformation of the calix[4]arenes (1,3-alternate conformer) that bound HCl (Figure 1.9A).[10] A design that combined calixarenes and crown ethers was developed jointly by the Mendoza and Gokel labs. The crown ethers served as headgroups while the 1,3-alternate conformer of calix[4]arene is used as a central relay (Figure 1.9B).[11]

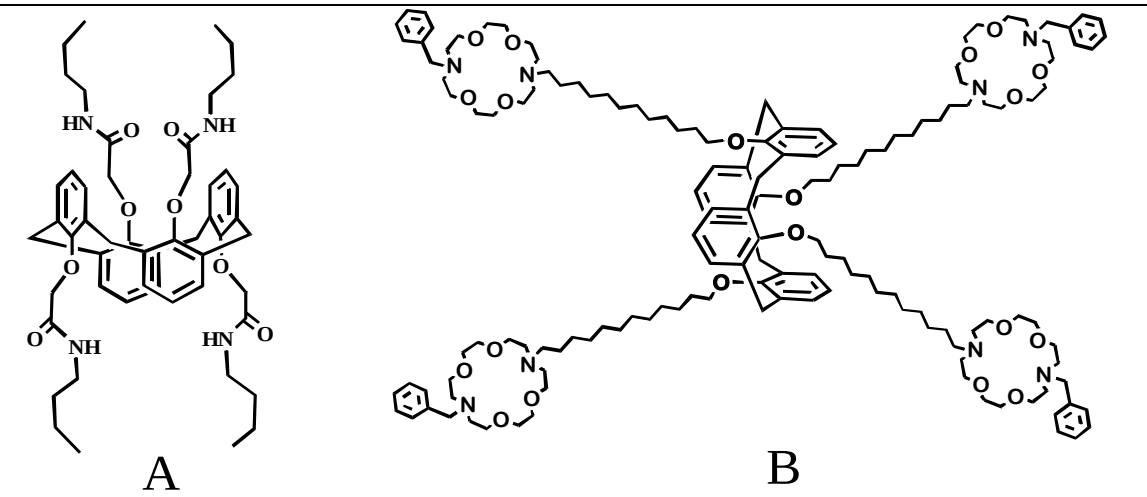

Figure 1.9 A) Davis's synthetic ion channels. B) calix[4]arene-crown synthetic ion channels

While a number of other macrocyles have been used in the design of ion channels, probably the most utilized are the crown ethers. In 1982, a channel-like arrangement of crown ethers was observed in the solid state structure of 18-crown-6.[12] Researchers envisioned the use of crown ethers as central scaffolds with hydrophobic chains attached

in order to favor the insertion into membranes and thus mediating the transport of ions.[13] Fyles and coworkers used a tartaric acid-18-crown-6 backbone to design a new family of active ion channels.[14] In a slightly different approach Voyer and coworkers used crown ethers and alpha-helical peptides that would self-assemble and form a transmembrane pore as shown in Figure 1.10B.[15] Matile and coworkers used a polyaromatic backbone composed of eight phenyl units that had six crown ethers attached (Figure 1.10C).[16] All of the structures discussed have well documented channel behavior.

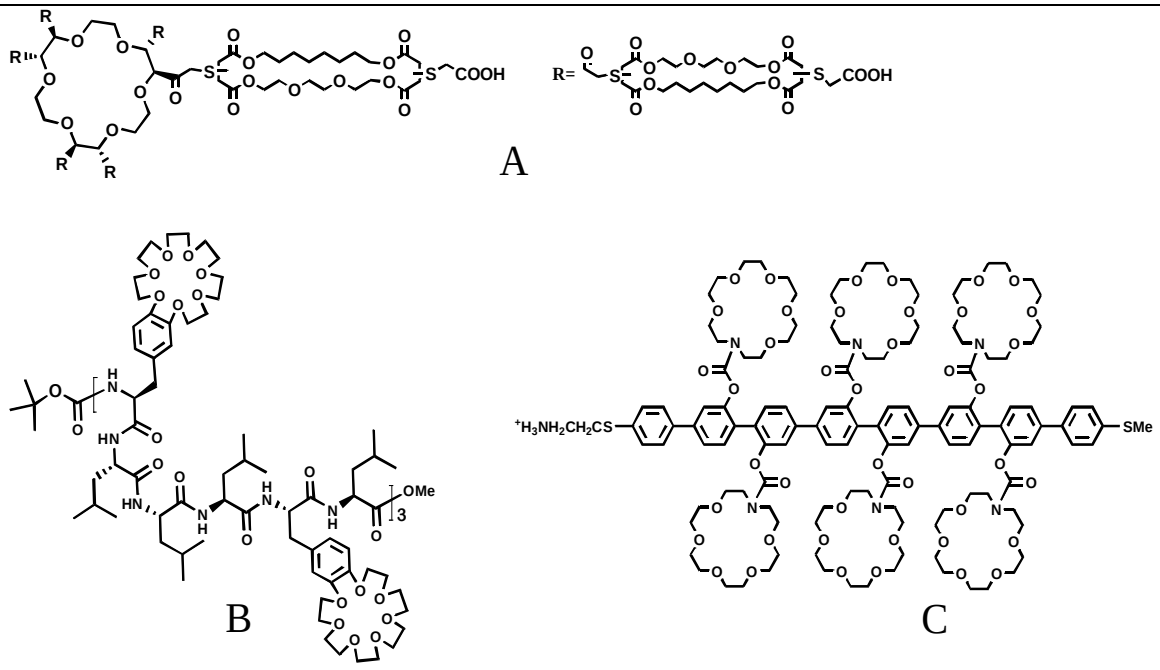

Figure 1.10 A) Flyes tartaric crown ether ion transporter. B) Voyer family of synthetic ion transporter. C) Matile polyphenylene ion transporter

The Gokel goup has reported a number of structures that act as ion transporters, and these families are presented briefly as follows.

Hydraphyles

One of the first families of compounds[17] that our group has developed is exemplified in Figure 1.11. The the two distal macrocyles (two diaza-18-crown-6 ethers) that are linked through an aliphatic spacer to a central relay (usually the third diaza-18-crown-6 ether is present here) are characteristic structural features for these compounds. The two headgroups are substituted at both nitrogens, and the spacer and the sidearm may or may not be identical.

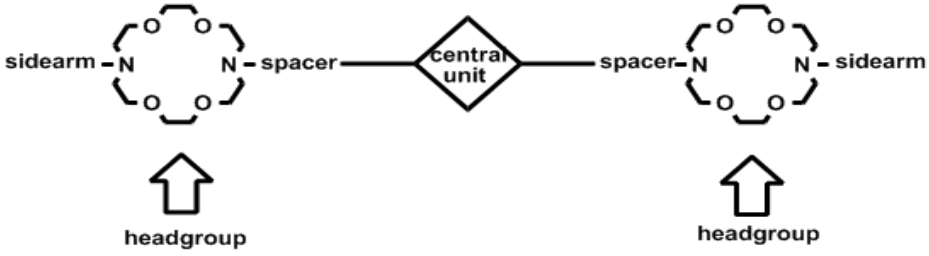

Figure 1.11 General structure of the hydraphiles.

This family of compounds proved to be a cation transporter with the two distal macrocycles acting as entry portals while the central relay is placed within the membrane. We believe that one molecule of hydraphyle can insert in the membrane and arrange in such a way as to create a pathway for ions and water molecules. A cartoon representation of this mechanism is depicted in Figure 1.12.

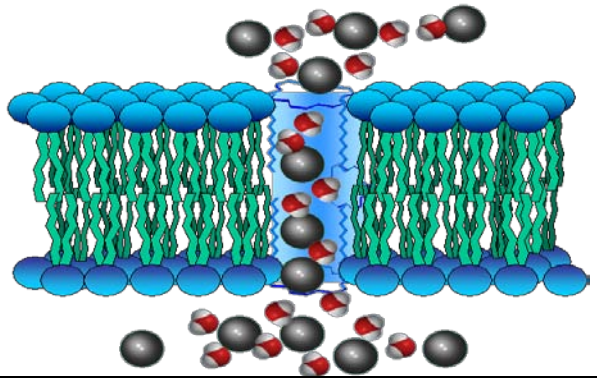

Figure 1.12 Putative transport mechanism for hydraphyles.

Applospans

Another group of compounds that proved to be active as ion transporters is what we called "applospans", a name suggested from the Greek απλόσ (simple) + span for simple, membrane-spanning structures that mediate ion transport.

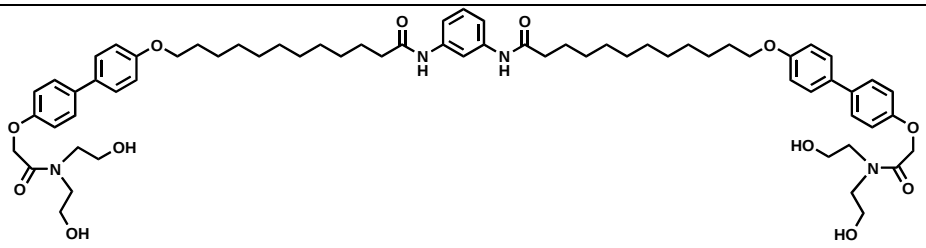

Figure1.13 Structure of an applospan

As the structure shown in Figure 1.13 suggests, they share structural features with the hydraphyles: a central relay, two entry portals and two spacers. Though the molecule is a lot simpler and the central relay and the two head groups are not moieties that we usually think as being capable of mediating the transport of ions the compound still exhibited ion transport with modest cation selectivity.[18]

Peptide based transporters

Chronologically the second family of ion transporters that was designed in our lab is one based on peptides. The general structure of these compounds is presented in Figure 1.14.

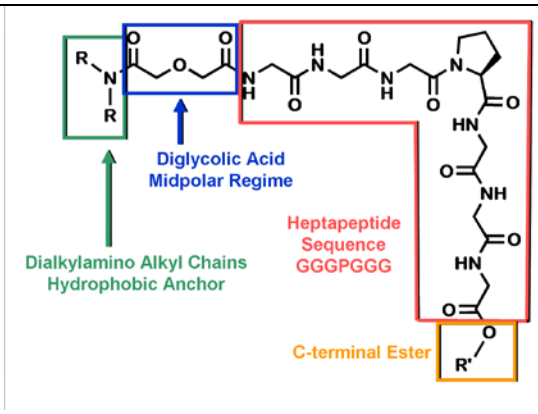

Figure 1.14 General structure of the peptide based ion transporters

The N-terminal end of the peptidic sequence (red in figure 1.14) is linked through a diglycolic acid residue (blue in Figure 1.14) to a dialkyl amino residue (green in Figure 1.14). The dialkyl groups can have different lengths and act as an anchoring point for the molecule in the membrane. The peptidic sequence is composed of three glycine residues followed by a proline. This amino acid sequence is inspired from the putative ion conduction pathway for the proteins in the ClC family where a G-X-X-P unit is conserved.[19] The proline is attached to another tri-glycine sequence which is capped as an ester to avoid potential electrostatic repulsions.

These compounds have been shown to be active as Cl^- transporters. We believe that two molecules insert in the membrane and aggregate to form a dimeric pore. The molecules are not long enough to span the whole bilayer so the dimeric pore is

responsible for disturbing the lower leaflet of the membrane as well and in this way creating a pore for the Cl^- ions to pass. This mechanism is depicted in Figure 1.15.

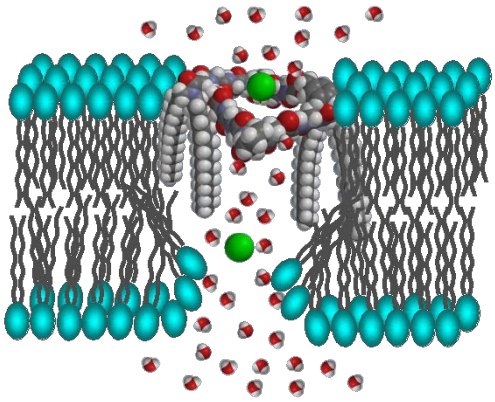

Figure 1.15 Putative transport mechanism for the peptide based transporters

Our group has studied extensively this family of compounds[20], performing structure relationship activity studies on all of the structural modules: the dialkyl amino group[21], the diglycolic acid residue[22], the peptide sequence[23] and the C-terminus ester[24].

Pyrogallol[4]arenes

Another group of compounds in which we became interested relatively recently are the pyrogallol[4]arenes.[25,26,27,28] The general structure of these compounds is presented in Figure 1.16.

This family of compounds was studied extensively by Atwood and coworkers.[29] A more in depth discussion of these molecules and their behavior in solution is the object of Chapter 3 of this thesis.

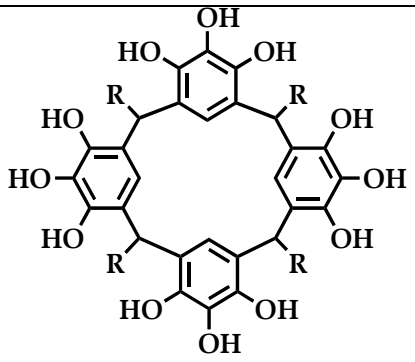

Figure 1.16 General structure of pyrogallol[4]arenes

Dipicolinic and Isophthalic acids deivatives

The latest family of compounds that we studied is a series of dianilides of dipicolinic and isophthalic acids that mediate the transport of anions through phospholipid bilayers.[30] The general structure of these compounds is presented in Figure 1.17.

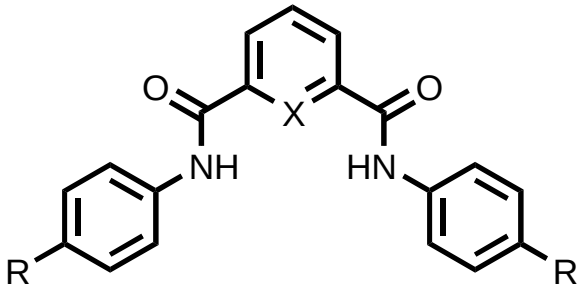

X=N	$R=CH_3$
X=N	R=H
X=N	R=CN
X=N	$R=NO_2$
X=CH	R=H
X=CH	$R=NO_2$

Figure 1.17. Dipicolinic and isophthalic acid derivatives

The study of the compounds in this family is the object of Chapters 4 and 5 of this thesis.

Conclusions

Our laboratory has extensive experience in the field of synthetic ion channels. Throughout this dissertation two families of ion transporters will be examined: pyrogallol[4]arenes and dianilides of dipicolinic and isophthalic acid. Along with well established tools in the ion channel field like planar bilayer experiments, fluorescence quenching or binding constants determination we have used in our studies methods such as gas-phase calculations, HPLC and electrospray mass spectrometry. The use of these methods might surprise but we have proven that they can be very effective and can provide insight and reliable data where other more traditional methods might fail to do so.

References

[1] Image reproduced from http://www.williamsclass.com/SeventhScienceWork/CellTheoryParts.htm

[2] Darnell, J. E.; Lodish, H. F.; Baltimore, D., *Molecular cell biology*. 2nd ed.; Scientific American Books : Distributed by W.H. Freeman: New York, N.Y., 1990; 1105 p.

[3] Hanahan, D. J. *A Guide to Phospholipid Chemistry*; Oxford University Press: Oxford, 1997 p 214.

[4] Hille, B. *Ionic channels of excitable membranes (third edition)*; 3rd ed.; Sinauer Associates: Sunderland, MA, 2001.

[5] Pedersen, C. J. *Journal of the American Chemical Society* **1967**, *89*, 7017-7036.

[6]Boehmer, V. *Angewandte Chemie, International Edition in English* **1995**, *34*, 713-745.

[7] Ohvo, H.; Slotte, J. P. *Biochemistry* **1996**, *35*, 8018-8024.

[8] Tabushi, I.; Kuroda, Y.; Yokota, K. *Tetrahedron Letters* **1982**, *23*, 4601-4604.

[9] Madhavan, N.; Robert, E. C.; Gin, M. S. *Angewandte Chemie, International Edition* **2005**, *44*, 7584-7587.

[10] Sidorov, V.; Kotch, F. W.; Abdrakhmanova, G.; Mizani, R.; Fettinger, J. C.; Davis, J. T. *J Am Chem Soc* **2002**, *124*.

[11] de Mendoza, J.; Cuevas, F.; Prados, P.; Meadows, E. S.; Gokel, G. W. *Angewandte Chemie, International Edition* **1998**, *37*, 1534-1537.

[12] Behr, J. P.; Lehn, J. M.; Dock, A. C.; Moras, D. *Nature* **1982**, *295*, 526-527.

[13] (a) Jullien, L.; Lehn, J. M. *Tetrahedron Letters* **1988**, *29*, 3803-3806; (b) Pechulis, A. D.; Thompson, R. J.; Fojtik, J. P.; Schwartz, H. M.; Lisek, C. A.; Frye, L. L. *Bioorg Med Chem* **1997**, *5*, 1893-1901.

[14] (a) Fyles, T. M.; James, T. D.; Pryhitka, A.; Zojaji, M. *Journal of Organic Chemistry* **1993**, *58*, 7456-7468; (b) Fyles, T. M.; James, T. D.; Kaye, K. C. *Journal of the American Chemical Society* **1993**, *115*, 12315-12321; (c) Carmichael, V. E.; Dutton, P. J.; Fyles, T. M.; James, T. D.; Swan, J. A.; Zojaji, M. *Journal of the American Chemical Society* **1989**, *111*, 767-769.

[15] Voyer, N.; Roby, J.; Deschenes, D.; Bernier, J. *Supramolecular Chemistry* **1995**, *5*, 61-69.

[16] Sakai, N.; Gerard, D.; Matile, S. *Journal of the American Chemical Society* **2001**, *123*, 2517-2524.

[17] O. Murillo, S. Watanabe, A. Nakano, G. W. Gokel. *J. Am. Chem. Soc*. **1995**, *117*, 7665

[18] W. Wang, R. Li, G. W. Gokel. *Chem. Commun*. **2009**, 911-913.

[19] Maduke, M.; Miller, C.; Mindell, J. A. *Annu. Rev. Biomol. Struct.* **2000**, *29*, 411-438

[20] (a) You, L.; Li, R.; Gokel, G. W. *Org. Biomol. Chem.* **2008**, *6*, 2914-2923. (b) You, L.; Ferdani, R.; Li, R.; Kramer, J. P.; Winter, R. E.; Gokel, G. W. *Chemistry* **2008**, *14*, 382-396. (c) Cook, G. A.; Pajewski, R.; Aburi, M.; Smith, P. E.; Prakash, O.; Tomich, J. M.; Gokel, G. W. *J. Am. Chem. Soc.* **2006**, *128*, 1633-1638. (d) Ferdani, R.; Pajewski, R.; Djedovic, N.; Pajewska, J.; Schlesinger, P. H.; Gokel, G. W. *New J. Chem.* **2005**, *29*, 673-680. (e) Schlesinger, P. H.; Ferdani, R.; Pajewski, R.; Pajewska, J.; Gokel, G. W. *Chem. Commun.* **2002**, 840-841. (f) Ferdani, R.; Li, R.; Pajewski, R.; Pajewska, J.; Winter, R. K.; Gokel, G. W. *Org Biomol Chem* **2007**, *5*, 2423-2432.

[21] a) Pajewski, R.; Ferdani, R.; Pajewska, J.; Li, R.; Gokel, G. W. *J. Am. Chem. Soc.* **2005**, *126*, 18281-18295.

[22] Pajewski, R.; Pajewska, J.; Li, R.; Daschbach, M. M. Fowler, E. A.; Gokel, G. W. *New J. Chem.* **2007**, *31*, 1960-1972.

[23] Ferdani, R.; Pajewski, R.; Pajewska, J.; Schlesinger, P. H.; Gokel, G. W. *Chem. Comm.* **2006**, 439-441

[24] Pajewski, R.; Pajewska, J.; Li, R.; Fowler, E. A.; Gokel, G. W. *New J. Chem.* **2007**, *31*, 1960-1972.

[25] Kulikov, O. V.; Rath, N. P.; Zhou, D.; Carasel, I. A.; Gokel, G. W. *New J. Chem.* **2009**, *33*, 1563-1569.

[26] Kulikov, O. V.; Daschbach, M. M.; Yamnitz, C. R.; Rath, N.; Gokel, G. W. *Chem Commun (Camb)* **2009**, 7497-7499.

[27] Li, R.; Kulikov, O. V.; Gokel, G. W. *Chem. Comm.* **2009**, 6092-6094.

[28] Kulikov, O.; Li, R.; Gokel, G. W. *Angew. Chem. Int. Ed.* **2009**, *48*, 375-377.

[29] (a) L. R. MacGillivray, J. L. Atwood, *Nature*, 1997, **389**, 469-472. (b) A. Shivanyuk, J. C. Friese, S. Doring, J. Rebek Jr., *J. Org. Chem.* **2003**, *68*, 6489-6496. (c) T. Gerkensmeier, W. Iwanek, C. Agena, R. Frölich, S. Kotila, C. Näther, J. Mattay, *Eur. J. Org. Chem.* **1999**, 2257-2262. (d) T. Evan-Salem, I. Baruch, L. Avram, Y. Cohen, L. C. Palmer, J. Rebek Jr., *Proc. Nat. Acad. Sci.* **2006**, *103*, 12296-12300.

[30] Yamnitz, C. R.; Negin, S.; Carasel, I. A.; Winter, R. K.; Gokel, G. W. *Chem. Commun.* **2010**, *46*, 2838-2840

Chapter 2. Triacsin C and derivatives: Synthesis and study of biological properties

Introduction

Triacsin C is part of a family of four naturally occurring compounds discovered in a culture of Streptomyces sp. in 1980.[1] The other members of the family are Triacsin A, B and D. They have been of interest in the biochemical community for some time because they inhibit a type of enzymes known as long chain acyl-CoA synthetases.[2,3,4,5] The structures are presented in Figure 2.1.

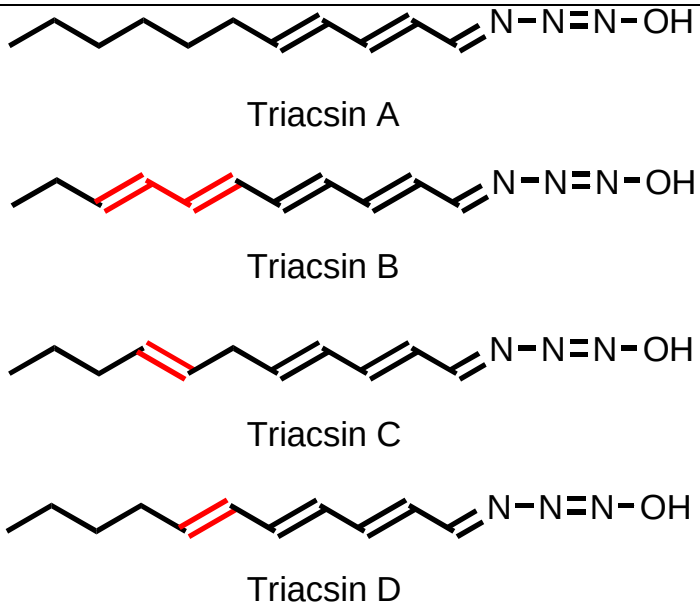

Figure 2.1. Structure of Triacsin A, B, C, D.

The four triacsin molecules share a number of structural characteristics. All of the Triacsins possess the unusual triazenol moiety (=N-N=N-OH) at one end of the molecule. The triacsins contain a linear chain of 11 carbons, several of which are unsaturated. The double bond system is generally, but not always, conjugated. The stereochemistry of the -C=C- is always *trans*.

The triazenol functional group and the carbon skeleton up to and including C_5 are identical in Triacsins A-D. The differences in structure begin at C_6 and these are

highlighted in red in Figure 2.1. Triacsins B and D have a double bond at C_6 while A and C do not. Triacsin B has another double bond between C_8-C_9 and triacsin C has a double bond between C_7-C_8.

Inhibitory potency of the Triacsin A, B, C and D

As noted above, the four triacsins inhibit the action of long chain acyl-CoA synthetases, although to different extents.[6] The results of an inhibition study are presented in Figure 2.2. The most active compound is triacsin C (red line in Figure 2.2) followed by A (blue line), both of which are much more active than B (green) and D (black).

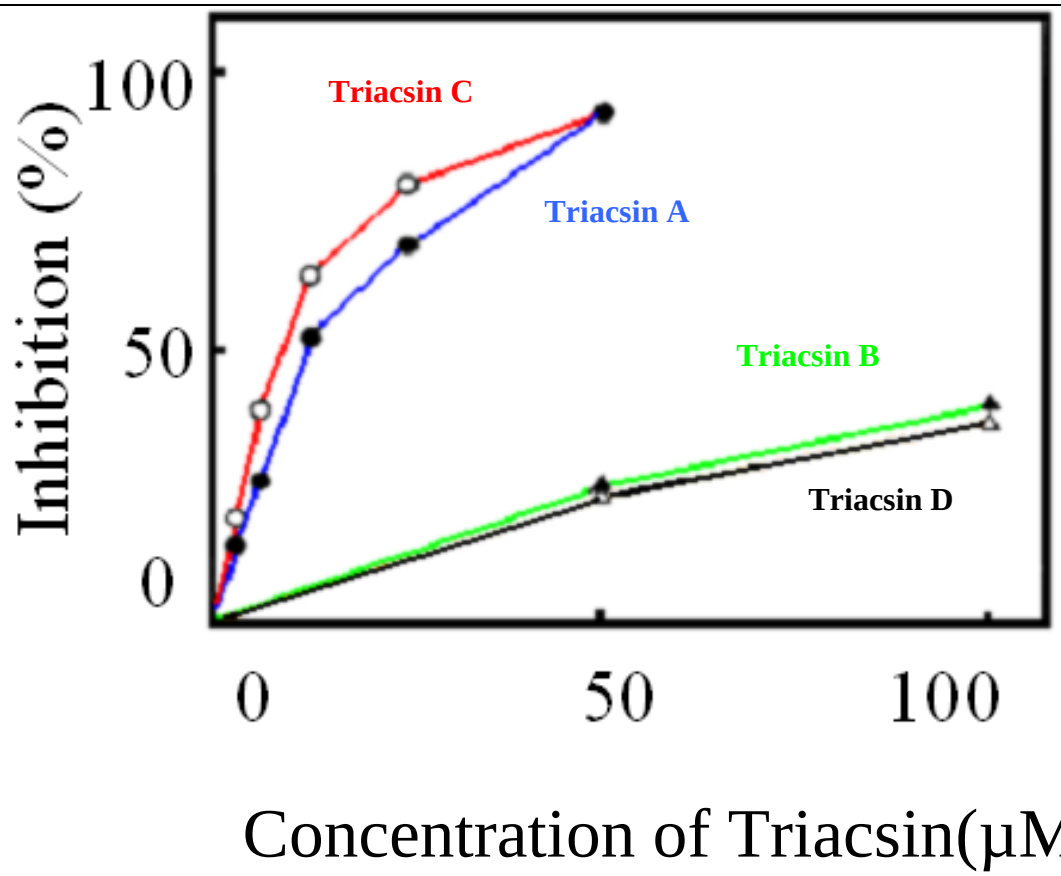

Figure 2. 2 Inhibitory activity of Triacsin A, B, C and D.

Triacsin C use in biochemical reseach

The ability of triacsins to inhibit acyl CoA enzymes has made this family of structures useful as tools in the field of biochemical research.[7,8,9,10,11] Acyl-CoA synthetase is an enzyme involved in the metabolism of fatty acids, transforming the free fatty acids into CoA esters. Several enzymes are known within the general family. They are generally designated “short”, “medium” and “long” chain variants. The short chain enzyme, usually designated “SC”, typically has as its substrate aliphatic acids in two- to four- carbon range. Substrates for the medium chain (“MC”) enzyme have acyl chains of four- to twelve carbons. The long chain (“LC”) enzyme acts on fatty acids having twelve carbons or more, typically 12-24.

Enzymatic mechanism for LC Acyl-CoA synthetase

LC Acyl-CoA synthetases react by a two-step mechanism (Figure 2.3).[12] In the first step, the fatty acids react with adenosine triphosphate (ATP) to form an acyl-adenosine monophosphate (acyl-AMP) mixed anhydride. Pyrophosphate is the byproduct of this step. The mixed anhydride activates the fatty acid so that coenzyme A can be attached. The enzyme requires Mg^{2+} as a cofactor and the hydrolysis of the pyrophosphate renders the enzymatic process irreversible.

It is the CoA activating group that will be important for subsequent metabolism of the fatty acids.

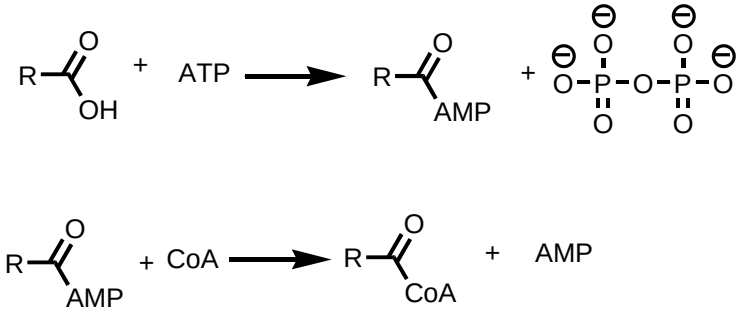

Figure 2. 3 Enzymatic reactions for fatty acids esterification.

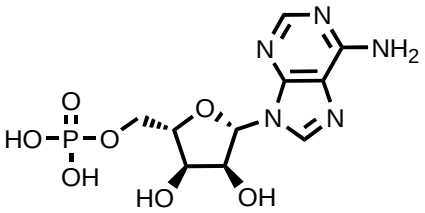

Adenosine Monophosphate (AMP)

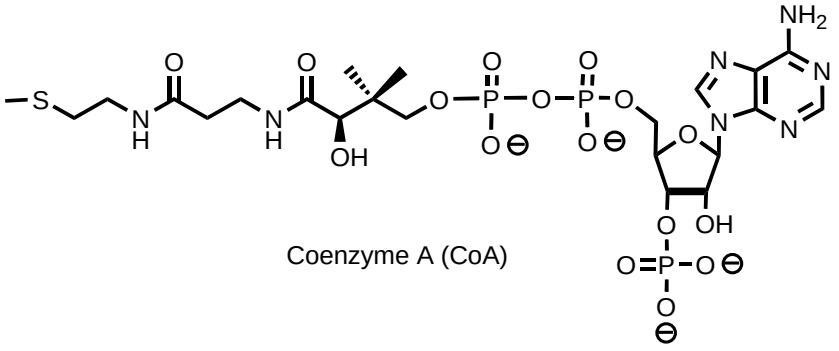

Coenzyme A (CoA)

Figure 2. 4 Structure of AMP and Coenzyme A

Acyl-CoA synthetases are almost ubiquitous in living organisms and thus adopt a large variety of structures and conformations. Despite their variety, the active site is highly conserved within this family of enzymes.[13] The similarity in active sites within the enzyme family probably accounts for the ability of triacsins to inhibit such a broad spectrum of enzymes.

The structure of LC Acyl-CoA synthetase from *Thermus thermophilus* was reported by Hisanaga in 2004[13] and is shown in Figure 2.5. This enzyme is a homodimeric structure. The two monomers are linked at the N-terminal ends.

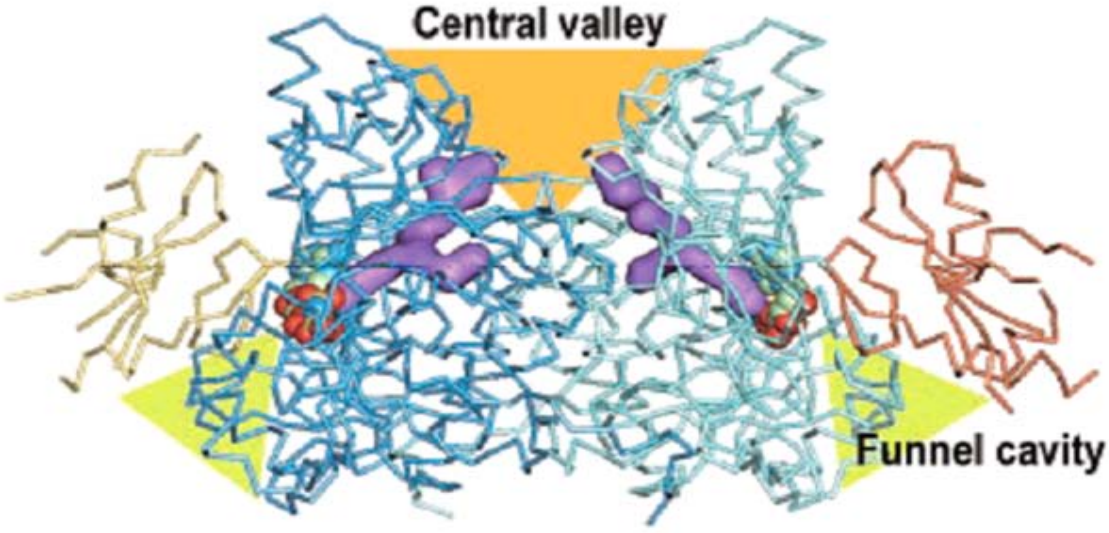

Figure 2. 5 The structure of LC Acyl-CoA synthetase from Thermus thermophilus (image reproduced from Hisanaga et al[13]).

Each part of the homodimer is linked in such a way that a cavity is created between them. This cavity is referred as the "central valley", which acts as an access point for the fatty acid substrate. It is important to notice that the fatty acids enter the active site of the enzyme with the carboxyl moiety pointing forward. After the esterification process occurred, the Acyl-CoA fatty acid molecule exits the enzyme through the "funnel cavity", which is situated opposite to the "central valley".

A more detailed representation of the active site of the enzyme is presented in Figure 2.6.

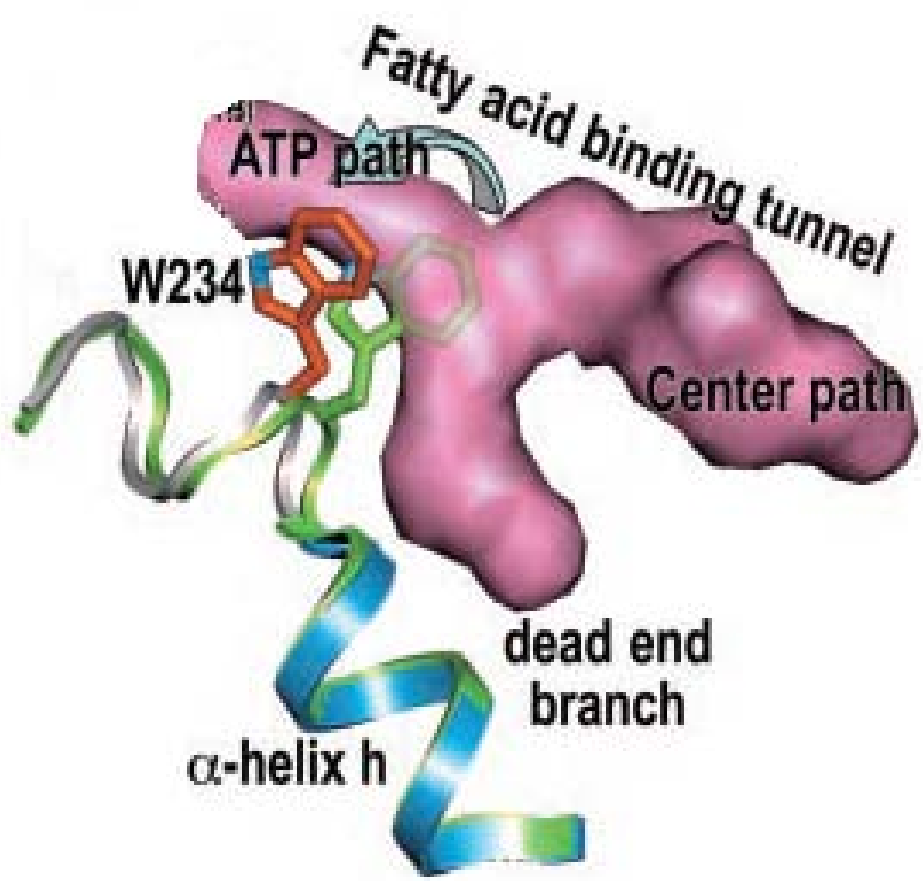

Figure 2. 6 The active site of the LC Acyl-CoA synthetase from Thermus thermophilus (image reproduced from Hisanaga et al[13])

When the enzyme is in the *apo* form, the fatty acids binding tunnel is occupied by the indole residue of a tryptophan molecule (W234). The esterification process begins with the binding of an ATP molecule at the end of the tunnel. This event triggers a series of conformational changes that result in the rotation of the W234 indole ring, clearing the path for the fatty acids to enter the active site. The tail of the fatty acid is placed inside the "dead end branch". This portion serves as a size selectivity filter: the fatty acids that

are not of appropriate size either can't fit or are too short and the esterification process does not occur. After the esterification is complete the product is released through the "funnel cavity".

Study of Triacsin C analogs

In a study published from the Gokel lab in 1995,[14] a group of structurally related compounds were assayed versus an Acetyl-CoA synthetase isolated from *S. cerevisiae*. These experiments were aimed at identifying the crucial structural elements necessary for the inhibitory activity. These structures are presented in Figure 2.7, along with Triacsin C for comparison.

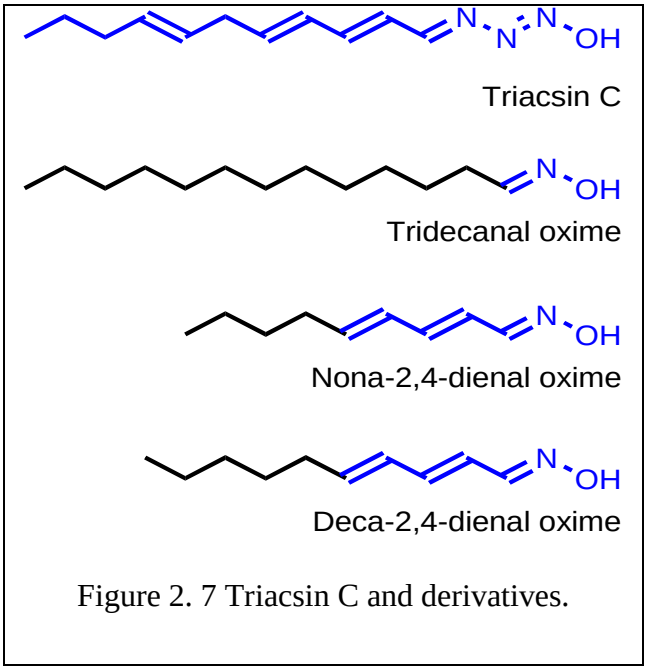

Figure 2. 7 Triacsin C and derivatives.

The structural similarities between the synthetic analogs and triacsin C are highlighted in blue. Tridecanal oxime has the same chain length as triacsin C and contains only the terminal oxime moiety. The two other compounds have extended

unsaturations (three conjugated double bonds) to mimic the triazenol moiety present in triacsin C's structure, but have overall shorter chains.

The inhibition values in the form of IC_{50} (the concentration at which 50% of growth is inhibited) are presented in Table 2.1.

Compound	*IC_{50} (μM)*
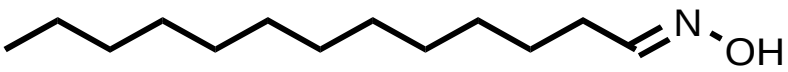 Tridecanal oxime	245 ± 17
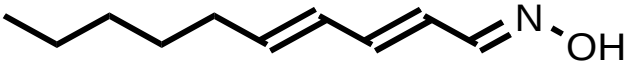 Deca-2,4-dienal oxime	16 ± 1
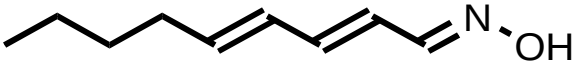 Nona-2,4-dienal oxime	6 ± 0.5
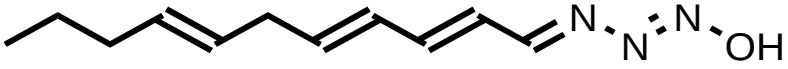 Triacsin C	0.080 ± 0.010

Table 2.1. IC_{50} determined for Triacsin C and derivatives.

While the study only included three new compounds and the most active analog turned out to be 75 fold less active than triacsin C a few interesting structure – activity relationships can be observed. First, the data in Table 2.1 show that the two unsaturated oximes are more active than tridecanal oxime. The high IC_{50} of tridecanal oxime (~3000 fold less active than triacsin C) indicates that the overall length and the presence of only the oxime moiety (=N-OH) is insufficient for achieving satisfactory inhibitory activity. Reducing the overall length of the carbon skeleton but adding adjacent unsaturations to

the oxime moiety dramatically reduces the IC_{50} (the case of nona- and deca- 2,4-dienal oximes) suggesting that the conjugated system is more important for the inhibitory activity than the overall length of the molecule. The higher activity observed for the unsaturated oximes points to the fact that the rather unusual triazenol moiety is important but not crucial. A conjugated system including two -CH=CH- double bonds and only one -CH=N- double bond, while not as active still results in significant enzyme inhibition. The overall length of the molecule does not seem to have such an important role.

While initially LC Acyl-CoA synthetases were regarded as being involved only in the fatty acid metabolism, more recent work points more and more towards a regulatory role for this family of enzymes. The regulatory role is exercised through variations in the concentration of their products – fatty acid CoA esters.

For example, the activity of endothelial nitric oxide synthase (eNOS – an enzyme responsible for production of NO) is inhibited upon palmitoylating two cysteine residues.[15] If the palmitoyl-CoA concentration is varied (by inhibiting or promoting the activity of LC Acyl-CoA responsible for the esterification of palmitic acid) a direct correlation is observed in the activity of eNOS. Same data suggest that palmitoylation is not only the rate limiting step but also a regulatory point in eNOS' activity.

Isoforms are proteins having similar amino acid sequences and with the same function.[16] Due to the important regulatory role of LC Ac-CoA enzymes refining the design of enzymatic inhibitors to the point where they can distinguish between isoforms has increased in importance.

In a collaborative effort with Professor Margaret Weis' laboratory at Texas Tech the response of two LC Acyl-CoA synthetase isoforms to Triacsin C and three oximes

(tridecanal oxime, nona- and deca- 2,4-dienal oximes) was studied. The two isoforms studied (named BP1 and BP2) were isolated from rat brain. If the two isoforms show significant differences in their IC_{50} values when exposed to a certain compound that is indicative of differences in the inhibitory mechanism; differences that could potentially be exploited for the development of isoform-specific inhibitors.

Due to its significance in enzymatic studies, Triacsin C is a commercially available compound obtained through biosynthesis. There is however a previously reported synthesis for Triacsin C.[17] To the best of my knowledge there are no reported syntheses for the other triacsins (A, B and D).

Results

The synthesis of tridecanal oxime, nona- and deca- 2,4-dienal oximes (Scheme 2.1) followed a previously reported synthetic route.[17]

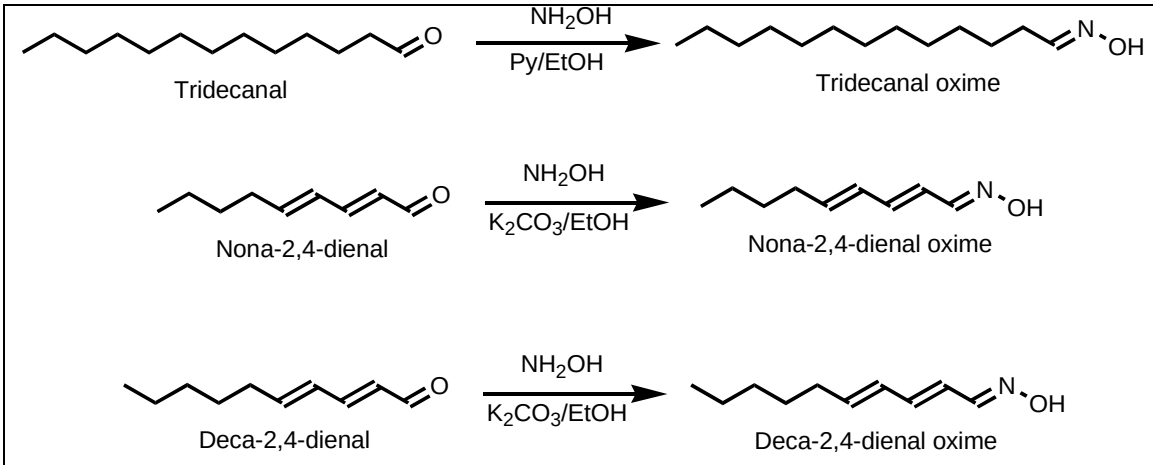

Scheme 2.1. Synthesis of Tridecanal oxime, Nona-2,4-dienal oxime and Deca-2,4-dienal oxime.

The two isoforms (BP1 and BP2) were exposed to triacsin C and the three synthesized oximes. The IC_{50} values for these two enzymes were recorded and a comparison of this data is presented in Table 2.2.

Compound	*IC_{50}(μM)*	
	BP1	*BP2*
Tridecanal oxime	303 ± 33	246 ± 31
Nona-2,4-dienal oxime	180 ± 32	74.0 ± 8.3
Deca-2,4-dienal oxime	80.6 ± 13	53.2 ± 8.0
Triacsin c	0.094 ± 0.013	0.098 ± 0.023

Table 2.2. IC_{50} for BP1 and BP2

Triacsin C inhibits both isoforms in a similar way, but significant differences in the IC_{50} values can be observed for the three oxime compounds. The three oximes clearly inhibit BP2 to a higher degree than BP1. The IC_{50} values are ~25% (for tridecanal oxime), ~150% (for nona-2,4-dienal oxime) and ~50% (for deca-2,4-dienal oxime) higher for BP1 than BP2. This result is encouraging for the development of isoform specific inhibitors.

Conclusions

Triacsin C and compounds structurally akin to Triacsin C can be used in a variety of ways. One obvious way is to explore the requirements for inhibitory activity with the goal of producing new compounds with enhanced activity and increased selectivity.

While the search for a stronger and more selective inhibitor is a worthy goal, not always a more potent inhibitor is necessary. Compounds eliciting lower but still

detectable activity can provide us with useful information helping us to better understand various facets of enzymatic mechanisms. We have used three of these derivatives (tridecanal oxime, nona-2,4-dienal oxime and deca-2,4-dienal oxime) to probe the differences in substrate requirement for two isoforms of LC Acyl-CoA synthetase. The variations observed in the inhibitory responses from these two isoforms when exposed to the three synthesized compounds are indicative that substrate selectivity for these two isoforms can be obtained. Further development of the present structures has potential to yield compounds eliciting inhibitory activity only on one isoform and thus providing us with tool to regulate various metabolic and signaling pathways.

Experimental section

Synthesis of tridecanal oxime, $CH_3(CH_2)_{11}$-CH=N-OH

Tridecanal oxime was synthesized as previously reported and the ^{1}H-NMR and melting points correlated well with published data.[14]

Synthesis of nona-2,4-dienal oxime $CH_3(CH_2)_3$-CH=CH-CH=CH-CH=N-OH

Nona-2,4-dienal oxime was synthesized as previously reported and the ^{1}H-NMR and melting points correlated well with published data.[14]

Synthesis of deca-2,4-dienal oxime $CH_3(CH_2)_4$-CH=CH-CH=CH-CH=N-OH

Deca-2,4-dienal oxime was synthesized as previously reported and the ^{1}H-NMR and melting points correlated well with published data.[14]

References

[1] Yoshida, K. M.; Okamoto, K.; Umehara, M.; Iwami, M.; Kohsaka, H.; Aoki H.; *J. Antibiotics,* **1982,** 151;

[2] Korchak H. M, Kane L.H., Rossi M.W., Corkey B.E.; *J Biol Chem* **1994**; 30281.

[3] Noel R.J., Antinozzi P.A., McGarry D.J., Newgard C.B., *J Biol Chem* **1997**; 18621.

[4] Tomoda H., Igarishi K., Cyong J.-C., Omura S., *J Biol Chem* **1991**; 4214.

[5] Vessey D.A., Kelley M., Warren R.S. *J Biochem Mol Toxicol* **2004**; 100.

[6] Omura, S.; Tomoda, H.; Xu, Q.M.; Takahashi, Y.; Iwai, Y; *J. Antibiot.*, **1986**, 39, 1211-1218;

[7] Van Horn, C. G.; Caviglia, J.M., Li, L.O.; Wang, S., Granger, D.A., Coleman, R., A.; *Biochemistry*, **2005**,1635

[8]., Crumley, J. L.; Young, L.H.; Stallone, J. L., Weis. M.T.; *Cardiovascular Research*, **2004,** 338

[9] Lam, T.K., Pocai1, A.; Gutierrez-Juarez1, R., Obici1, S., Bryan, J., Aguilar-Bryan, L., Schwartz1, G. J., Rossetti, L.; *Nature Med*, **2005**, 320

[10] Thimmarayappa, J., Sun, J., Schultz, L. E., Dejkhamron, P., Lu, C., Giallongo, A., Merchant, J. L.; Menon, R.K., *Molecular Endocrinology* **2006**, 2747

[11] Shumilina, E., Klocker, N., Korniychuk, G., Rapedius, M., Lang, F., Baukrowitz, T., *J Physiol,* **2006,** 433

[12] Cleland, W. W. (1963) *Biochim. Biophys. Acta* **67,** 104

[13] Hisanaga, Y., Ago, H., Nakagawa, N., Hamada, K., Ida,K., Yamamoto, M., Hori, T., Arii, Y., Sugahara, M., Kuramitsu, S., Yokoyama, S., Miyano, M. *J. Biol. Chem.* 2004, 31717-31726;

[14] Knoll, L. J.; Schall, O. F.; Suzuki, I.; Gokel, G.W.; Gordon, J. I.; *J. Biol. Chem*, **1995**, 20090-20097.

[15] Liu, J.; Garcia-Cardena, G.; Sessa W. C., , *Biochemistry*, **1996**, 13277-13281.

[16] http://ghr.nlm.nih.gov/glossary=isoforms

[17] Tanaka, H.; Yoshida, K.; Itoh, Y.; Imanaka, H.; *Tetrahedron Letters*, **1982**, 3421-3422;

Chapter 3. Pyrogallol[4]arenes solution equilibrium studies

Introduction

In a patent[1] that issued in 1909 with the title "Condensation Product and Method of Making Same," Leo Baekeland reported the formation of a new polymeric material resulting from the condensation of phenol and formaldehyde. This product bears a name derived from its inventor "Bakelite", and it gained rapid popularity due to its electrical and thermal insulating properties.

This basic reaction between phenols and various aldehydes led to the formation of many other materials, one of the most notable being the cyclic structures named calixarenes[2] and resorcinarenes.[3] The aromatic reagents used for the synthesis of macrocycles similar to calixarenes are phenol, resorcinol or pyrogallol. The nomenclature for calixarene is quite simple and is formed from the name of the phenol followed by the number of the repeating aromatic unit: for example a calixarene-analog containing four resorcinol units rather than four phenols would be named resorcinol[4]arene.

Pyrogallol[4]arene synthesis

The condensation products that pyrogallol forms and especially pyrogallol[4]arenes were extensively studied by Atwood and coworkers for their properties as capsule forming units.[4,5,6,7,8] These compounds are synthesized by refluxing pyrogallol with the corresponding aldehyde in ethanol, in the presence of HCl. Upon cooling, a solid separates from the reaction mixture. After washing the solid with ethanol, the product is typically pure enough for further experiments. The general reaction for the synthesis of these compounds is shown in Scheme 3.1.

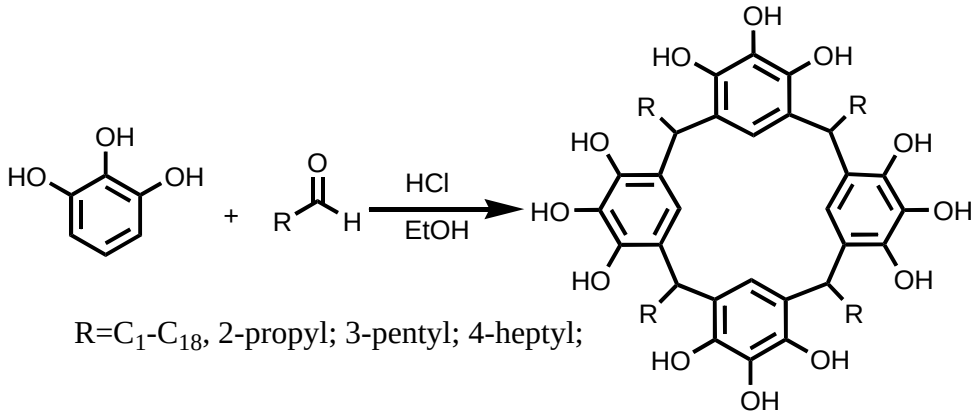

R=C_1-C_{18}, 2-propyl; 3-pentyl; 4-heptyl;

Scheme 3.1. Synthesis of pyrogallol[4]arenes

As in all macrocycle syntheses the question of the conformation of the four aromatic rings must be addressed. In calixarene chemistry the various conformations are cone (rccc), partial cone (rcct), 1,3-alternate and 1,2-alternate(Figure 3.1).

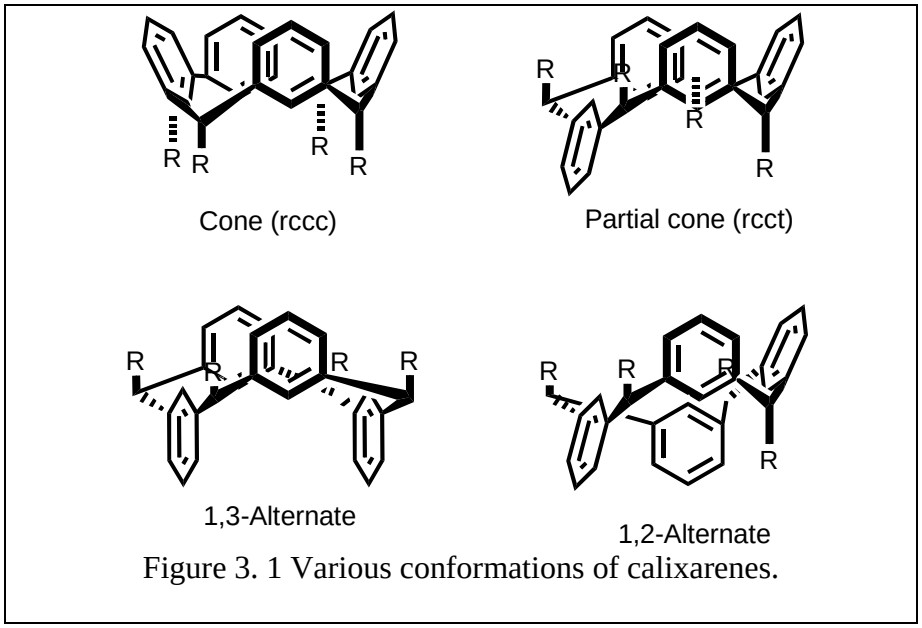

Figure 3. 1 Various conformations of calixarenes.

Previously, the formation of up to five pyrogallol[4]arene conformers has been reported,[9] the boat, crown, chair, diamond, and saddle configurations. The 12 hydroxyl groups present on the outer rim make an extended hydrogen-bond network likely, which

in turn would favor an all *cis* conformation of the sidechains. Even so, it is possible that all other possible conformations form.

Significant effort has been expended in elucidating the conformation or conformations of the material(s) isolated from the synthetic process. According to the X-ray analysis, the isolated material is in the cone conformation. We attribute this to the higher symmetry of this conformer that allows it to crystallize more readily than the other conformational possibilities.

Crystallization motifs for pyrogallol[4]arenes

These tetrametric cone arrangements can crystallize in at least two different forms: a bilayer type structure[10] and a hexameric hydrogen bonded capsule[11] (exemplified by the C_{11} pyrogallol[4]arene in Figure 3.2 both in a schematic and in a CPK version).

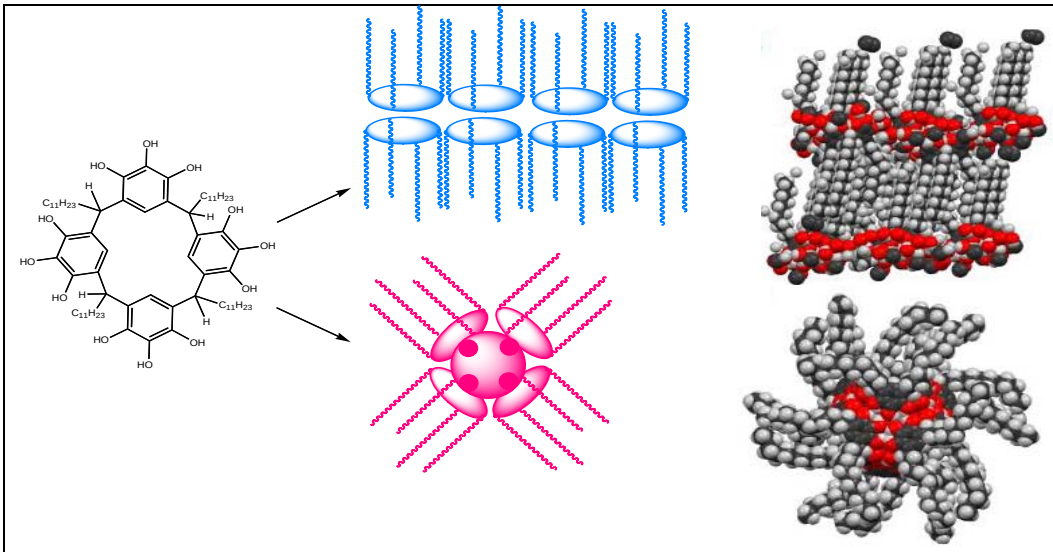

Figure 3. 2 Bilayer and Capsule structure for pyrogallol[4]arenes

Both the bilayer and the hexameric capsule have been characterized by X-ray analysis to confirm the identity of the unit cell.

Membrane properties of C11 pyrogallol[4]arenes

In a paper published from our group in 2009 the ion transport properties of these compounds through membranes have been studied using the planar bilayer method.[12] The study focuses on both the bilayer and the hexameric arrangements of the C_{11} pyrogallol[4]arene.

The planar bilayer conductance method is an analytical technique that studies the membrane properties of compounds with a focus on their ability to mediate the transport of ions through a phospholipid bilayer.[13] A schematic representation of this apparatus is presented in Figure 3.3.

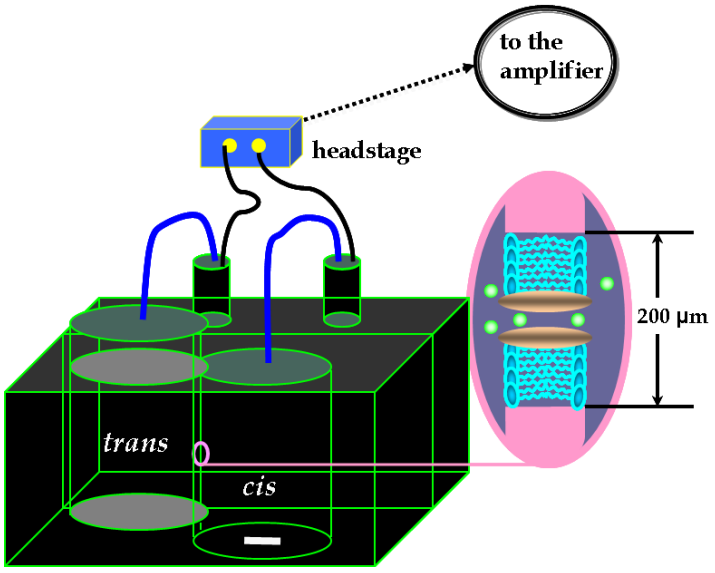

Figure 3. 3 Schematic representation of a planar bilayer apparatus.

The apparatus is composed of two chambers (labeled *cis* and *trans*) that are communicating through a small orifice of ~200 µm in diameter. The two chambers are filled with aqueous buffer and in each chamber an electrode is connected to a detector. A phospholipid bilayer is painted on the orifice so that the two chambers are completely isolated. At the start of the experiment, the compound to be studied is added in the cis chamber and the resulting current is monitored. If the compound is able to insert in the bilayer and mediate the transport of ions, an electrical current is detected. A typical planar bilayer trace is presented in Figure 3.4.

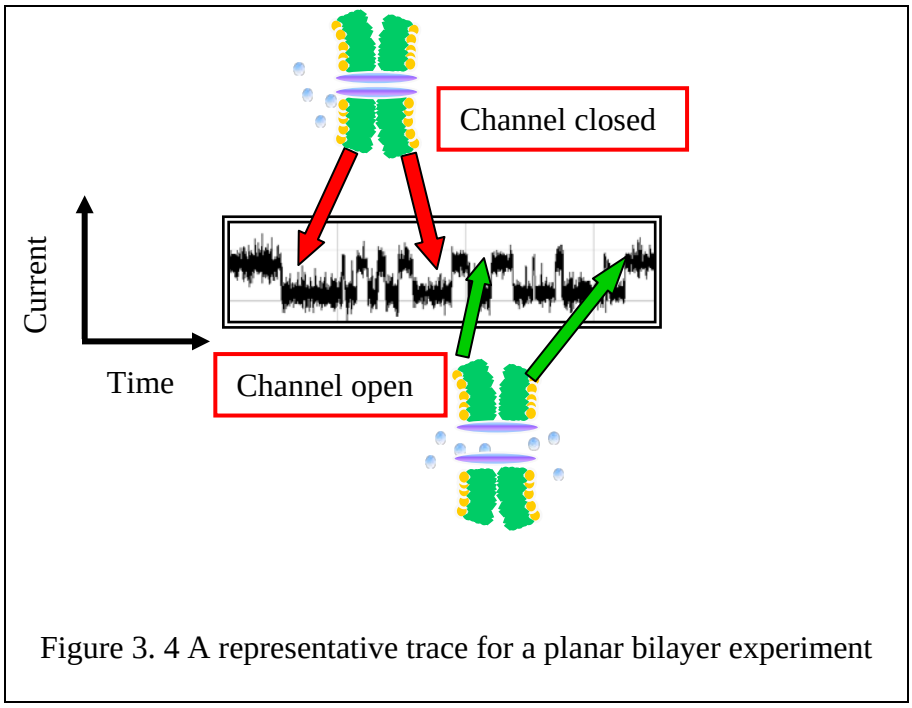

Figure 3. 4 A representative trace for a planar bilayer experiment

In Figure 3.4 the traces indicated by the red arrows represent the portions of the experiment where the channel inserted in the bilayer is not functional/open and is not transporting ions. The traces indicated by the green arrows represent channel openings. When the channel is open, ions can pass from one chamber to the other and the resulting

electric current is being detected. The open–closed behavior exemplified in Figure 3.4 is characteristic of channels and not of carriers so this experiment is the definitive proof for a channel mechanism.

These pyrogallolarene compounds contain both long hydrocarbon chains (which are lipophilic) and hydroxyl groups (which are hydrophilic and can hydrogen bond with various anions) making this family of compounds a likely candidate for insertion and pore formation in a membrane. Planar bilayer experiments for both the bilayer and the hexameric capsule were performed in order to investigate the membrane properties of these compounds.

In Figure 3.5 the traces obtained from the C_{11} bilayer in the presence of Cl^- are presented (the horizontal arrow indicates a 10 s span).

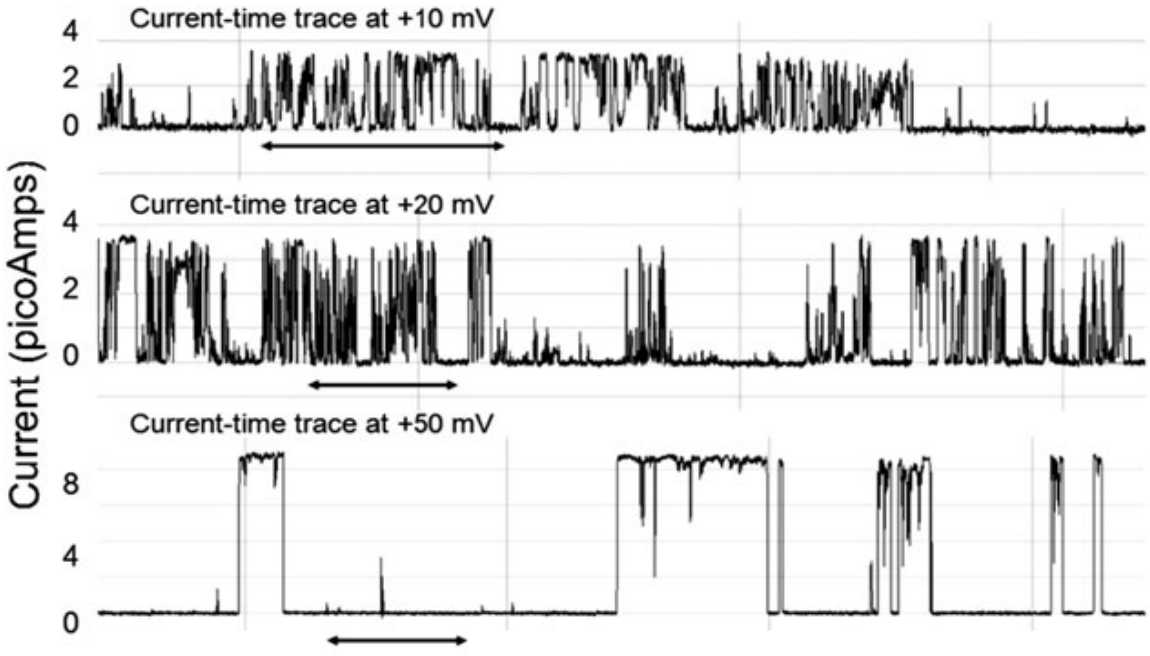

Figure 3. 5 Planar bilayer traces for C_{11} bilayer.

Observing stable open-closed behavior is often a time dependent process. When the putative ionophore is added to the buffer, it may not immediately insert into the planar bilayer and form a functional pore. Often transient opening events are observed initially and after a certain period of time a stable open-closed behavior is recorded. The three traces presented in Figure 3.5 pertain to the same experiment and were recorded consecutively at three different voltages. In the first two traces, we observe open and closed states. Many of these are very short although some more clearly defined states are apparent. At the beginning of the experiment the ionophores are still inserting in the phospholipid bilayer and are inducing transient disturbances in the membrane that are responsible for the currents observed. Over time, a stable open-closed behavior with longer, better-defined openings can be observed (third trace). The intensity of the current is also twice that observed in the first two traces, giving more credit to the formation of a functional channel. Most likely C_{11} bilayer breaks apart into monomers and these monomers can then insert into the membrane and form aggregates of various sizes that then mediate the transport of anions.

When the same experiment was conducted on the C_{11} hexameric capsule, no transport event was observed for more than an hour, after which behavior similar to that shown in Figure 3.5 was observed.

We expected that if transport was mediated by both forms (bilayer and capsule) it might occur by different mechanisms or involve different species. The fact that the capsules seemed inactive (and were for ~60 minutes) but eventually gave results similar to those observed with the bilayer was troubling. The time necessary for the capsule to begin transporting ions seemed too long for a simple induction/insertion phase. These

results begged the question whether or not the discordance in the time necessary to obtain transport was due to different transport mechanisms or the formation of a similar transport mediator that occurred at different rates from the bilayer and capsule. If the bilayer and capsule share the same transport mechanism, then the extra time necessary for achieving transport by the capsule variety is most likely due to the breaking apart of the hexameric assembly into smaller oligomers. These oligomers are then responsible for the ion transport in a similar fashion as the C_{11} bilayer.

To our knowledge, the only data available about these compounds was structural information from the solid state experiments (X-ray analysis of crystals).[4,5] There was little information available about their stability in solution, aggregation behavior, or whether or not an equilibrium existed between the various forms. In order to investigate the stability of the hexameric capsules in solution and the existence of such an equilibrium we decided to use the high performance liquid chromatography (HPLC) method to analyze the starting materials.

HPLC is an analytical technique used mostly for purification and separation of complex mixture of compounds. It uses high purity solvents and tightly packed columns to obtain clear separation between the components. Based on the polarity of the chromatographic column (stationary phase), there are essentially two types of HPLC: normal phase and reverse phase. In the normal phase, the stationary phase (usually silica packed columns) is relatively polar and for reverse phase HPLC, the stationary phase is nonpolar (long hydrocarbon chains grafted on a thin silica coating). For all the HPLC experiments the solvent system (mobile phase) is of opposite polarity to the stationary phase. For instance, in an experiment using a reverse phase column a common solvent

system is water/methanol. The mixture of compounds is injected into the column and then the different components are identified and separated based on their elution time. Based on their relative affinity for the stationary or mobile phase, the components elute at different times, times that are characteristic and can be used to identify them. Detectors used for HPLC can be based on UV-VIS absorbance, refractive index or ES-MS.

Results

The work presented in this section is part of a paper published in 2009 from our group.[12] It appeared that the ability of an HPLC column to resolve complex mixtures of structurally related compounds might be useful in the investigation of the dynamics of pyrogallolarene bilayer and capsule samples. If the bilayer dissociated homogenously into monomer, we would only observe one peak, whereas if multiple species are present, several peaks would be apparent in the HPLC trace. Different peaks can be observed only if the corresponding structures have different partition coefficients. While our compounds are oligomers of the pyrogallol[4]arenes we assumed that doubling or tripling the molar mass of the monomer would result in different partition coefficients which would allow us to distinguish them. The same would be true of the capsule sample. If the capsule remained stable in solution and no decomposition or deaggregation occurred, only one peak would be observed. Again if in both cases we would get several peaks, by comparing the elution times for the capsule and bilayer traces we can draw conclusions on the composition of those samples.

The HPLC experiments performed are presented in more detail bellow.

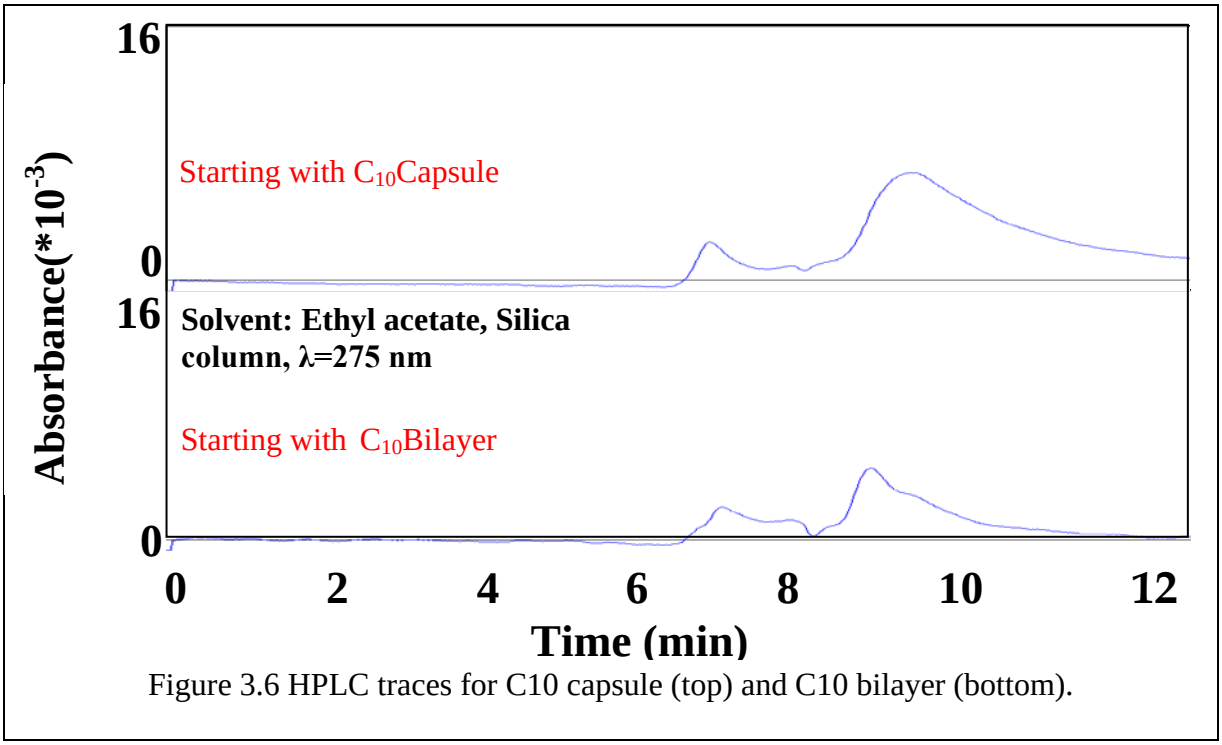

Figure 3.6 HPLC traces for C10 capsule (top) and C10 bilayer (bottom).

The same mass of both the capsule and the bilayer were dissolved in ethyl acetate. Identical masses of compounds were used to ensure that the same amount of monomeric material would be present, in whatever form, in both experiments. After preparing the solutions, they were held at room temperature for one hour to account for the induction period noted in the planar bilayer experiments. Aliquots of each sample were then injected into the HPLC and the resulting HPLC traces were recorded. A comparison between the traces from C_{10} capsule (top trace) and C_{10} bilayer (bottom trace) is presented in Figure 3.6 (the experiments were monitored on a longer time scale but the only peaks observed were the ones shown in Figure 3.6).

The similarities between the two HPLC traces are highlighted in Figure 3.7.

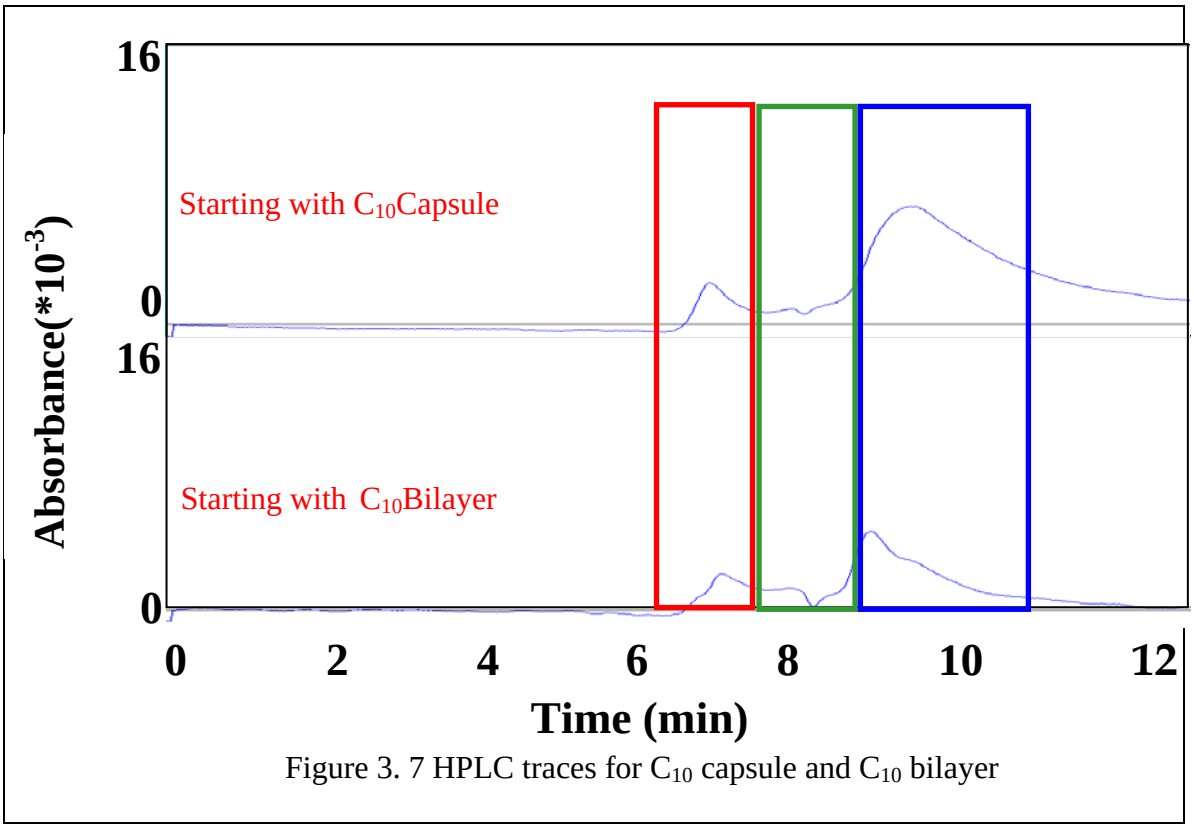

Figure 3. 7 HPLC traces for C_{10} capsule and C_{10} bilayer

The similarity between the two traces is apparent in Figure 3.7. The first peak in both mixtures begins eluting at ~7 minutes and the overall traces are nearly identical. In both traces three similar regions can be observed and they are highlighted in red, green, and blue in Figure 3.7.

The first region (highlighted in red in Figure 3.7) includes a peak, which we attribute to the monomer. The smaller size of this structure makes it the most likely component of the first peak with the fastest elution time. The second region (green in Figure 3.7) contains a number of less well-defined shoulders that we attribute to various oligomers (dimmers, trimers, tetramers). These are most likely forming as intermediates between the long array of linked monomers present in bilayer or capsule and the monomer. The last region in the trace (blue in Figure 3.7) contains a broader and more

intense peak which we attribute to the hexameric capsule and to any other higher oligomers that might form in this environment.

Conclusions

Long chain pyrogallol[4]arenes have very interesting membrane properties. Based on their crystallization motif, they can insert in and mediate the transport of anions through bilayers membranes in a time dependent fashion. The bilayer structure inserts and forms aggregates capable of mediating the transport of ions faster than the capsule.

Our efforts were channeled in the direction of understanding the mechanism of action for these compounds. We investigated their anion transport behavior with planar bilayer experiments (which confirmed the anion transport) and with HPLC experiments aimed at examining the solution stability of these compounds.

HPLC experiments are presented that show similar compositions for the solutions of both bilayer and capsule. These compositions are complex but the many similarities in the traces make us confident in concluding that they are in essence the same. Based on these arguments we believe that both the bilayer and the capsule are breaking apart into monomers in solution. These monomers are in turn responsible for inserting into the membrane and forming oligomeric pores of various sizes that can mediate the transport of ions.

Data from the planar bilayer experiments allow us to estimate the dimensions of the pores that are responsible for the current passing through the phospholipid membrane.[13] Correlating that data with the sizes of the monomer we can hypothesize on

the number of monomers required to form those pores. Our estimates along with the capsule <-> monomer <-> bilayer equilibrium are presented in Figure 3.8.

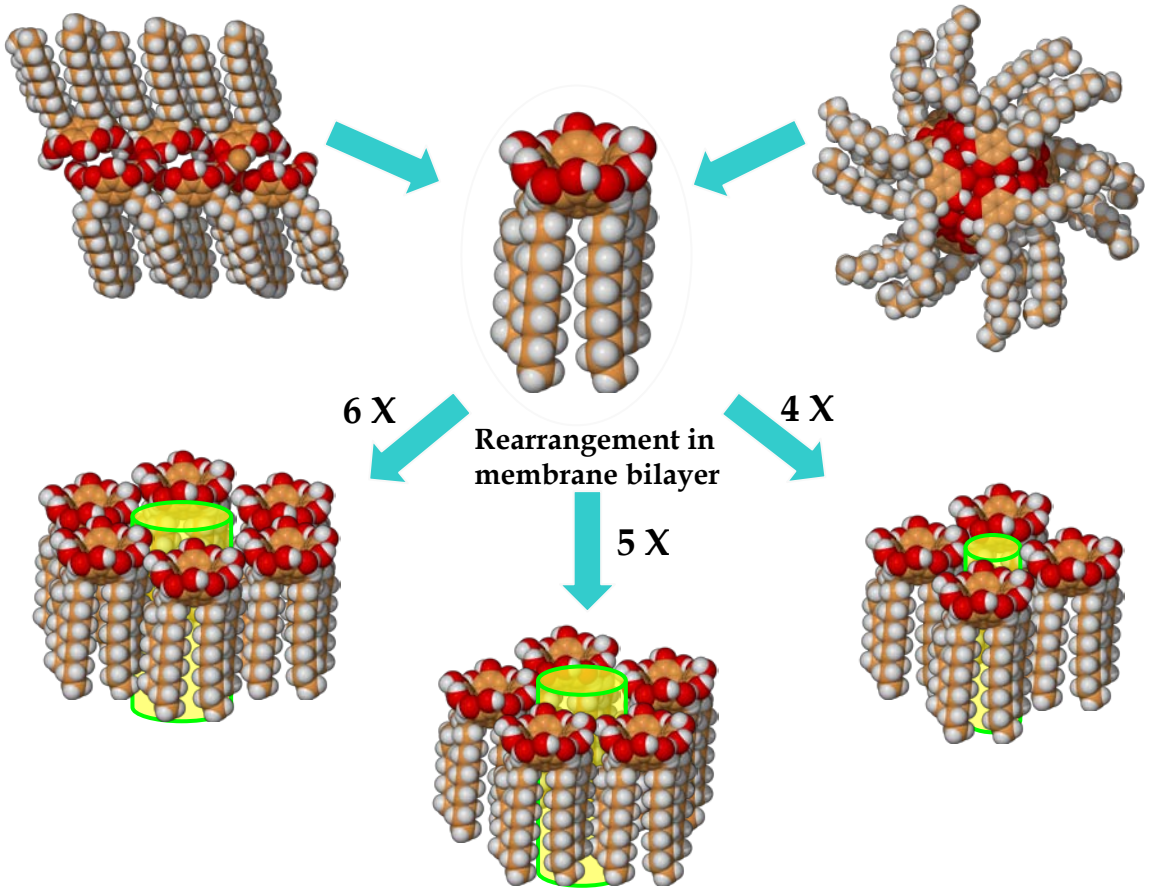

Figure 3. 8 Aggregation behavior of pyrogallol[4]arenes.

As Figure 3.8 shows, both the bilayer and the capsule crystallization motifs break apart in solution and form the monomer, which then reaggregates and forms tetra, penta and hexameric pores that permit the passage of ions through the phospholipid bilayer.

Experimental Section

Pyrogallol[4]arenes have been synthesized and purified previously reported and have been used without further purification.[12]

High performance liquid chromatography

HPLC experiments were conducted on an Xper-Chrom Model 1400 HPLC equipped with a UV-vis detector (λ = 275nm) using a Shodex 5SIL 10E normal phase column. Experiments were performed at least in triplicate, and traces were recorded using Peak Simple v. 2.08 software. Samples were dissolved in EtOAc, and the mobile phase was also EtOAc.

References

[1] L. H. Baekeland, "Condensation Product And Method Of Making Same", United States Patent 942, 809 **1909**.

[2] a) C. D. Gutsche, Calixarenes; Royal Society of Chemistry: Cambridge, **1989**; *Vol. 1*; (b) C. D. Gutsche, Calixarenes Revisited; Royal Society of Chemistry: Cambridge, **1998**; Vol. *6*.

[3] Sliwa, W.; Kozlowski, C. *Calixarenes and Resorcinarenes: Synthesis, Properties, and Applications*; Wiley-VCH Verlag GmbH & Co.: Weinheim, 2009.

[4] Cave, G. W.; Antesberger, J.; Barbour, L. J.; McKinlay, R. M.; Atwood, J. L.; *Angewandte Chemie International Edition*, **2004**, 5263.;

[5] J. L. Atwood, L. J. Barbour, A. Jerga, *Chem. Commun*. **2001**, 2376 – 2377.;

[6] S. J. Dalgarno, G. W. V. Cave, J. L. Atwood, *Angew. Chem. Int. Ed.*, 2006, **45**, 570-574.;

[7] S. J. Dalgarno, D. B. Bassil, S. A. Tucker, J. L. Atwood, *Angew. Chem. Int. Ed.*, **2006**, *45*, 7019-7022.

[8] S. J. Dalgarno, N. P. Power, J. L. Atwood, *Coordination Chemistry Reviews*, **2008**, *252*, 825-841

[9] Dueno, E. E.; Hunter, A. D.; Zeller, M.; Ray, T. A.; Salvatore, R. N.; Zambrano, C. H., Crystal Structure of 2,8,14,20-tert-Butylpyrogallol[4]arene, *J. Chem. Crystallogr.* **2008**, *38*, 181-187.

[10] Kulikov, V. O.; Rath, N. P.; Zhou, D.; Carasel, I. A.; Gokel, G. W.; *New Journal of Chemistry*, **2009**, 1563.

[11] G. W. V. Cave, S. J. Dalgarno, J. Antesberger, M. C. Ferrarelli, R. M. McKinlay, J. L. Atwood, *Supramol. Chem*. **2008**, *20*, 157 –159.

[12] Li, R.; Kulikov, O. V.; Gokel, G. W.; *Chemical Communications*, **2009**, 6092.

[13] Hille, B. *Ionic Channels of Excitable Membranes (Third Edition)*; 3rd ed.; Sinauer Associates: Sunderland, MA, 2001, p814

Chapter 4. Dipicolinamides and Isophthalamides Anion transport studies

Introduction

Ion binding and transport are of fundamental interest for biology and of compelling interest to chemists who strive to better understand binding selectivity and the interactions that control them. Inorganic anions and cations are pervasive in natural systems and their concentrations are closely regulated by numerous complex proteins. Many ions also play a role as enzymatic cofactors, in forming buffer systems, or in maintaining the cellular membrane potential necessary for signaling. Understanding the ability to bind, to transport, and to regulate ion concentrations is of fundamental importance as a scientific matter and of the greatest consequence in the control of biological processes.

The transport of anions in nature occurs most often through two mechanisms. The mechanisms are usually referred to as carrier and channel[1] (Figure 4.1).

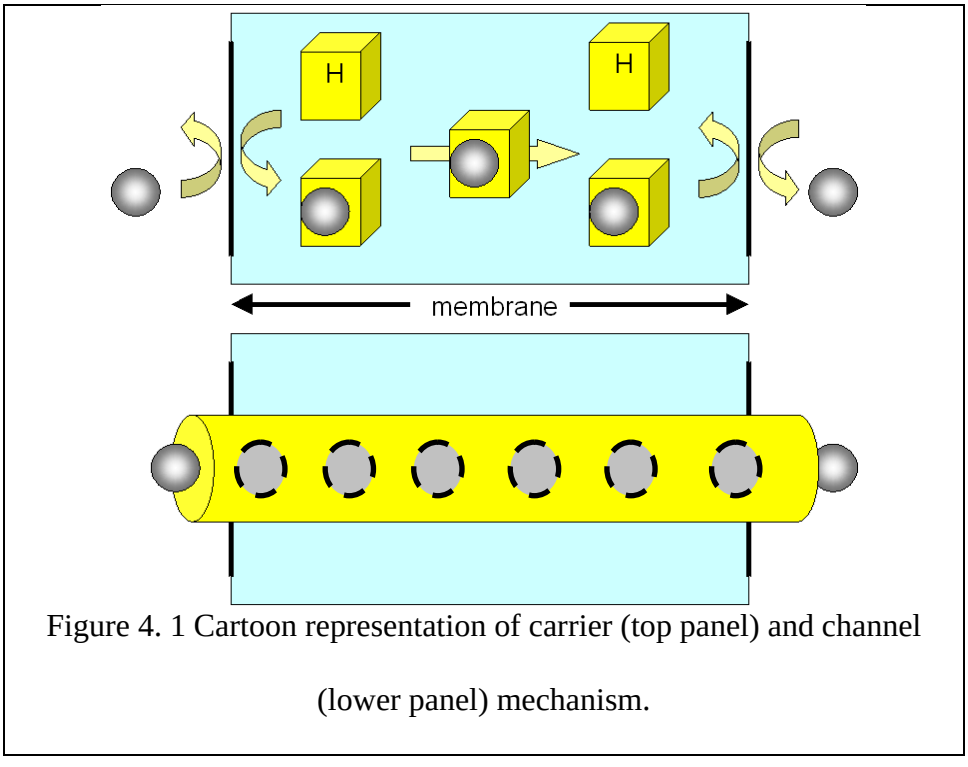

Figure 4. 1 Cartoon representation of carrier (top panel) and channel (lower panel) mechanism.

The carriers are typically smaller than channels and transport ions by a "receptor binding, diffusion, ion release" mechanism. The ions bind to the carrier at either the extracellular or intracellular surface of the membrane; the carrier envelops an ion in order to solvate it and to shield it from the lipophilic environment at the core of the membrane. The receptor-cation complex then diffuses down its concentration gradient to the opposite side of the membrane. The rate at which the carriers transport ions varies but can be as high as 10^4 ions per second. This maximal rate is significantly slower than cation transport by a channel,[2] which can exceed 10^7 ions per second. The rate limiting step in carrier transport is most likely the diffusion through the membrane.[3]

Natural ion channels are large proteins that reside inside the membrane. Their transport mechanism is based on forming an opening or pore allowing ions to pass through the membrane through a low energy pathway. The naturally occurring channels tend to be selective for the ions that they transport. The origin of the selectivity is certainly not known for all channels but for the KcsA voltage gated potassium channel[4] an array of main chain carbonyl groups are positioned so that only certain ions can pass. This section of the channel is often called "the selectivity filter." The transport rate of channels can be up to 10^8 ions per second.[2]

The transport of ions, whether by a carrier or channel mechanism, will naturally be driven by the concentration gradient. This type of transport does not require the consumption of additional energy in order to occur. In certain situations there is a need to transport ions in the opposite direction (from the lower concentration to the higher concentration) and this comes at an energy cost (usually obtained in natural systems by the hydrolysis of ATP). This kind of transport is performed by channels.

Reports of anion binding receptors date back several decades[5,6,7,8,9] but in recent years as a result of a few seminal papers[10,11,12] interest in anion binding has rekindled and burgeoned. One of the most influential of the more recent papers was authored by Crabtree[12] and coworkers, who synthesized an anion receptor based on isophthalic acid and aniline (Figure 4.2).

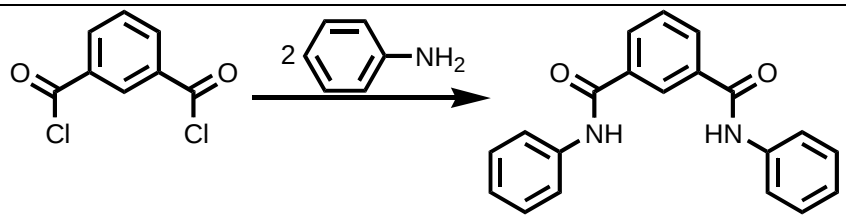

Figure 4. 2 Synthesis and structure of Crabtree's anion receptor.

In the same article Crabtree reported a crystal structure in which the receptor acted as a host for a Br^- anion guest (Figure 4.3).

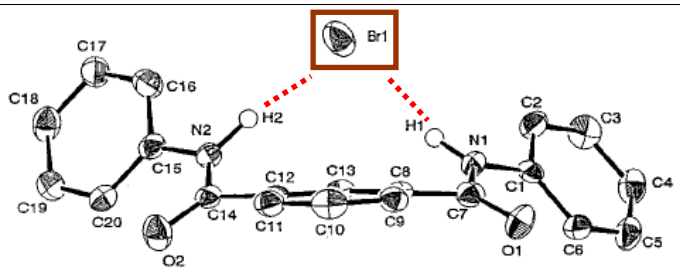

Figure 4. 3 Side view of the crystal structure of the host-guest complex formed by Crabtree's receptor.

The solid state structure shows that the anion resides above the plane of the molecule and forms hydrogen bonds with the two amidic protons. While Crabtree did not pursue the study of this family of compounds, the binding properties of this structure triggered the interest of a number of groups that saw the potential of such a molecule. Gale and coworkers used this model molecule as a starting point and produced an

impressive library of isophthalic acid dianilides.[13] The receptor has been used as an anion-binding subunit into ion-pair hosts,[14] while isophthalamides that replace the aniline subunit with other aromatics such as aminoindoles[15,16] or with alkylamines[17] have been reported. Numerous pyridine-2,6-dicarboxylic acid dianilides are known as well although most were prepared for study in a context other than anion complexation.[18] Dipicolinamides have been incorporated as subunits into structures such as Lehn's helices[19] and Anslyn's cyclophane receptor for trigonal planar anions.[20]

Another interesting result obtained with compounds bearing structural similarities with Crabtree's receptor was published by Li and coworkers.[21] They demonstrated by use of a planar bilayer experiment that the molecule in Figure 4.4 mediates the transport of chloride through a phospholipid bilayer and exhibits channel – like behavior.

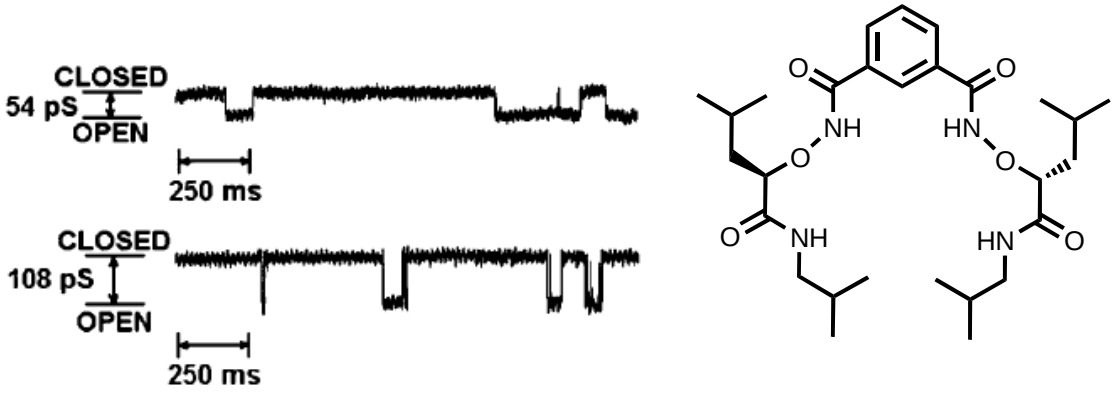

Figure 4.4 Li's receptor and the planar bilayer traces.

The planar bilayer traces shown indicate the formation of two conductance states, one corresponding to 54 pS and another one to 108 pS.

This result was both surprising and interesting. First, it shows that Crabtree–like molecules are able to mediate the transport of ions through a phospholipid bilayer. Second, this work suggests that such structures organize into ion channels. The planar

bilayer conductance results confirm the latter but the authors neither disclosed structural information nor speculated upon it.

In order to bridge a phospholipid bilayer, a molecule or assembly must span ~35-40 Å. The size of the Li *et al.* channel former is about half of that at best depending on conformation. The size issue alone suggests that it is impossible for a single molecule to be responsible for the channel behavior observed. The size requirements point to the formation of oligomeric aggregates either in the aqueous media or through lateral diffusion inside the phospholipid bilayer. The inference we draw is that aggregates must form a pore that mediates the transport of chloride ions.

Results

The results discussed below are presented in the paper that our group published in *Chemical Communication* in 2010.[22] I have performed the electrospray-ionization mass spectrometry studies detailed here. The calculations, syntheses, proton NMR binding studies, chloride transport studies, and optical spectroscopy were performed by a former coworker Dr Carl Yamnitz. Saeedeh Negin, another member of the Gokel research group and a graduate student at the University of Missouri-St. Louis, performed the planar bilayer studies.

The combination of numerous Crabtree-type variants that have appeared in the literature and the intriguing but surprising results of Li *et al*. inspired our interest in this group of compounds. The family of compounds shown in Figure 4.5 was prepared and their anion transport properties were investigated. Four of the compounds shown in Figure 4.5 are dianilides of dipicolinic acid and two are dianilides of isophthalic acid.

Differences in between these compounds stem from the substitution on the aniline ring. Substituents range from the electron donating CH_3, H to the electron withdrawing CN and NO_2.

Compounds studied

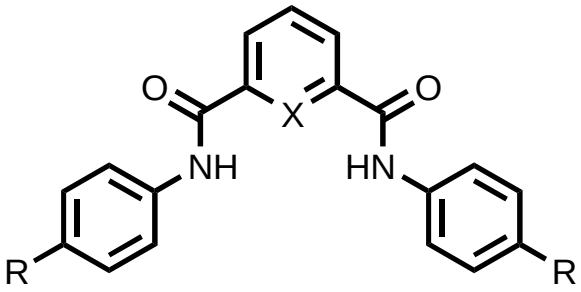

Pyr-CH_3 X=N R=CH_3
Pyr-H X=N R=H
Pyr-CN X=N R=CN
Pyr-NO_2 X=N R=NO_2
ISO-H X=CH R=H
Iso-NO_2 X=CH R=NO_2

Figure 4. 5 Structures of the compounds studied

The synthesis of these compounds is straightforward and begins either from dipicolinic acid (2,6-pyridinedicarboxilic acid) or from isophthalic acid. The diacid is converted to the diacid chloride using $SOCl_2$ and then treated with the appropriate aniline to yield the desired compound (Figure 4.6).

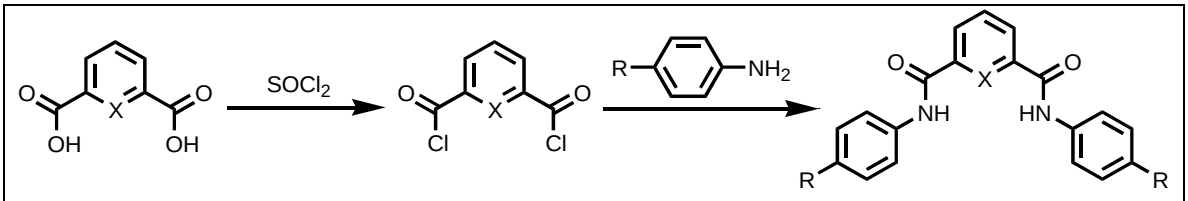

Figure 4. 6 The synthesis of studied compounds

Computational studies

The resulting dianilides have been studied by using a variety of analytical techniques. First a series of computational studies have been performed in order to obtain

information about the gas phase conformations. These computational studies have been performed by Dr Carl Yamnitz, at the DFT level of theory using Spartan 06 software package. In Figure 4.7 the gas phase calculations for the unsubstituted isophthalamide (left) and dipicolinamide (right) derivatives without any anions present are shown.

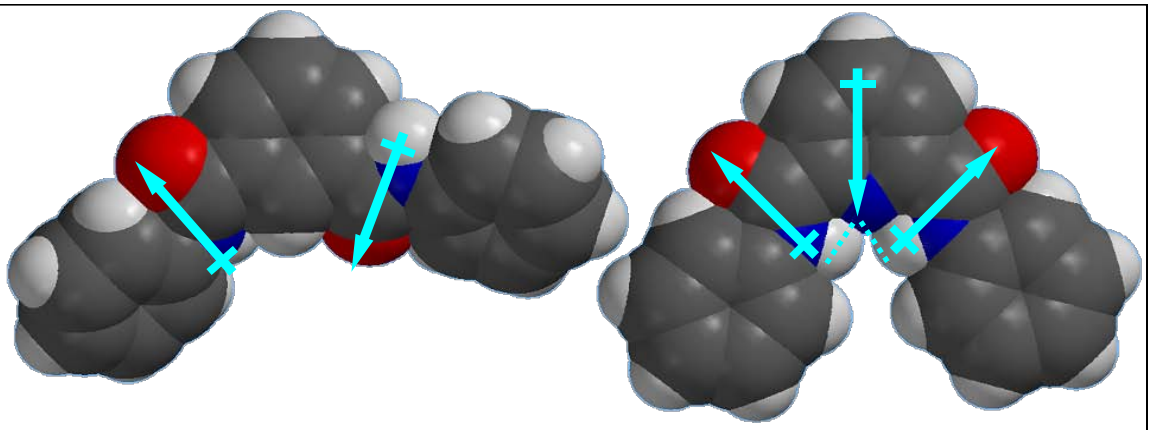

Figure 4. 7 Gas phase conformation of unsubstituted isophthalamide (left) and dipicolinamide (right) in the absence of guest anions

Isophthalanilides have a *syn-anti* conformation with one of the aromatic sidearms twisted. This particular conformation can be explained by the tendency of these compounds to minimize the overall dipole of the molecule. The optimal conformation is to have the dipoles of the carbonyl moieties pointing in opposite directions.

The unsubstituted dipicolinamide has a different conformation where the two aromatic side-arms are in a *syn–syn* conformation. Again minimization of the overall molecular dipole is the driving force for the conformation. In this particular case we also have the dipole induced by the nitrogen atom incorporated in the pyridine ring. Another difference is the opportunity for hydrogen bonding between the pyridyl nitrogen and the two amidic protons, which locks the molecule in this planar arrangement and makes the

syn–syn conformation more favorable. The computational results correspond well with crystal structures reported in the literature for isophthalamides[23] and dipicolinamides.[24]

Calculations performed for dipicolinamides and isophthalamides in the presence of guests yielded conformations similar to the one presented in the crystal structure in Figure 4.3. In Figure 4.8 the calculations for the nitro substituted isophthalamide (A) and dipicolinamide (B) in the presence of Cl^- anions are shown.

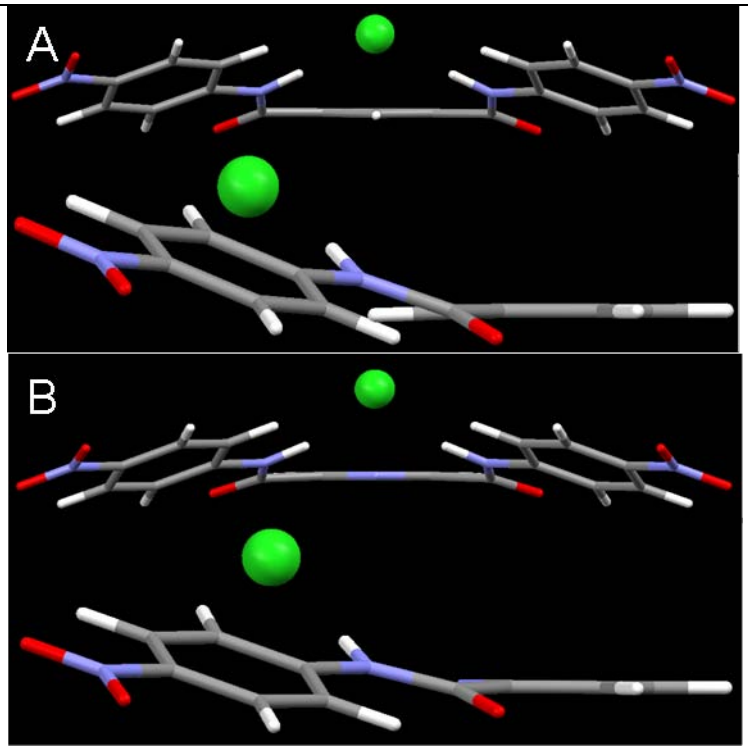

Figure 4. 8 Conformations of p-nitro substituted isophthalamide (A) and dipicolinamide (B) with a Cl^- guest

In both cases, the Cl^- resides above the plane of the molecule and the two aromatic sidearms are rotated in order to favor the formation of hydrogen bonds between the anion and the two amidic hydrogens.

Solution based studies

The experimental behavior of these compounds was determined by the following studies. Chloride release from the vesicles was measured by ion selective electrode and fluorescence quenching methods as well as by planar bilayer experiments. Binding constants were determined in solution by using a previously reported NMR method[25]. The data from all of these experiments are in agreement and provide us with a trend for the ability of these six compounds to bind and transport chloride. The two nitro compounds and the cyano derivatives are the most active compounds, followed by the unsubstituted and the methyl derivatives. This trend is in accordance with the electronic properties of the *para*-substituents. The electron withdrawing substituents (*p*-nitro and *p*-cyano) reduce the electron density on the aromatic ring and consequently on the N-H amidic bond, weakening it. A proton involved in a weaker bond is more likely to form hydrogen bonds with anions. This effect is no longer present for the unsubstituted and *p*-methyl derivatives which exhibit lower activity.

While the data was piecing together nicely, what our work was lacking was direct comparisons in between these compounds to clearly establish a ranking for the binding and transport activity. A key issue was that differences in solubility precluded us from obtaining binding constants data in the same solvent for all of the compounds. This, in turn, made direct comparisons impossible.

Electrospray mass sprectrometry

We decided to use mass spectrometry to overcome the solubility problem. The dianilides were therefore studied using electrospray mass spectrometry (ES-MS). The ES-MS method is a milder ionization technique than electron impact so little or no fragmentation of the hosts is usually observed.[26] Another advantageous feature of the ES-MS technique is that it uses solution samples instead of solid samples thus being better fitted for our needs. A cartoon representation of the ES-MS ionization and detection process is presented in Figure 4.9.[27]

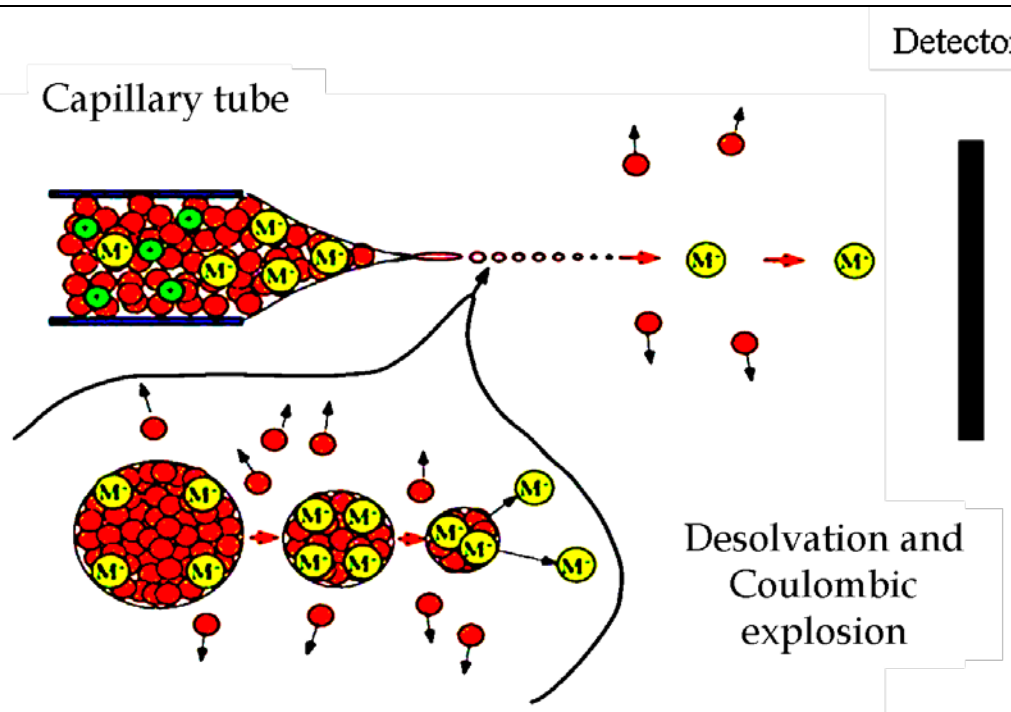

Figure 4. 9 ES-MS ionization process

The solution is injected through a capillary placed inside another capillary tube through which nitrogen gas (called nebulizing gas) is flowing. The tip of the capillary is maintained at a high electric potential and this electric potential splits the sample into an aerosol of small droplets. The flow of nitrogen gas directs the droplets towards the mass

spectrometer. In their path the droplets lose most of the solvent molecules thus increasing the concentration of ions inside the droplet. When the electrostatic repulsion becomes too great, a “Coulombic explosion” occurs that releases the ions into the vapor phase. These ions are then detected based on their m/Z ratios.

The experiments were run using methanol solutions of the compounds studied and tetrabutylammonium chloride. Compounds Pyr-NO_2 and Iso-NO_2 which are less soluble in methanol were dissolved in a 10/90 (v/v) DMSO/methanol. Admittedly, methanol and 10% DMSO-methanol are not identical. However, both solvents are predominantly methanol and the dielectric constants of methanol and DMSO are 33 and 44, respectively.

Our goal was to let the hosts compete for the anions so each experiment was designed accordingly. In each experiment, the concentrations of the two hosts were the same and the chloride (as tetrabutylammonium salt) was present in a substoichimetric amount (usually 10-fold lower concentration) to permit the competition.

An example of the data collected from such an experiment is presented in Figure 4.10.

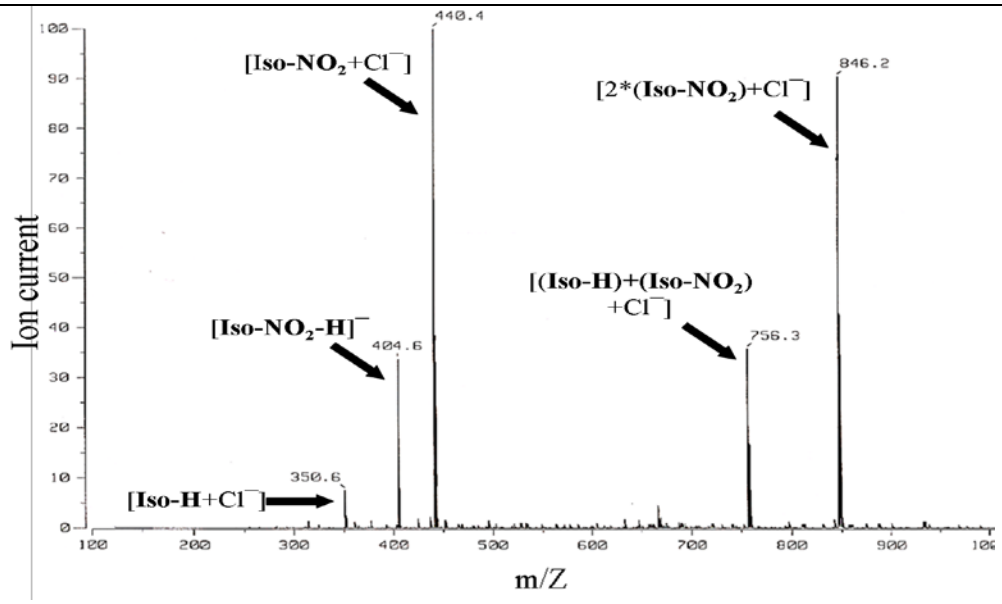

Figure 4. 10 Competitive ES-MS experiment between the p-nitro and the unsubstituted isophthalamide

The data were processed as follows. In each MS experiment, the most intense peak was used as a reference peak, called the "base peak" and assigned the reference intensity (height) of 100. The intensities of all the other peaks in the spectrum are normalized to this base peak so their intensities will be lower than or equal to 100%. The intensity of the peak is a quantitative measure of the ions that are detected by the instrument and of the ions that are formed in the mixture. By using ratios between the peak intensities of the chloride adducts that the two hosts form, we can determine a selectivity ranking for the two hosts.

In Figure 4.10 the competitive experiment is performed between two isophthalamide derivatives: the *p*-nitro and the unsubstituted derivative. All of the peaks are labeled and they correspond either to the deprotonated hosts or to chloride adducts. The chloride adducts can be monomeric (one host and one Cl^-) or dimeric (two molecules of host and one Cl^-). The dimers can be homodimers (the two molecules of the

same host) or heterodimers (a molecule of each host). When calculating the ratios of peak abundances the homodimers are counted twice and heterodimers are counted once for each host. For example the number of molecules of Iso-NO_2 that bind Cl^- are calculated with the following formula: [(Iso-NO_2)+Cl^-] + [(Iso-NO_2)+(Iso-H)+Cl^-] + 2*[2x(Iso-NO_2)+Cl^-].

The data accumulated from the various competitive experiments is presented in Table 4.1.

Table 4. 1Competitive ES-MS experiment data for the compounds studied.

Compound	X	p-substituent	Ratios vs Iso-H
Pyr-CH_3	CH	CH_3	0.14 ± 0.01
Pyr-H	CH	H	0.13 ± 0.02
Pyr-CN	CH	CN	3.27 ± 0.26
Pyr-NO_2	CH	NO_2	2.82 ± 0.07
Iso-H	N	H	1.00
Iso-NO_2	N	NO_2	5.44 ± 0.65

In these competitive experiments, the compounds Pyr-CN, Pyr-NO_2 and Iso-NO_2 bound more Cl^- than the designated control compound (Iso-H) did and even more than compounds Pyr-CH_3 and Pyr-H did. Compounds Pyr-CN, Pyr-NO_2 and Iso-NO_2 have electron withdrawing substituents in the *para*-position of the aniline ring (cyano or nitro). The presence of these electron withdrawing substituents reduces the electron density on

the aromatic system, which in turn reduces the electron density of the N-H bond. The resulting N-H is weaker (more acidic) making hydrogen bonding with chloride easier.

The compound Iso-H was chosen to be the reference for several reasons. The reference structure was required to provide enough binding in order to have a reliable comparison with the stronger binders, but at the same time it could not be so potent that it would totally suppress the signal from the weaker binders. Before starting the experiments, we suspected that compounds Pyr-CH_3 and Pyr-H and Iso-H would be the weaker binders so our standard should be one of them. Our first experiments were directed to rank these three compounds in order to pick a suitable standard. As can be seen in Table 4.1, Iso-H is the strongest binder in this series. It was therefore chosen to be the control structure.

We performed direct comparisons using other potential standards as well. For instance, we performed a competitive experiment using **Pyr-NO_2** and **Iso-NO_2**. The experiment was successful, but the data obtained were difficult to interpret and quantify. This is because compounds **Pyr-NO_2** and **Iso-NO_2** differ only through the identity of the atom in position 1 on the central arene: N for **Pyr-NO_2** and CH for **Iso-NO_2**. This difference translates to only one atomic mass unit difference between the adducts of these two compounds, so the [**Host**+Cl^-] is a mixture of [(**Iso-NO_2**)+Cl^-] and [(**Pyr-NO_2**)+Cl^-] peaks overlapping, while the dimer adduct cluster is composed of three species: [2x(**Iso-NO_2**)+Cl^-], [(**Pyr-NO_2**)+(**Iso-NO_2**)+Cl^-] and [2x(**Pyr-NO_2**)+Cl^-]. An example of the composition of the cluster of peaks corresponding to a dimmer is exemplified in Table 4.2.

Table 4. 2Species present in the cluster of peaks corresponding to a dimmer chloride adduct

m/Z value	Species present
848	[(**Iso-NO_2**)+Cl^-]
849	[2x(**Iso-NO_2**)+1+Cl^-] + [(**Pyr-NO_2**)+(**Iso-NO_2**)+Cl^-]
850	[2x(**Iso-NO_2**)+2+Cl^-] + [(**Pyr-NO_2**)+(**Iso-NO_2**)+1+Cl^-] + [2x(**Pyr-NO_2**)+Cl^-]
851	[2x(**Iso-NO_2**)+3+Cl^-] + [(**Pyr-NO_2**)+(**Iso-NO_2**)+2+Cl^-] + [2x(**Pyr-NO_2**)+1+Cl^-]
852	[2x(**Iso-NO_2**)+4+Cl^-] + [(**Pyr-NO_2**)+(**Iso-NO_2**)+3+Cl^-] + [2x(**Pyr-NO_2**)+2+Cl^-]

Deconvoluting these clusters is difficult but possible by using isotope distribution charts. Starting with the first peak we know it is composed only of the homodimer of **Iso-NO_2** and Cl^-. From the isotope distribution charts we get the percentage of the [2x(**Iso-NO_2**)+1+Cl^-] from [2x(**Iso-NO_2**)+Cl^-]. Subtracting that from the second peak we are left with only [(**Pyr-NO_2**)+(**Iso-NO_2**)+Cl^-]. Using a similar procedure but taking into consideration the isotope distribution charts for [(**Pyr-NO_2**)+(**Iso-NO_2**)+Cl^-] we obtain [2x(**Pyr-NO_2**) +Cl^-] from the third peak and so on.

Interpreting the results of this procedure, while having a lot of merit as a control experiment, is very tedious and time consuming. We performed it for the Pyr-NO_2 and

Iso-NO_2 pair and it resulted in a 1.3:1 selectivity for Iso-NO_2 as well as for Pyr-H and Iso-H pair and it resulted in a 7:1 selectivity for Iso-H. The results from these experiments correlate well with the data presented in Table 4.1.

The data from the ES-MS experiments points towards the following binding strength ranking: Iso-NO_2, Pyr-CN, Pyr-NO_2>Iso-H, Pyr-H, Pyr-CH_3. This trend correlates very well with the results from our other studies.

Conclusions

The ability of dianilides of dipicolinic and isophthalic acids to bind and transport chloride through phospholipid bilayers is clear. Studies using independent analytical techniques (computational experiments, planar bilayer, influx of chloride into vesicles, binding constant determination by NMR and ES-MS assays) all point towards the same activity trend for the members of this family of compounds. The most active compounds are the ones bearing the electron withdrawing substituents (*p*-nitro and *p*-cyano) on the aniline ring. These three compounds are far superior to the non-substituted compounds or those molecules having electron donating substituents (methyl) as far as their ability to bind and transport chloride ions.

While planar bilayer and chloride influx experiments give us data on the anion transporter character of these compounds, we obtained more detailed data on the binding process by using ^{1}H-NMR-determined binding constants. The caveat of the NMR experiments was the difference in solubility between these compounds, which impeded direct comparisons. To overcome this difficulty we devised competition experiments using ES-MS so that direct comparisons of these compounds in solution can be made.

As is the case with the remarkable results of Li *et al*., the ion transport mechanism by which these compounds operate remains unclear. The most plausible hypothesis at present is a stacking mechanism whereby a number of monomers aggregate within the membrane and form pores that allow the passage of anions. How many monomers are aggregating and what exactly is the morphology of these pores still needs to be determined.

Experimental Section

Synthesis of the compounds studied was performed as previously described[15] and the physical properties of these compounds correlated well with the previously published compounds.

Competitive chloride binding assayed by electrospray mass spectrometry

In each experiment, competing hosts were present in equimolar concentrations (50 μM) and chloride (as NBu_4Cl salt) was kept sub-stoichiometric (5 μM). The ratios shown in Table 4.1 were calculated from the total integration of relevant m/Z peaks for host-Cl^- adducts. In every case, the total relative abundance of the unsubstituted isophthalamide, was normalized to 1, with a value established for the competing compound. Errors are the calculated standard deviations of ratios from at least three independent experiments.

References

[1] Hille, B. *Ionic channels of excitable membranes (third edition)*; 3rd ed.; Sinauer Associates: Sunderland, MA, **2001** p 814.

[2] Stark, G.; Ketterer, B.; Benz, R.; Lauger, P. *Biophys. J.* **1971**, *11*, 981-994.

[3] Buck, R. P. *J. Phys. Chem.* **1987**, *91*, 2347-2350.

[4] Doyle, D. A.; Cabral, J. M.; Pfuetzner, R. A.; Kuo, A.; Gulbis, J. M.; Cohen, S. L.; Chait, B. T.; MacKinnon, R., *Science* **1998**, *280*, 69-77.

[5] (a) C. H. Park and H. E. Simmons, J. Am. Chem. Soc., **1968**, 90, 2431;

[6] F. P. Schmidtchen, Angew. Chem., **1977**, 89, 751;

[7] E. Graf and J.-M. Lehn, J. Am. Chem. Soc., **1975**, 97, 5022

[8] A. Echavarren, A. Galan, J. De Mendoza, A. Salmeron and J.-M. Lehn, Helv. Chim. Acta, **1988**, 71, 685;

[9] M. Newcomb and M. T. Blanda, Tetrahedron Lett., **1988**, 29, 4261

[10] (a) Anion Receptor Chemistry, ed. A. Bianchi, K. Bowman-James and E. Garcia-Espana, Wiley-VCH, New York, **1997**; (b)

[11] J. L. Sessler, P. A. Gale and W.-S. Cho, Anion Receptor Chemistry, Royal Society of Chemistry, Cambridge, **2006**.

[12] (a) Kavallieratos, K.; de Gala, S. R.; Austin, D. J.; Crabtree, R. H. *J. Am. Chem. Soc.* **1997**, *119*, 2325-2326. (b) Kavallieratos, K.; Bertao, C. M.; Crabtree, R. H. *J. Org. Chem.* **1999**, *64*, 1675-1683.

[13] (a) Gale, P. A. *Acc. Chem. Res.* **2006**, *39*, 465-475. (b) Bates, G. W.; Gale, P. A.; Light, M. E. *Chem. Commun.* **2007**, 2121-2123.

[14] Koulov, A. V.; Mahoney, J. M.; Smith, B. D. *Org. Biomol. Chem.* **2003**, *1*, 27-29.

[15] (a) Bates, G. W.; Gale, P. A.; Light, M. E. *Chem. Commun.* **2007**, 2121-2123.

[16] Zielinski, T.; Dydio, P.; Jurczak, J. *Tetrahedron* **2008**, *64*, 568-574.

[17] Santacroce, P. V.; Davis, J. T.; Light, M. E.; Gale, P. A.; Iglesias-Sanchez, J. C.; Prados, P.; Quesada, R. *J. Am. Chem. Soc.* **2007**, *129*, 1886-1887.

[18] Lizarraga, E.; Zabaleta, C.; Palop, J. A. J. Thermal Anal. Colorim. **2007**, 89, 783-792.

[19] Berl, V.; Huc, I.; Khoury, R. G.; Lehn, J.-M., Chem. Eur. J. **2001**, 7, 2798-2809.

[20] Bisson, A. P.; Lynch, V. M.; Monahan, M.-K. C.; Anslyn, E. V. Angew. Chem. Int. Ed. Engl. **1997**, *36*, 2340-2342.

[21] (a) Li, X.; Shen, B.; Yao, X.-Q.; Yang, D. *J. Am. Chem. Soc.* **2007**, *129*, 7264-7265. (b) Li, X.; Shen, B.; Yao, X.-Q.; Yang, D. *J. Am. Chem. Soc.* **2009**, *131*, 13676–13680.

[22] Yamnitz, C. R.; Negin, S.; Carasel, I. A.; Winter, R. K.; Gokel, G. W. *Chem. Commun.* **2010**, *46*, 2838-2840

[23] Nimmanpipug, P.; Tashiro, K.; Maeda, Y.; Rangsiman, O. *J. Phys. Chem. B* **2002**, 106, 6842-6848.

[24] Malone, J. F.; Murray, C. M.; Dolan, G. M. *Chem. Mater.* **1997**, *9*, 2983-2989.

[25] Connors, K. A. *Binding Constants*, 1st ed.; John Wiley & Sons: New York, **1987**, 189-215.

[26] Silverstein, R. M.; Webster, F. X.; Kiemle, D. J.; "*Spectrometric Identification of Organic Compounds; Seventh Edition*", John Wiley & Sons, Inc, **2005**, p 7.

[27] Image reproduced from http://rsl.eng.usf.edu/Pages/ResearchElectrospray.html

Chapter 5. Gas Phase Ion Selectivity of 1,3-Diarylamides

Introduction

The study of ligands, hosts, receptors, etc. for cations and anions has been underway for a century or more.[1,2,3,4,5,6,7,8,9,10] Historically, cation complexation has received more attention, but during recent years the study of receptors for anions such as halides has become an area of vigorous research effort. In this range of studies, many interactions have proved to be important in the complexation process but the most frequent binding motif for anion complexation is typically hydrogen bonding.[11,12,13,14,15,16]

The slower development of anion sensors, compared to cation sensors, is due to the fact that detecting small inorganic anions is often more difficult than detecting cations. This difficulty stems in part from the fact that the anions are larger than the isoelectronic cations[17] which lowers their charge density and reduces the effectiveness of electrostatic interactions with a potential ligand. Polyatomic inorganic anions exhibit a wide range of geometries with charges delocalized over a number of atoms which makes designing a suitable receptor more difficult.

Another feature of anions is their higher free energy of solvation compared to cations of almost the same size, which means that the receptor must compete more effectively with the solvent. For example, F^- (radius = 1.36 Å) has a ΔG hydration of -465 kJ/mol, which is significantly greater than a potassium cation with almost the same size (radius = 1.38 Å) and ΔG hydration of -295 kJ/mol[18]. These particularities of anions make the task of binding and detecting anions more difficult.

In a recent paper[19] from our group, compounds having the general structure presented in Figure 5.1 have been shown to bind and transport Cl^- through phospholipid bilayers. Binding and transport involving or mediated by these compounds has been

investigated using gas-phase calculations and experiments such as planar bilayer conductance studies, ion release from vesicles, fluorescence studies, and electrospray mass spectrometry (ES-MS).

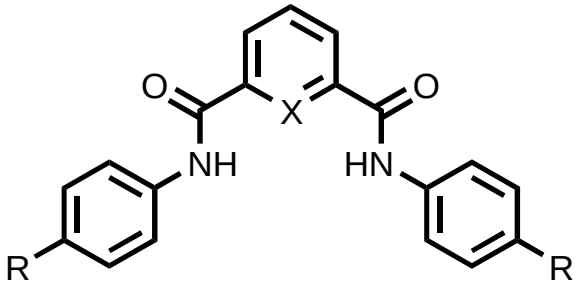

1 X=N R=CH_3
2 X=N R=H
3 X=N R=CN
4 X=N R=NO_2
5 X=CH R=H
6 X=CH R=NO_2

Figure 5. 1 General structure of compounds **1**-**6**

The combination of results obtained by the application of these various techniques established a trend for Cl^- binding and transport activity. Broadly expressed, binding and transport mediated by **3**, **4** and **6** was greater than observed for **1**, **2** and **5**.

Each of the experimental techniques enumerated above provides information about an aspect of the overall ion transport process. For instance, the planar bilayer experiments provide evidence for transport through a "membrane-like" structure while fluorescence experiments give data from which the aggregation behavior of these compounds can be inferred. The electrospray mass spectrometry technique, ES-MS (a solution based mass spectrometry technique),[20] may be used to investigate the anion binding abilities of these compounds. Experiments are designed so that anions will compete for a host. This is done because the ES-MS method is not sufficiently quantitative to compare separate experiments to reliably obtain selectivity data. To ensure competition the anion concentrations in all experiments significantly exceeded the host concentration.

It was found in earlier work that compounds such as **4** and **6** (see above) are effective Cl^- binders.[19] This result begged the question of halide ion selectivity and, indeed, selectivity in binding other types of anions. The first phase of this study was therefore to probe selectivity in the halogenated anion series (F^-, Cl^- and Br^-).

Computational data

Computational studies were conducted by Dr. Carl Yamnitz in our laboratory, using the Spartan Software Package at the density functional theory (DFT) level. Details of the computational work are presented in his doctoral dissertation. Certain results are recounted here as they help us understand the binding and selectivity properties of the isophthalamides and the picolinamides. The three halogenated anions used in this study (F^-, Cl^- and Br^-) all have the same charge (1^-) but differ in their ionic radii. This difference is represented visually in Figure 5.2.[17]

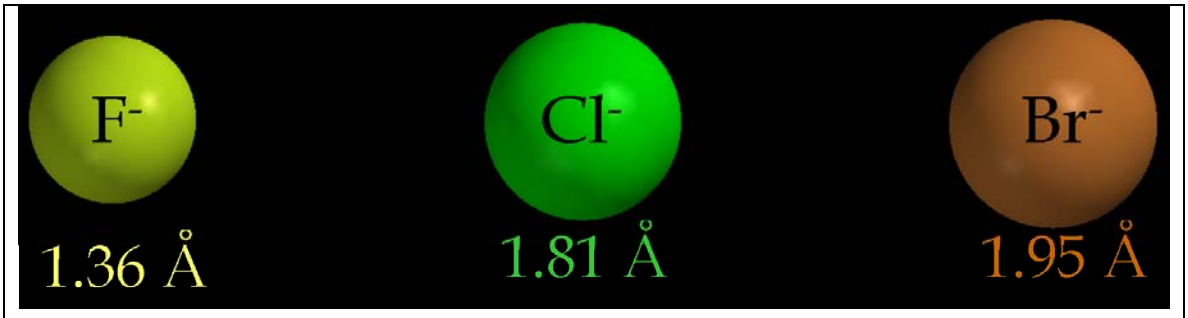

Figure 5. 2 Ionic radii for F^-, Cl^- and Br^-

Gas phase calculations were performed using both **Pyr (4)** and **Iso (6)** either by themselves or when binding F^-, Cl^-, or Br^-. The results are shown in pictorial form in Figure 5.3.

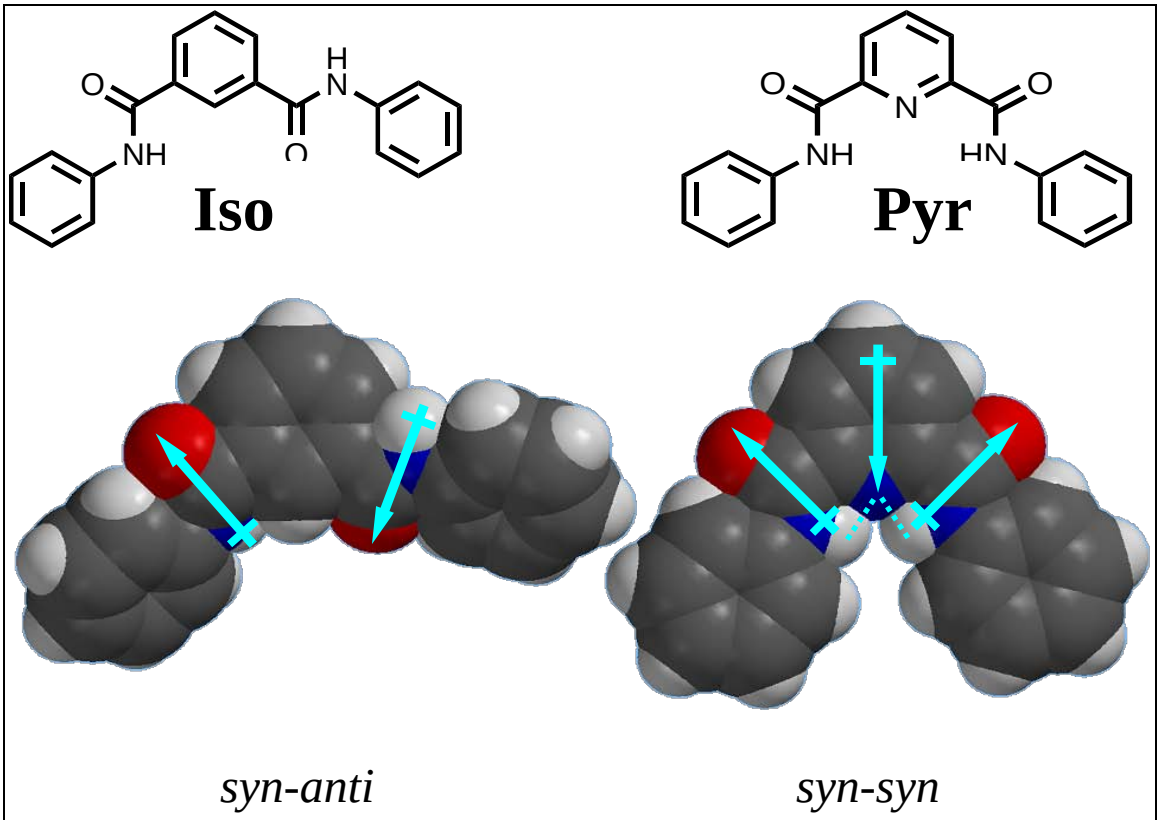

Figure 5. 3. Conformation of unsubstituted isophthalamides (left) and dipicolinamides (right).

The computational studies suggest that hosts **Pyr** and **Iso** exist in different conformations in the absence of any guest (see Figure 5.3): **Iso** is in a *syn-anti* conformation while **Pyr** is in a *syn-syn* conformation. For **Iso,** the driving force for attaining the *syn-anti* conformation is minimizing the molecular dipole that arises from the presence of two amidic moieties. In the case of **Pyr,** an additional dipole is contributed by the pyridyl N. There is also the possibility of intramolecular hydrogen bonding between the pyridyl N and the amidic NH bonds in the **Pyr** host. The result of these interactions is a *syn-syn* conformation.

The gas phase calculations of host–anion adducts were used to estimate the distance between the anion and the amidic N (in yellow in Figure 5.4), the angle that the anion and the central arene form (pink), the torsion angle of the side-arms (green) and the host-guest binding energies.

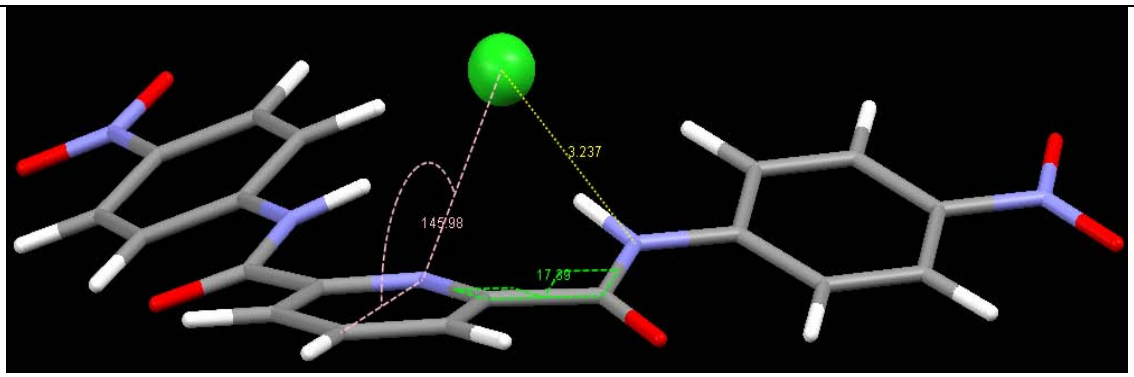

Figure 5. 4 The method of data collection used for gas phase calculations.

Both **Pyr** and **Iso** bind Cl^- in a similar manner (exemplified by **Iso** in Figure 5.5). The calculations show that Cl^- resides above the plane of the central arene at a 148º angle. The two sidearms are rotated to minimize the distance between the amidic protons and the anion. The dihedral angle between the central benzene ring and the side-arms is 23º and the distance between Cl^- and the amidic N is 3.29Å.

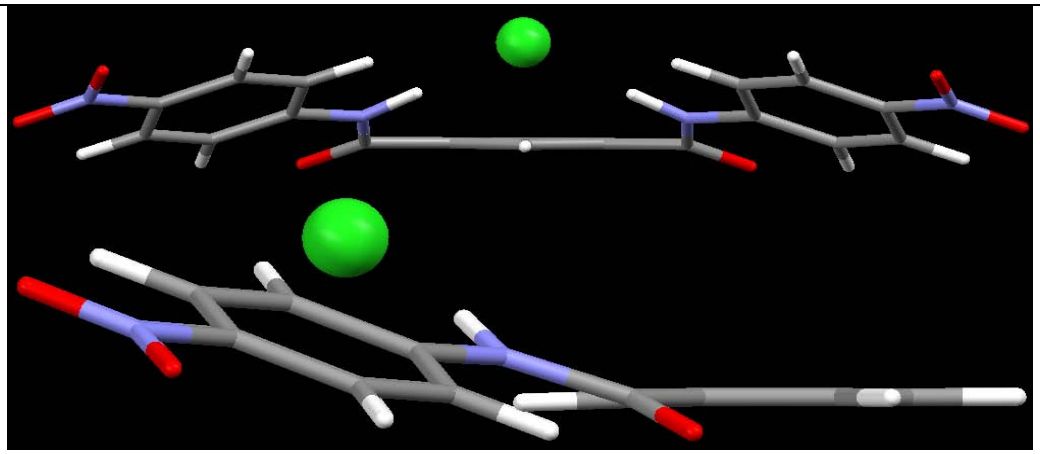

Figure 5. 5 Host **Iso** binding Cl^-

The results of gas phase calculations for hosts **Pyr** and **Iso** binding F^- are shown in Figures 5.6 and 5.7.

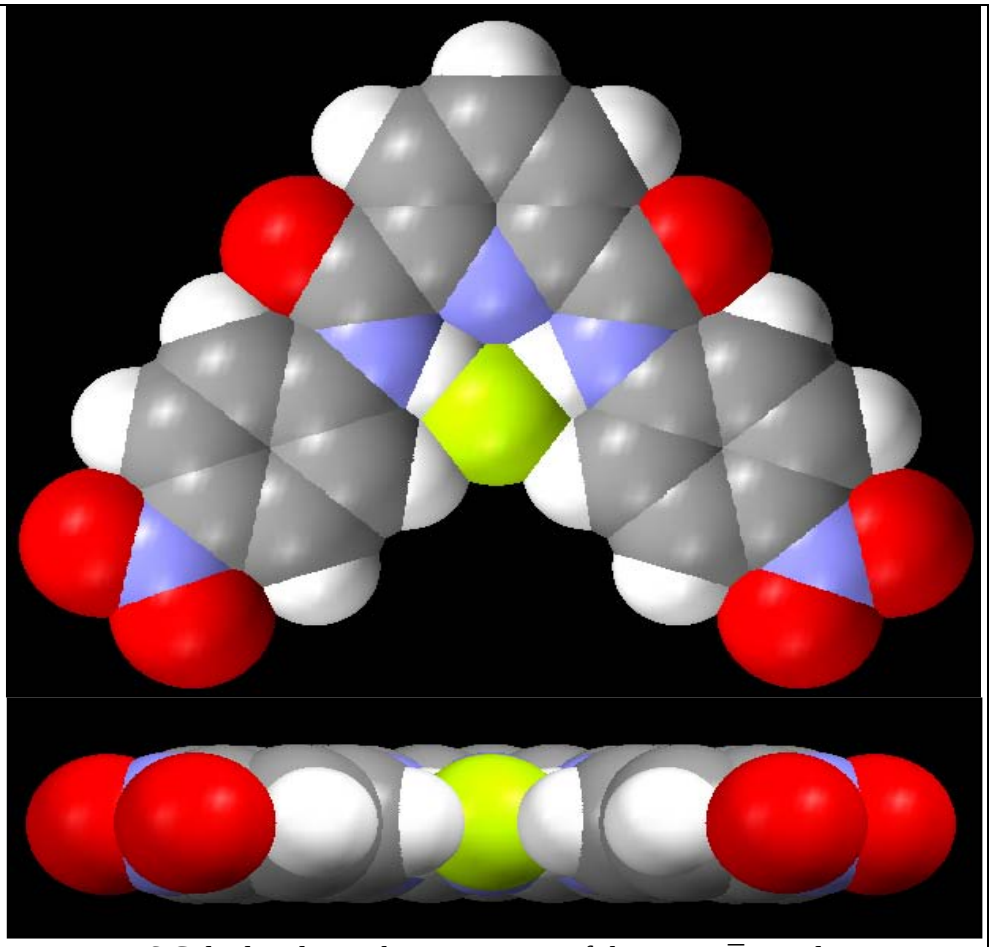

Figure 5. 6 Calculated gas phase structure of the Pyr+F^-complex.

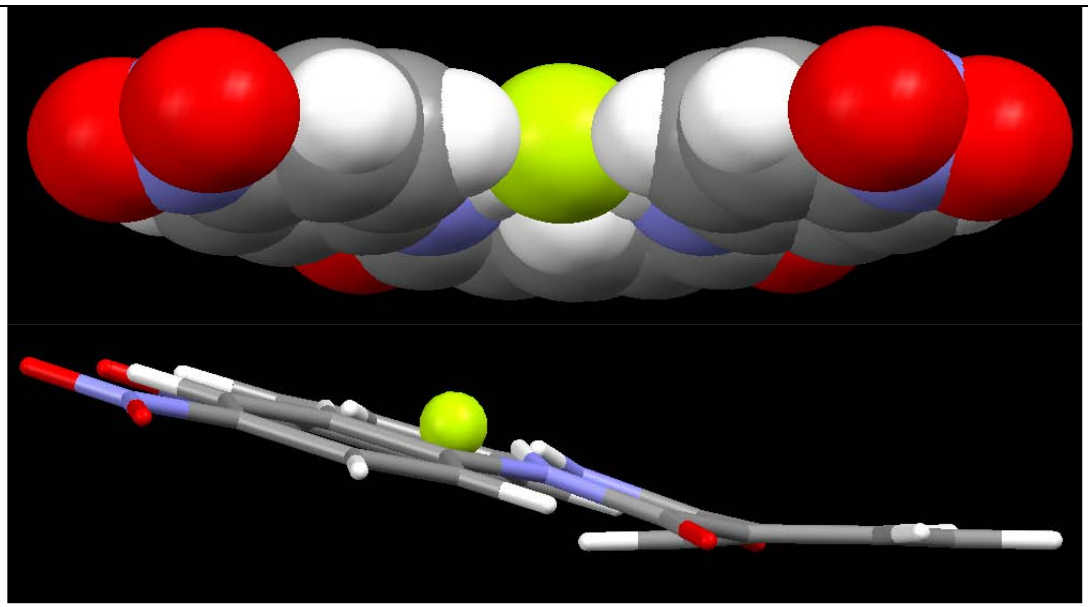

Figure 5. 7 Calculated gas phase structure of the **Iso**+F^-.

Data are not shown here for the analogous Br^- adducts, but they exhibit similar conformations when binding Cl^-.

The calculated data for all six [**host**-X^-] adducts are summarized in Table 5.1.

Table 5. 1. Computational data collected for adducts of **Pyr** and **Iso** with halogenated anions (F^-, Cl^-, and Br^-). All experiments were performed at the DFT level of theory.

Adduct	*X^- - amidic N distance (Å)*	*Central arene – X^- angle (º)*	*Side-arm torsion (º)*	*[Host-X^-] Kcal/mol*
[**Pyr**+F^-]	2.58	178	1	-123
[**Pyr**+Cl^-]	3.23	146	17	-37
[**Pyr**+Br^-]	3.45	142	18	-41
[**Iso**+F^-]	2.66	154	18	-132
[**Iso**+Cl^-]	3.29	148	23	-42
[**Iso**+Br^-]	3.47	144	25	-51

In the series of adducts formed by **Pyr**, the selectivity (F^->Cl^->Br^-) can be explained based on differences in hydrogen bond length, the angle that the anion forms with the plane of the central arene, and side-arm torsion. Both the hydrogen bond distance and the side-arm torsion increase with increasing atomic mass of the complexed anion. Concurrently the angle formed by the anion and the central arene decreases, meaning the respective anion resides higher above the plane of the molecule. These three changes result in weaker bonding interactions and a corresponding decrease in anion selectivity.

An analysis of this series using the same parameters as above (H-bond length, angles and side-arm torsion) shows that the situation is similar for the series of adducts that host **Iso** forms with halide ions. F^- is the preferred anion followed by Cl^- and Br^-.

An interesting conformation is exhibited by the [**Pyr**-F^-] adduct (Figure 5.6). In this case the anion resides in the same plane as the central arene. There is very little twisting of the two side-arms (~1º) and this lack of rotation results in less disruption of the conjugation with the amide bond. At the same time the pre-existing hydrogen bonds between the amidic NH and the pyridyl N are not disturbed, further favoring the planar conformation. Also the smaller ionic radii of F^- (1.33Å) and the fact that **Pyr** has a nitrogen atom instead of an CH in the 1 position makes accommodating the anion in the planar conformation possible.

The [**Iso**-F^-] adduct (Figure 5.7) has different structural characteristics. The F^- ion resides above the plane of the central arene at an angle of 154º. The two side-arms are twisted with the N-H bonds pointing towards the F^- at an angle of 18º and the distance between F^- and the amidic N is 2.66Å. So in a direct experiment with **Pyr** and **Iso**

competing for F^- we would probably see more of the [**Pyr**+F^-] forming than the **Iso** analog. This is most likely due to the presence of the extra hydrogen atom in the binding cleft of **Iso** that occupies part of the space that F^- would require and pushes the anion out of the plane, resulting in partial disruption of conjugation.

The Cl^- complexes of both **Pyr** and **Iso** are similar. The only notable difference is seen in the side-arm torsion angles: 17º for **Pyr** and 23º for **Iso**. The difference is probably caused by the hydrogen bonding that exists between the amidic NH and the pyridyl N. The existence of these two hydrogen bonds makes the system less prone to twisting, hence the smaller torsion angle. These data suggests that in a direct comparison experiment, both hosts would exhibit similar complexation modes. A similar conclusion can be drawn for the bromide adducts.

Electrospray mass spectrometry experiments

Solutions of hosts **Pyr** and **Iso** (0.5 mM) in 10% DMSO/MeOH were prepared along with solutions of tetrabutylammonium fluoride, chloride, and bromide in MeOH. Aliquots from solutions of one host and two competing anions were mixed to yield a final concentration of host equal to 4.5 μM with a ratio of host to anions that is usually 1:10:10 (exceptions are discussed below). This mixture was injected in the ES-MS instrument and the resulting spectra were collected.

The resulting peaks were analyzed as follows: the intensity of every peak is normalized to the most intense peak (the base peak) which is set to an arbitrary value of 100. The intensities of each peak are proportional to the amount of anion adduct that is formed. The hypothesis is that the more anion adduct that is formed, the stronger must be

the bond between X^- and the host. The peak intensities for monomers and the dimers (either homodimers or heterodimers) of a certain anion are summed and the composite values are used to determine the ratios between various anion adducts. The resulting ratios establish rankings of binding strength among anions. These rankings provide us with information on the selectivity of a certain host for various anions.[19]

Control experiments

A) ES-MS response to **Pyr** and **Iso**

Experiments were preformed that directly compare adducts formed by the two hosts and one anion. Solutions of hosts **Pyr** and **Iso** (0.5 mM) in 10% DMSO/MeOH were prepared along with solutions of tetrabutylammonium chloride in MeOH. Aliquots from solutions of the two competing hosts and Cl^- were mixed to yield a final concentration of host equal to 4.5 μM with a ratio of **Iso**:**Pyr**:Cl^- of 1:1:10. This mixture was injected in the ES-MS instrument and the resulting spectra were collected. The mass spectral peak intensities, obtained from these experiments for [**Iso**+Cl^-]/[**Pyr**+Cl^-], gave a ratio of 1.3:1 (three replicates). Thus, the behavior of the hosts is similar but not identical. A limitation of this approach is the fact that the molecular weights of **Iso** and **Pyr** differ by only one atomic mass unit. Thus, complexes formed with these two hosts and the same anion were difficult to distinguish (*i.e.* the peaks in the ES-MS spectra overlap). When selectivities observed in subsequent experiments differed by only 30%, they were interpreted as being the same within experimental error. However, most selectivity or partition ratios were well outside 30%.

B) Partitioning of **Pyr** and **Iso** between deprotonation and complexation

The tendency of the two hosts to form adducts or deprotonate has been studied using ES-MS experiments. For this particular series of experiments solutions of hosts **Pyr** and **Iso** (0.5 mM) in 10% DMSO/MeOH were prepared along with solutions of tetrabutylammonium fluoride and chloride in MeOH. Aliquots from solutions of the host and the studied anion were mixed to yield a final concentration of host equal to 4.5 μM. The binding/deprotonation behavior was studied at host:anion ratios of 1:1 and 1:10. The mixture (host:Bu_4NX or host:10 Bu_4NX) was injected into the ES-MS instrument, the resulting spectra were collected, and the ratios between [**Host**+X^-] / [**Host**-H]$^-$ were determined. These ratios are presented in Table 5.2 for **Pyr** and Table 5.3 for **Iso**.

Table 5.2 Host single anion control experiments for **Pyr**

Host[a]	*Anion*[b]	*Host-X*$^-$ *ratios*	*[Host-X*$^-$*] / [Host-H]*$^-$	*% Interaction*	
				Binding%	*Deprotonation%*
Pyr	F^-	1:1	2.4:1	70	30
Pyr	F^-	1:10	0.42:1	30	70
Pyr	Cl^-	1:1	17.2:1	94	6
Pyr	Cl^-	1:10	5.5:1	85	15

[a]Stock [**Host**]=0.5 mM in 10% DMSO/MeOH; Final [**Host**]=4.5 μM in 0.5% DMSO/MeOH. [b]Stock [TBAX]=1 mM in MeOH

Table 5.3 Host single anion control experiments for Iso

Host[a]	*Anion*[b]	*Host-X*$^-$ *ratios*	*[Host-X*$^-$*] / [Host-H]*$^-$	*% Interaction*	
				Binding%	*Deprotonation%*
Iso	F^-	1:1	3.1:1	75	25
Iso	F^-	1:10	0.2:1	17	83
Iso	Cl^-	1:1	21.3:1	96	4
Iso	Cl^-	1:10	15.6:1	94	6

[a]Stock [**Host**]=0.5 mM in 10% DMSO/MeOH; Final [**Host**]=4.5 μM in 0.5% DMSO/MeOH. [b]Stock [TBAX]=1 mM in MeOH

At least two things can be inferred from the data presented in Tables 5.2 and 5.3, above. First, at a host:F^- ratio of 1:1 the ability of F^- to deprotonate either **Iso** or **Pyr** is similar. Although pyridine is more electron poor than benzene, the nitroaniline components of each diamide likely dominate the dissociation. The first and second dissociation constants for isophthalic acid are 3.5 and 4.6, respectively. The corresponding values for dipicolinic acid are 2.2 and 4.8.[21] The difference in pK_1 for the acids is a little more than a power of ten. This difference is likely to be reduced for the diamides. Thus, **Pyr** shows approximately 30% deprotonation in the presence of one equivalent of F^- compared to 25% by **Iso**.

Second, in the presence of a 10-fold excess of F^-, deprotonation of **Iso** is greater than deprotonation of **Pyr**, although it is the dominant process in both cases. The **Pyr** host is likely more acidic than **Iso**, but removal of a proton from **Pyr** leaves two adjacent lone pairs (deprotonated amide and pyridyl nitrogen lone pair). This is obviously

unfavorable but the difference in the two values may well be within the error of the experiment.

The deprotonation reaction is clearly undesirable in terms of complexation. First, it depletes the pool of host available for binding, leaving less host available to bind with anions. In this way the selectivity measurements reflect what happens only to some of the host and not to the majority of the host. Second, a deprotonated host has a negative charge in the anion binding cleft. A negative charge can only have a repelling interaction with an anion.

The data in tables 5.2 and 5.3 show that Cl^- prefers anion binding over deprotonation. Very little deprotonation occurs either if Cl^- is present in a 1:1 ratio (94-96% binding) or 1:10 ratio (85-94% binding). The higher percent of binding that occurs for **Iso** when compared to **Pyr** can be explained by the higher acidity of the amidic protons of **Pyr** caused by the internal hydrogen bonding that causes slightly more deprotonation to occur. On the other hand F^- shows 70-75% binding at a 1:1 ratio and 17-30% binding at a 1:10 ratio. If we compare these numbers, either at a 1:1 or at a 1:10 molar ratios, in either case the propensity for deprotonation for F^- is superior to that of Cl^- by a significant margin. Hence in a direct experiment with F^- and Cl^- we can expect that the deprotonation reaction can be attributed mostly to F^-.

The ES-MS control experiments show that F^- deprotonates the two hosts more than Cl^-. So even if a stronger binding interaction is expected to occur in the host-F^- complex than in the Cl^- or Br^- analogs this cannot be directly quantified and translated into the predicted complexation order of $F^->Cl^->Br^-$ within our set of conditions due to the competition from the deprotonation process.

C) UV-vis controls

In our analysis of the UV-vis properties of these compounds we tried to assign the peaks to the anion adduct and the deprotonated host respectively. To observe the UV-vis properties of the fully deprotonated host we added excess DMSO solution of a strong base: dimsyl sodium (pK_a of DMSO is 35 making dimsyl sodium a very strong base) and recorded the UV-vis spectrum in DMSO. The resulting spectrum is presented in Figure 5.8.

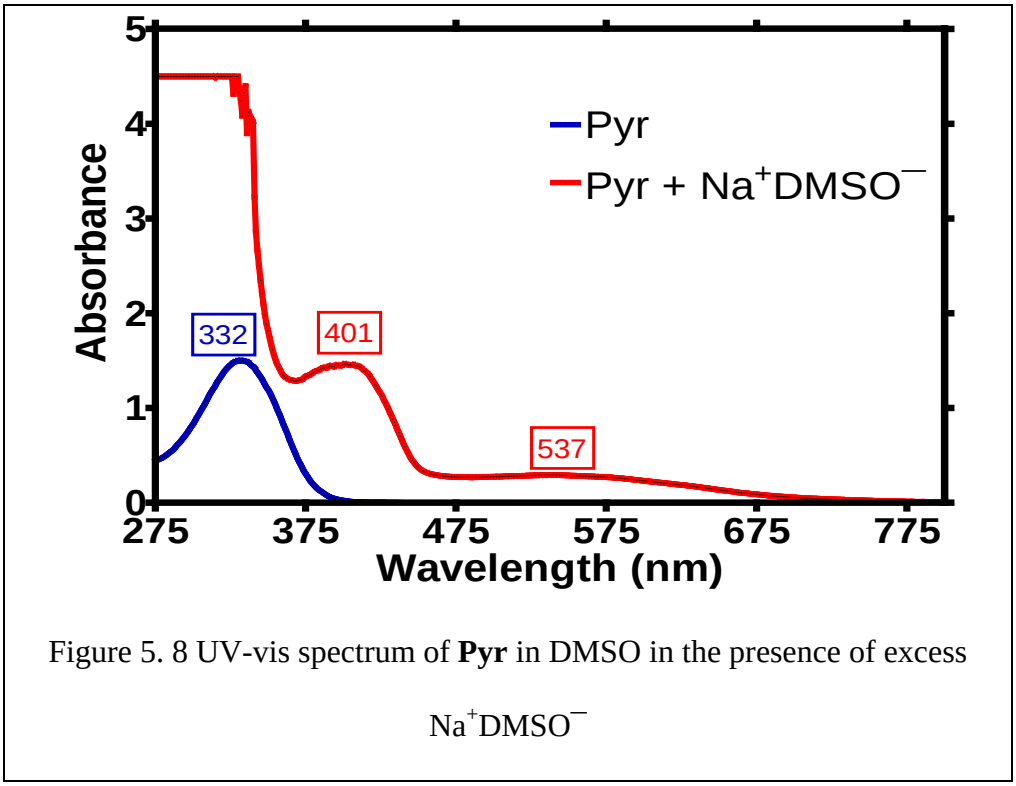

Figure 5. 8 UV-vis spectrum of **Pyr** in DMSO in the presence of excess Na^+DMSO^-

There are significant changes between the two traces. The blue trace that contains only **Pyr** has a λ_{max} at 332 nm. The red trace that contains **Pyr** and dimsyl sodium has a maximum at 401 nm which probably pertains to the doubly deptotonated host.

In a different UV-vis experiment ran in EtOAc, in which 1 equivalent of **Pyr** is exposed to 10 equivalents of TBAF (Figure 5.9) a maximum at 343 nm is apparent which most likely corresponds to the single deprotonated host.

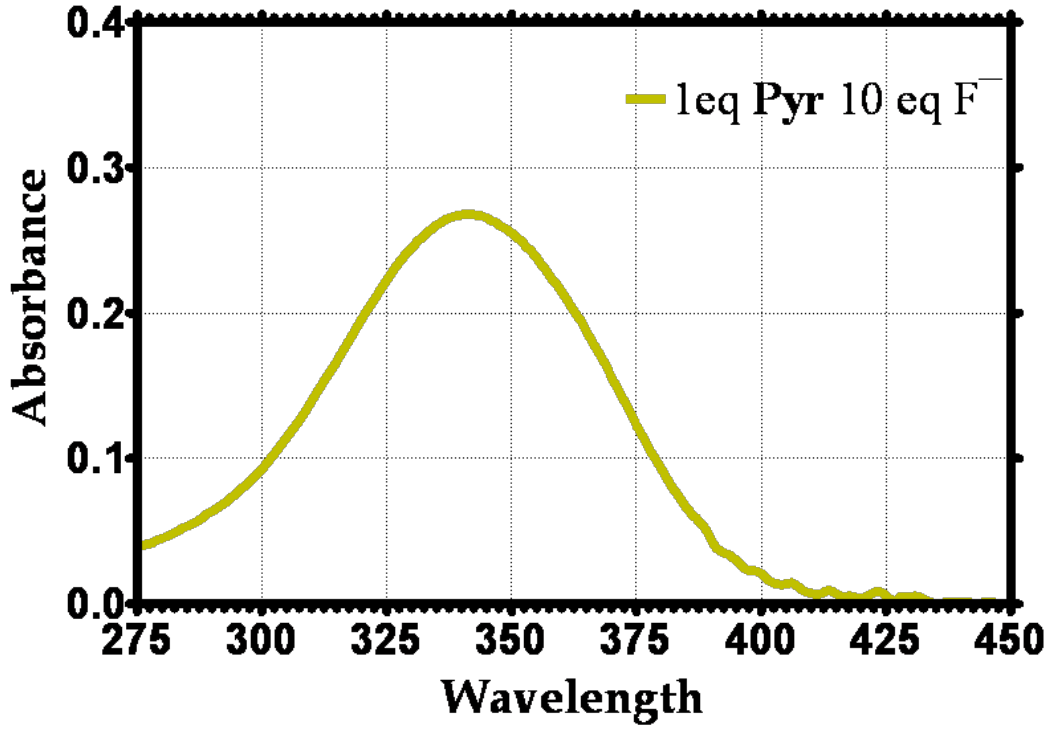

Figure 5. 9 UV-Vis traces in EtOAc for 1 eq **Pyr** and 10 eq F^-. Final [**Pyr**]=33 µM.

Titration of **Pyr** with TBACl

UV-vis titration of **Pyr** with TBACl resulted in the graph presented in Figure 5.10. 1 mL of a 1 mM solution of **Pyr** in DMSO was added to 2 mL of EtOAc and the resulting solution was titrated with aliquots of a 1 mM DMSO solution of TBACl to yield the molar ratios presented in Figure 5.10.

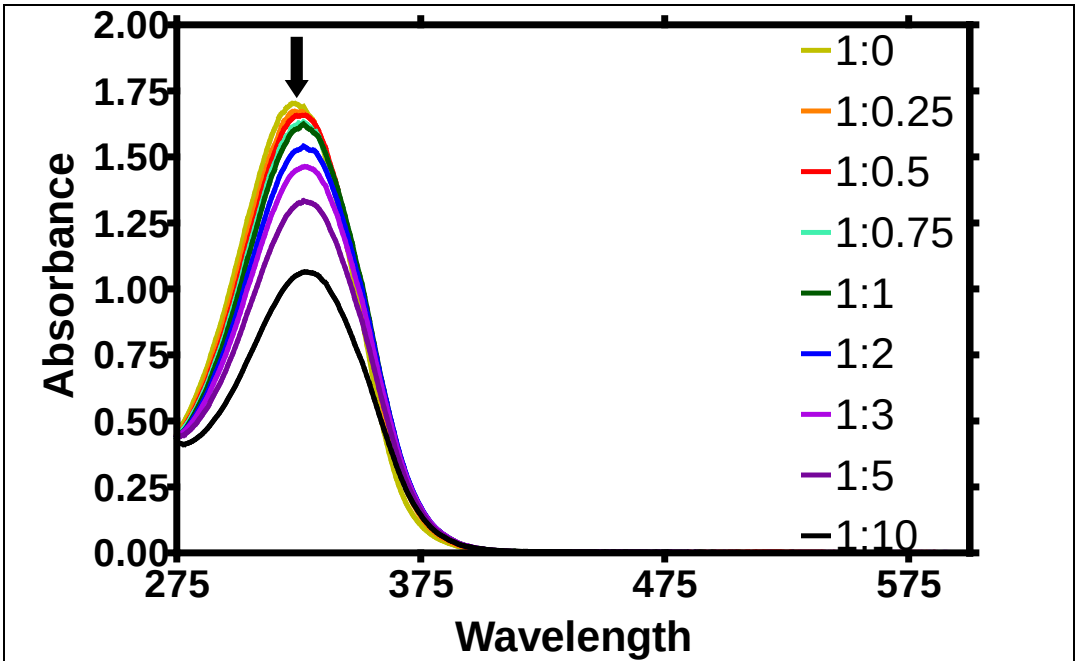

Figure 5. 10 UV-vis titration of **Pyr** with Cl^-

The λ_{max} changes from 322 nm (yellow trace) to 332 nm (black trace). Also the intensity of the traces is diminishing as we titrate due to dilution. No isosbestic point or other absorption bands are observed. This data along with the ES-MS study that showed 84-94% Cl^- binding going from mixtures containing the host:Cl^- in a 1:1 ratio to 1:10 ratio indicate the prevalence of binding over deprotonation in this experiment.

Results

Anion selectivity data for the **Pyr** and **Iso** hosts with halogenated anions, obtained by the ES-MS method, are summarized in Table 5.4. Each value presented is the average of at least three trials. Solutions of hosts **Pyr** and **Iso** (0.5 mM) in 10% DMSO/MeOH were prepared along with solutions of tetrabutylammonium fluoride, chloride, and bromide in MeOH. Aliquots from solutions of one host and two competing anions were mixed to yield a final concentration of host equal to 4.5 μM with a ratio of host to anions

of 1:10:10. This mixture was injected in the ES-MS instrument and the resulting spectra were collected and the ratios between the two different anion adducts were determined.

Table 5. 4. Anion selectivity for hosts **Pyr** and **Iso** with halide ions.

Host[a]	*[Host+Cl⁻[b]]/ [Host+F⁻[b]]*	*[Host+Cl⁻]/ Host+Br⁻[b]]*	*[Host+F⁻]/ [Host+Br⁻]*
Pyr	0.35 ± 0.1	6.7 ± 0.4	11.5 ± 3
Iso	3.5 ± 1.2	6.9 ± 1	1.1 ± 0.1

[a]Stock [**Host**]=0.5 mM in 10% DMSO/MeOH; Final [**Host**]=4.5 μM in 0.5% DMSO/MeOH. [b]Stock [TBAX]=1 mM in MeOH

The data presented in Table 5.4 (column 3) show that both **Pyr** and **Iso** hosts are selective for Cl^- over Br^- by ~7 to 1. The situation changes when F^- and Cl^- are used as competing anions: **Iso** prefers Cl^- over F^- by 3.5 to 1, while in the case of **Pyr,** F^- is the preferred anion by a ratio of ~ 3 to 1.

The results of the F^- *vs* Br^- comparisons are in line with the F^- *vs* Cl^- and Br^- *vs* Cl^- experiments. **Pyr** binds F^- more strongly than it binds Br^- by a factor of about 12 to 1. Considering that **Pyr** prefers F^- over Cl^- (~3 to 1) and at the same time **Pyr** prefers Cl^- over Br^- by about 7 to 1, 12 to 1 seems to be a reasonable number. Likewise, **Iso** prefers Cl^- over F^- by about 4 to 1 and Cl^- over Br^- by about 7 to 1 so a ratio of F^- vs Br^- of about 1.1 seems sensible.

The data presented in Table 5.4 show different selectivity trends for hosts **Pyr** and **Iso**. For host **Pyr** the selectivity is $F^- > Cl^- > Br^-$ while for host **Iso** is $Cl^- > F^- > Br^-$. The selectivity trend for **Iso** differs from the predicted results. The contradiction between the expectation and the observations impelled a reexamination of the ES-MS data

collected. The most significant difference observed in the ES-MS experiments involved those in which F^- was present. In most experiments that have F^- as one of the competing anions the base peak corresponds to the deprotonated host and not to one of the anion adducts. This means that the majority of host is not available to form an anion adduct. We inferred that the selectivity trends determined in these experiments were not reliable. A search of the literature revealed reports of F^- behaving as a base rather than as a guest.[22]

To examine the selectivity trend for **Pyr** in a set of conditions where binding was favored over deprotonation a series of ES-MS experiments was conducted in which the molar ratios of anions to host were varied. We started with the same conditions used previously (host : anion molar ratios 1:10:10 in 0.5%DMSO/MeOH) and gradually reduced the molar ratios of the anions while keeping the concentration of host constant. We examined the binding/deprotonation equilibrium at host : anion molar ratios of 1:5:5, 1:3:3 and 1:1:1. For each of these experimental conditions we determined the ratio of the Cl^- adduct to the F^- adduct. The results that were obtained are shown in Table 5.5.

Table 5. 5. Base peak and selectivity ratios for **Pyr** at various anion molar ratios.

Molar Ratio **Pyr**[a] *: Cl^-[b] : F^-[b]*	*[**Pyr** + Cl^-] / [**Pyr** + F^-]*	*Base Peak M/z*	*Base peak identity*
1 : 1 : 1	4.3 ± 1.1	441 [**Pyr** + Cl^-]	Chloride adduct
1 : 3 : 3	1.8 ± 0.7	405 [**Pyr**-H]$^-$	Deprotonated host
1 : 5 : 5	1.2 ± 0.3	405 [**Pyr**-H]$^-$	Deprotonated host
1 : 10 : 10	0.4 ± 0.1	405 [**Pyr**-H]$^-$	Deprotonated host

[a]Stock [**Host**]=0.5 mM in 10%DMSO/MeOH; Final [**Host**]=4.5 μM in 0.5%DMSO/MeOH. [b]Stock [TBAX]=1 mM in MeOH

The data in Table 5.5 show that at high anion molar ratios (10:1, 5:1 and 3:1) the base peak was the deprotonated host. At a molar ratio of **Pyr** : Cl^-: F^- = 1 : 1 : 1 the base peak was an anion adduct indicating that the majority of the host is involved in complexation reactions. In this set of experimental conditions the complexation preference of **Pyr** is indeed $Cl^- > F^- > Br^-$, similar to the one for **Iso**.

Having established the apparent halide ion selectivities of **Pyr** and **Iso**, it was of obvious interest to more closely examine the two competing processes: binding and deprotonation. Closer examination of ES-MS spectra with the goal of quantifying both deprotonation (represented by how much deprotonated host is present) and binding (represented by how much of the anion adducts are present) yielded the ratios presented in Table 5.6 (one host in the presence of one anion) and Table 5.7 (one host with two competing anions).

Table 5. 6. Binding / deprotonation ratio for **Pyr** and **Iso** in the presence of one anion.

Host[a]	*Anion*[b]	*Molar ratio Host : A^-*	*Base peak M/z*	*Major process*	*Binding/ Deprotonation*
Pyr	F^-	1:10	405[**Pyr**-H]$^-$	Deprotonation	0.42:1
Iso	F^-	1:10	404[**Iso**-H]$^-$	Deprotonation	0.2:1
Pyr	Cl^-	1:10	441[**Pyr** +Cl^-]	Binding	5.5:1
Iso	Cl	1:10	440[**Iso** + Cl^-]	Binding	15.6:1
Pyr	Br^-	1:10	485[**Iso** + Br^-]	Binding	5.8:1
Iso	Br^-	1:10	484[**Iso** + Br^-]	Binding	9.0:1

[a]Stock [**Host**]=0.5 mM in 10%DMSO/MeOH; Final [**Host**]=4.5 µM in 0.5%DMSO/MeOH. [b]Stock [TBAX]=1 mM in MeOH

To determine the binding/deprotonation ratios the peak intensities of the anion adducts (monomers and dimers) were summed and divided by the sum of the peak intensities corresponding to the deprotonated host (monomers and dimers).

Table 5. 7. Binding/deprotonation ratio for **Pyr** and **Iso** in the presence of two competing anions.

Host[a]	*Anion 1(A_1)*[b]	*Anion 2 (A_2)*[b]	*Molar ratio Host:A_1:A_2*	*Overall Binding/ Deprotonation*	*Major process*	*Selectivity A_1/A_2*
Pyr	F^-	Cl^-	1:10:10	0.17	Deprotonation	2.8
Pyr	F^-	Cl^-	1:5:5	1.38	Binding	0.83
Pyr	F^-	Cl^-	1.3:3	1.51	Binding	0.55
Pyr	F^-	Cl^-	1:1:1	3.49	Binding	0.23
Pyr	Cl^-	Br^-	1:10:10	1.51	Binding	6.7
Pyr	F^-	Br^-	1:10:10	0.2	Deprotonation	11.5
Iso	F^-	Cl^-	1:10:10	2.56	Binding	0.28
Iso	Cl^-	Br^-	1:10:10	1.51	Binding	6.9
Iso	F^-	Br^-	1:10:10	0.92	Deprotonation	1.1

[a]Stock [**Host**]=0.5 mM in 10% DMSO/MeOH; Final [**Host**]=4.5 μM in 0.5% DMSO/MeOH. [b]Stock [TBAX]=1 mM in MeOH

To determine the overall binding/deprotonation ratios the peak intensities of the anion adducts (monomers and dimers) corresponding to both anions were summed and divided by the sum of the peak intensities corresponding to the deprotonated host (monomers and dimers). The selectivity between anions (A_1/A_2 in table 5.7) was

determined by dividing the sum of the peak intensities corresponding to A_1 by the sum of the peak intensities corresponding to A_2.

For both hosts, anion binding is favored for Cl^- and Br^-, whereas F^- acts primarily as a base in these control experiments. The binding/deprotonation ratio is higher for **Iso** than for **Pyr** when comparing experiments with the same anions, presumably due to the higher acidity of **Pyr**'s amidic protons.

Molar ratios of host : F^- = 1:10 result in an overall net preference for deprotonation. Lowering the host:F^- molar ratios to 1:5, 1:3 and 1:1 promotes complexation. Deprotonation events are inimical to complexation studies as they result in a skewed selectivity ratio.

The ratio in which these two competing processes (binding and deprotonation) interact and what is their dynamic for various anions merited further exploration. This was done in a series of experiments described below.

NMR titration experiments

The first experiment was an ^{1}H-NMR titration in DMSO-d_6 in which one equivalent of **Pyr** was titrated with increasing quantities of tetrabutylammonium fluoride (TBAF). Solutions of the receptor molecule in DMSO-d_6 were prepared at a concentration of 1 mM. A 1 mL solution thus prepared was transferred to a glass NMR tube and titrated with aliquots from a 1 mM solution containing the titrant anion as the tetrabuthylammonium salt in DMSO-d_6. The chemical shifts of the NH and aromatic protons were monitored as a function of the number of equivalents of anions added. The ^{1}H-NMR spectrum of **Pyr** is shown in Figure 5.11.

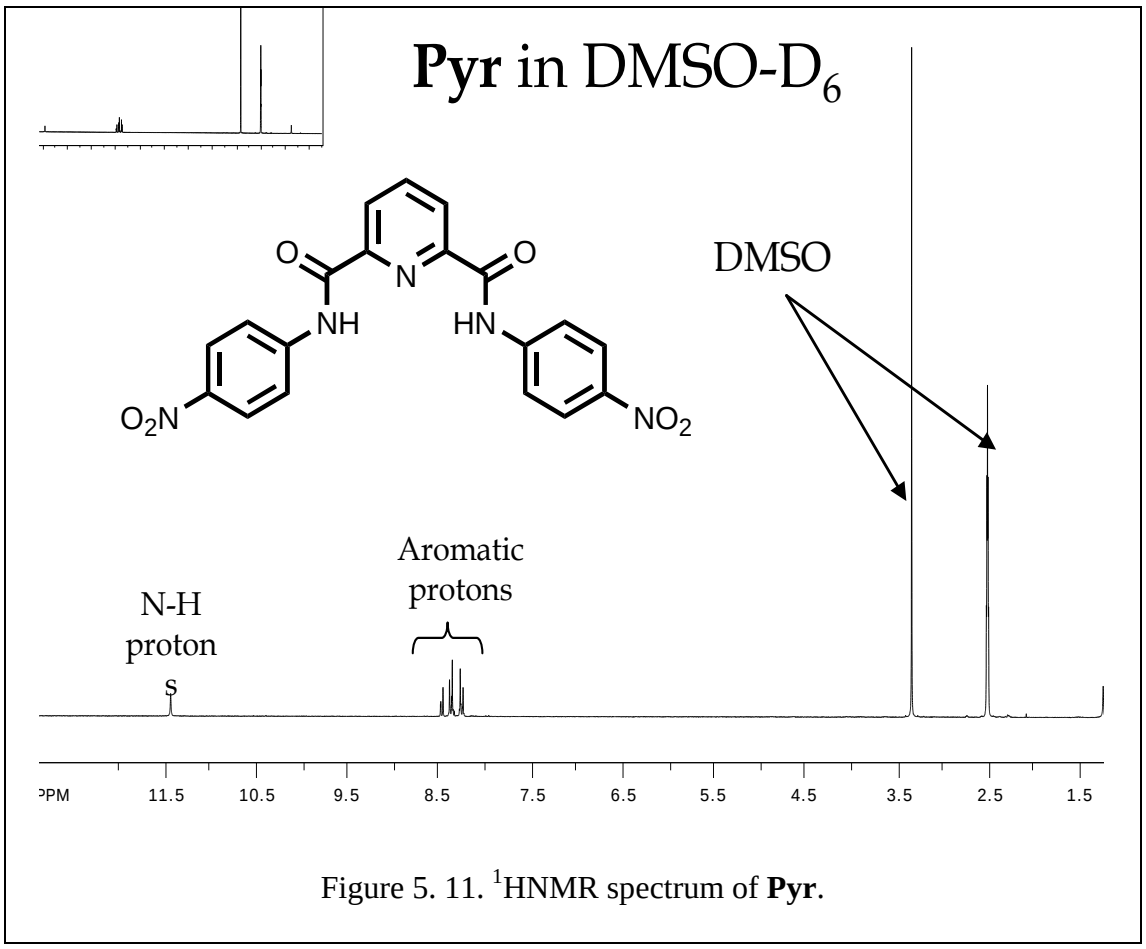

Figure 5. 11. [1]HNMR spectrum of **Pyr**.

An expanded image of the aromatic peaks present in the spectrum and the detailed assignment of aromatic peaks are shown in Figure 5.12.

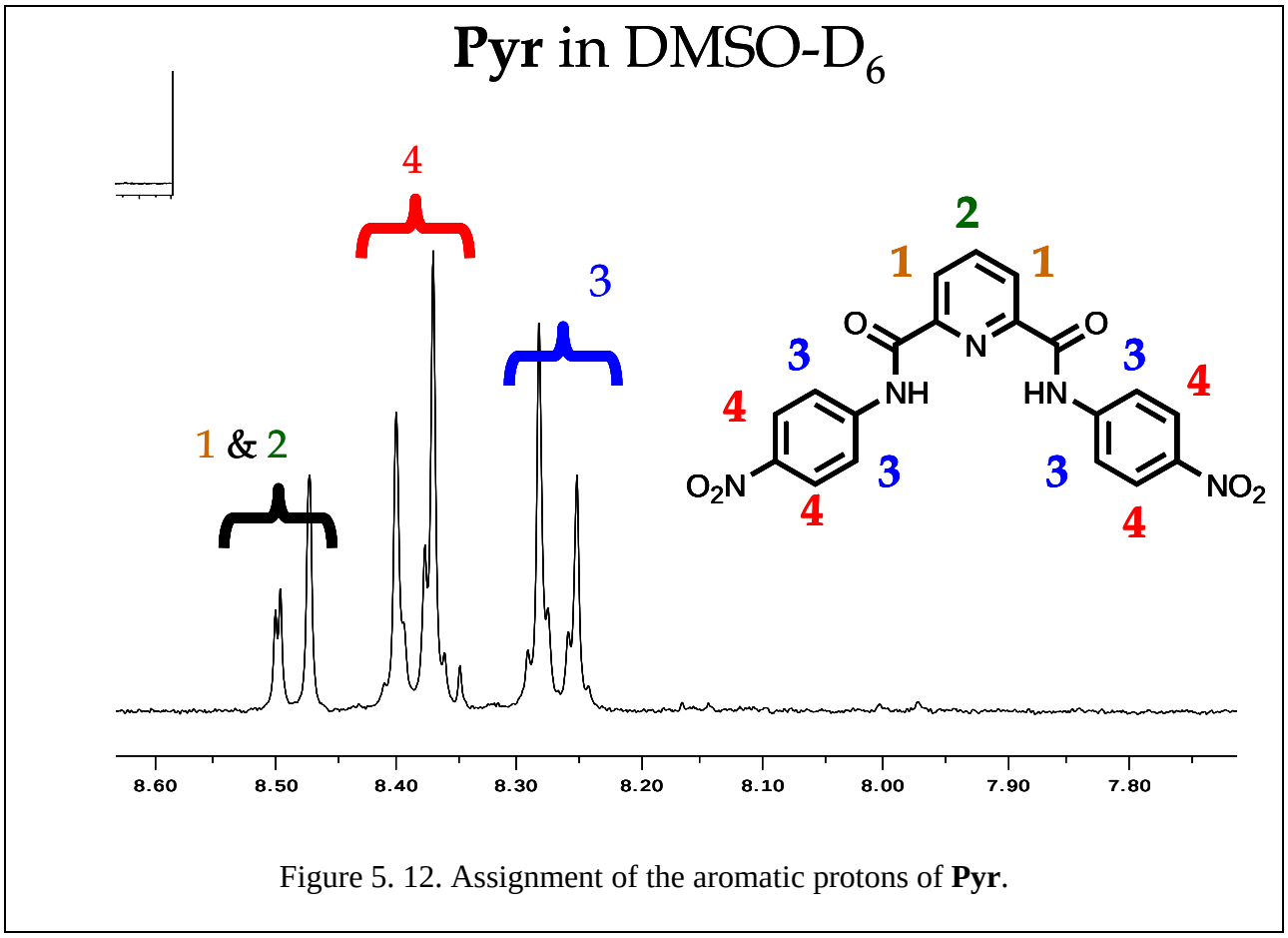

Figure 5. 12. Assignment of the aromatic protons of **Pyr**.

The assignment of the protons in the aromatic region was done using 2D COSY ^{1}H-NMR. The peaks are presented in Figure 5.13. Based on the structure of **Pyr** we should observe interactions between protons 1 and 2 for one and 3 and 4 on the other hand. The peaks at 8.5 ppm only interact with themselves while the other two peaks are interacting between them as well. Based on these interactions and the peak integration we assigned the peaks at 8.5 ppm to protons 1 and 2, the one around 8.4 ppm to protons 4 (which being in the para position to the electron withdrawing $-NO_2$ group they will be more downfield) while the peaks around 8.25 ppm belong to protons 3.

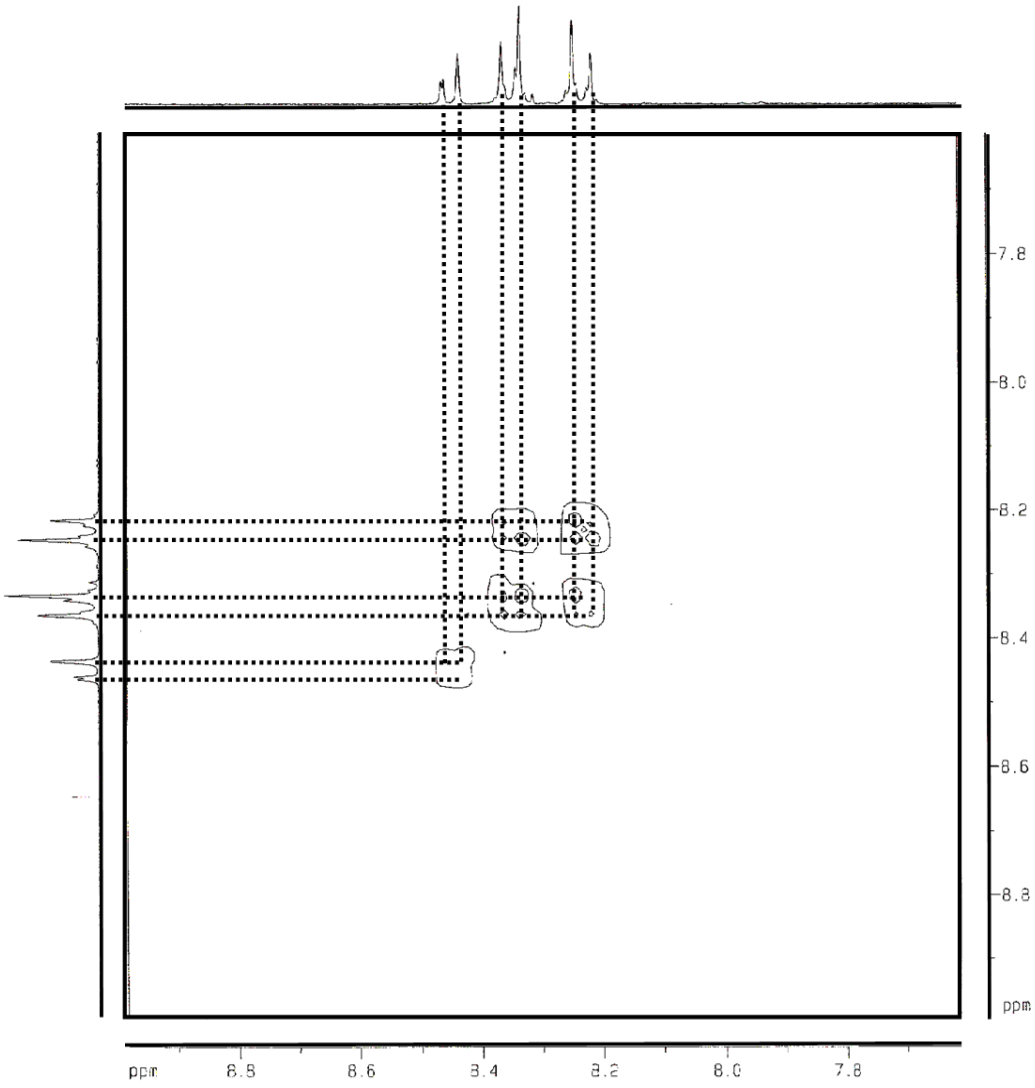

Figure 5. 13. 2D ^{1}HNMR of the aromatic region for **Pyr**.

This ^{1}H-NMR experiment was expected to proceed as follows: if two species (a deprotonated host and an anion adduct) formed after adding the TBAF titrant, the shifts of the protons labeled 3 and 4 in Figure 5.12 should be separated enough to be clearly observed. By comparing the integration of these peaks, we can get a ratio of formation for these two species at different amounts of titrant. Figure 5.14 shows a comparison between the spectra of 1 eq **Pyr** with no titrant and 1 eq **Pyr** with 1 eq TBAF.

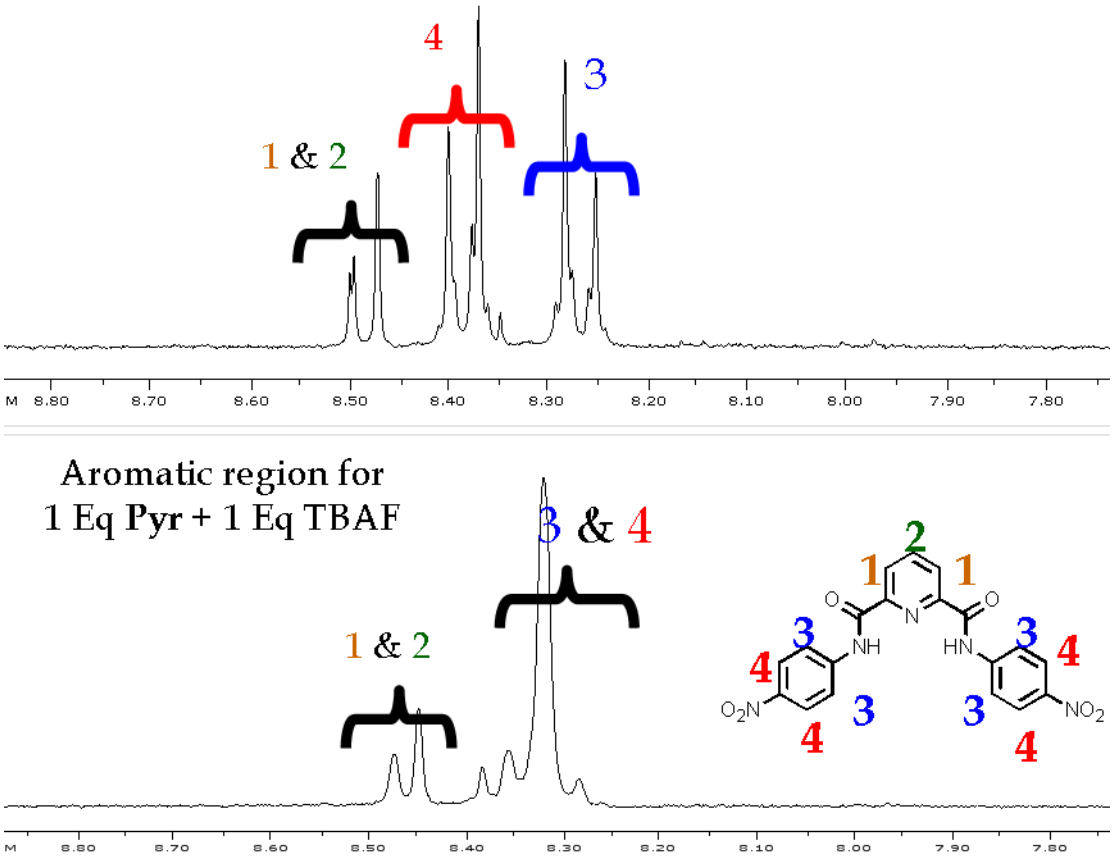

Figure 5. 14. Comparison of the spectra of **Pyr** (top panel) and **Pyr** with 1 eq TBAF (bottom panel).

Figure 5.14 shows the significant changes that occur in the spectrum during the titration experiment. The cluster located near 8.50 ppm (protons 1 and 2) shifts upfield while the peaks assigned to protons 3 and 4 shift and coalesce at about 8.25 ppm. Based on the ES-MS experiments that were conducted at this ratio of titrant, we infer that both deprotonation and binding occur. Thus, the resulting peak cannot pertain to only one of these species, but must reflect a mixture of the two. The high degree of overlap precluded drawing more specific conclusions from this NMR titration experiment.

HPLC studies

In previous studies discussed in chapter 3 of this thesis, HPLC was used to investigate solution equilibria involving closely related species. An HPLC study was undertaken in this case in the expectation that individual species could be resolved and perhaps even quantified. The goal was to deconvolute the "mixture peak" into separate and identifiable peaks that could be assigned either to deprotonated or complexed species.

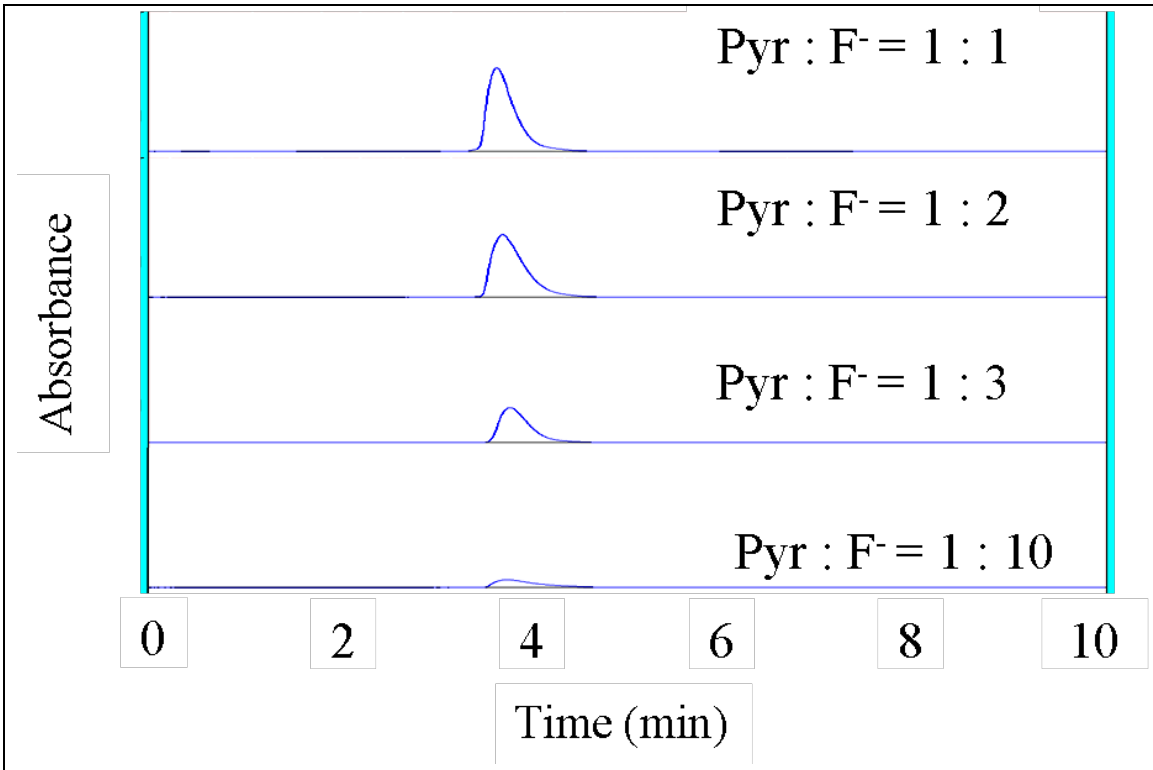

Figure 5. 15. HPLC traces for the titration of **Pyr** with increasing equivalents of TBAF.

In this experiment **Pyr** (1 mM in DMSO) was titrated with TBAF (1 mM in DMSO) in increasing molar ratios. 0.1 mL of **Pyr** solution and aliquots of TBAF solution were mixed separately and the resulting solution was added to 2 mL of EtOAc. The sample prepared in this way was injected into an HPLC having a normal phase silica

column and a UV-vis detector using EtOAc as the mobile phase. The results are recorded in Figure 5.15.

The results presented in Figure 5.15 show that as the amount of TBAF is increased, the intensity of the initial peak diminishes, but there is no change in the peak's elution time. The diminished intensity of the initial peak can be attributed to a dilution effect: as we are titrating we are adding more and more solvent, resulting in a net dilution of the sample.

UV-Vis studies

We performed a series of UV-VIS experiments in which the λ_{max} values were determined for a number of mixtures containing **Pyr** and Cl^- and F^-. Figure 5.16 shows spectra of the initial species. These comprise the baseline for the ensuing studies. The change in λ_{max} was followed for two mixtures: 1 eq **Pyr** and 10 eq Cl^- (green trace in Figure 5.16) and 1 eq of **Pyr** and 10 eq F^- (yellow trace in Figure 5.16).

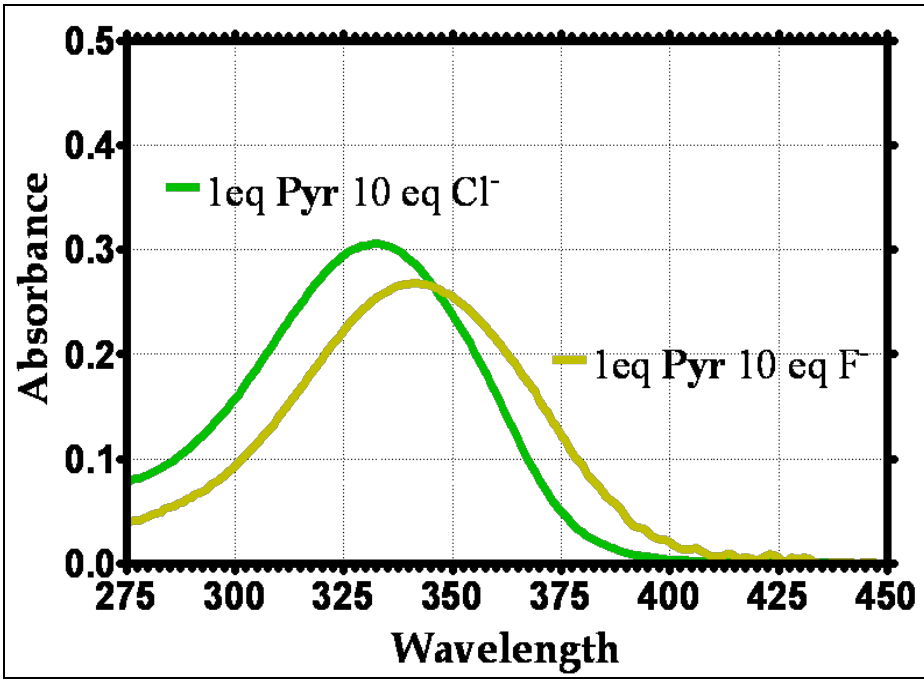

Figure 5. 16. UV-Vis traces in EtOAc for 1 eq **Pyr** with 10 eq Cl^- (green) and 1 eq **Pyr** with 10 eq F^- (yellow). Final [**Pyr**]=33 µM.

1 mM DMSO solutions of **Pyr** and tetrabutylammonium salts of F^- and Cl^- were prepared. 0.1 mL of **Pyr** stock solution was added to 2 mL of EtOAc and the resulting mixture was titrated with aliquots of the stock anion solution, added in the necessary amount to yield the desired molar ratios.

We know from our ES-MS experiments that the "green line" mixture reflects mostly binding and the "yellow line" mixture reflects mostly deprotonation. It is apparent in Figure 5.16 that there is an 11 nm difference in between the maxima of the two traces, reflecting the difference in composition between the two mixtures.

An experiment where 1 eq of **Pyr** was titrated with increasing amounts of TBAF yielded the curves shown in Figure 5.17. 1 mM DMSO solutions of **Pyr** and tetrabutylammonium fluoride were prepared. 0.1 mL of **Pyr** stock solution was added to 2 mL of EtOAc and the resulting mixture was titrated with aliquots of the stock anion solution, added to yield the desired molar ratios.

Comparing the maxima for 1 eq of **Pyr** and 0 eq TBAF (yellow trace) to 1 eq **Pyr** and 10 eq TBAF (blue trace) there is a 21 nm shift (343-322 nm) in the λ_{max}.

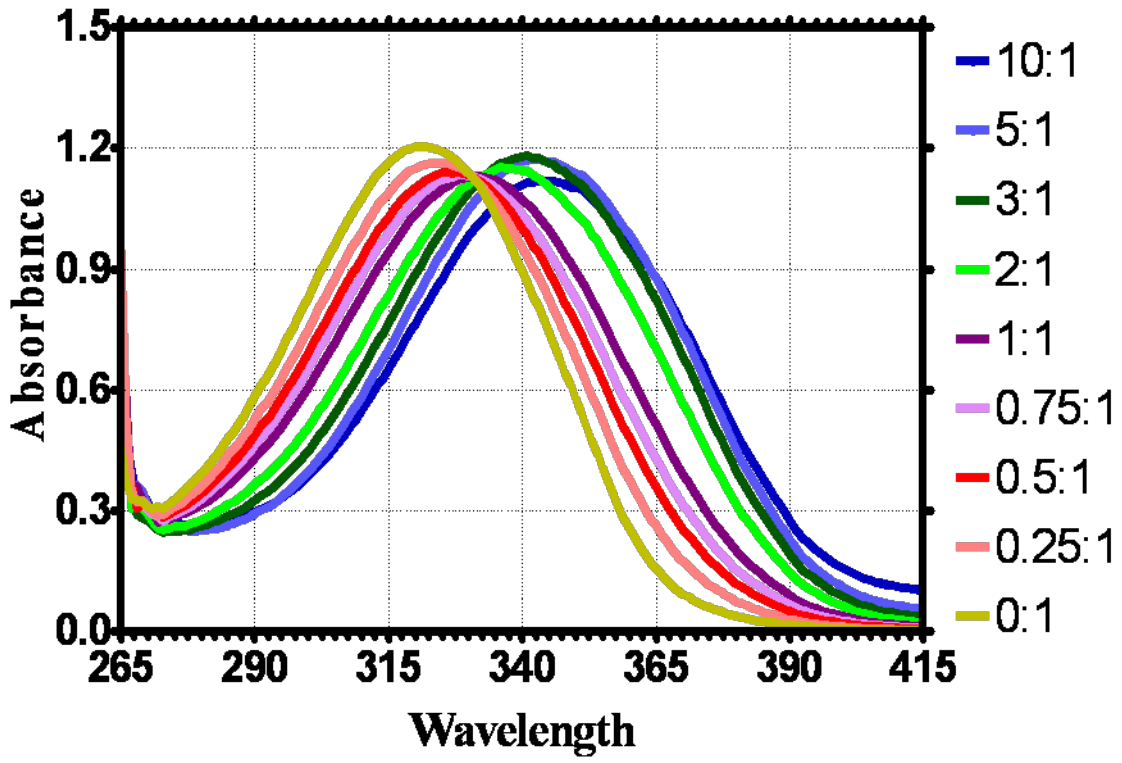

Figure 5. 17 Titration of **Pyr** with TBAF in EtOAc.

A closer look at the graph reveals the presence of an isosbestic point at 331 nm (Figure 5.18). The last curve that intersects the isosbestic point is the curve corresponding to a 1:2 ratio of **Pyr** : TBAF. An isosbestic point for a reaction mixture is observed when the stoichiometry of the reaction doesn't change.[23] In other words, up until that point there was a constant ratio between binding and deprotonation and for all the mixtures whose curves do not intersect the isosbestic point this ratio changes, most likely favoring deprotonation.

Figure 5. 18. Isosbestic point observed in the titration of Pyr with TBAF.

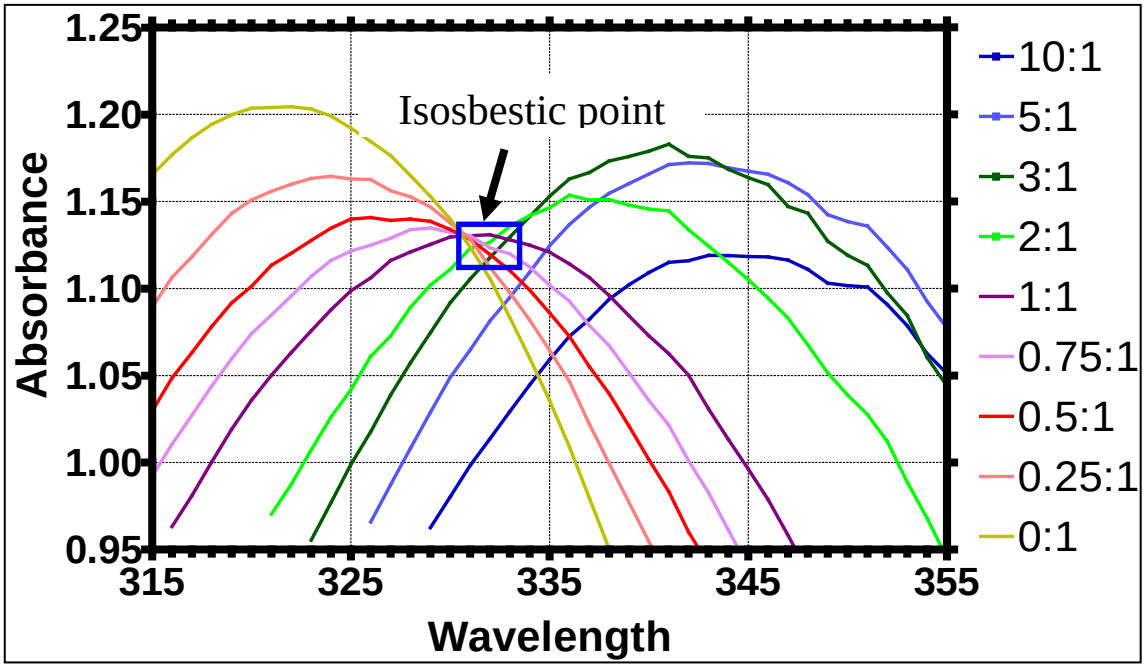

Plotting the changes in λ_{max} as a function of the number of equivalents of F^- added gives the graph shown in Figure 5.19.

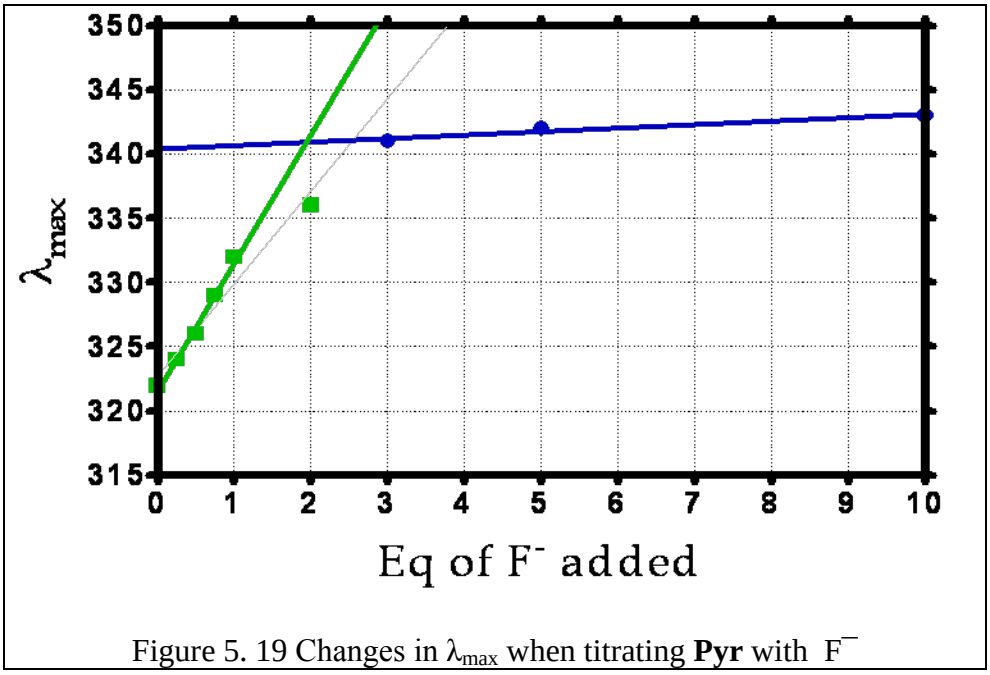

Figure 5. 19 Changes in λ_{max} when titrating **Pyr** with F^-

Fitting the data points to straight lines rather than a curve makes more chemical sense and it correlates well both with the presence of the isosbestic point and the ES-MS data. The two lines intersect close to the point corresponding to the **Pyr** : F^- = 1 : 2 mixture. This agrees with the inference that up until that point a certain mixture composition is present but as the F^-concentration increases beyond that point, the mixture composition changes more dramatically.

The fact that the λ_{max} values for the data points corresponding to mixtures with 0-2 eq F^- are close to the λ_{max} of the control experiment using 10 eq Cl^- indicates that binding predominates in these mixtures. At higher concentrations of F^- the λ_{max} increases (in correlation with the control experiment that used 10 eq F^-) pointing to deprotonation as the predominant process.

Colorimetric behavior of Pyr and Iso in the presence of various anions.

During the course of the experiments described above, it was noted that solutions of **Pyr** and **Iso** changed color when certain anions were added. This color change is concentration dependent and anion dependent. The color change was assumed at first to result from the deprotonation event that occurs when F^- comes into contact with the host. Subsequently, it was noticed that color changes also occurred when anions such as $H_2PO_4^-$ (DHP) and acetate were present. Figure 5.20 shows example of host solutions that change color or fail to do so in the presence of anions.

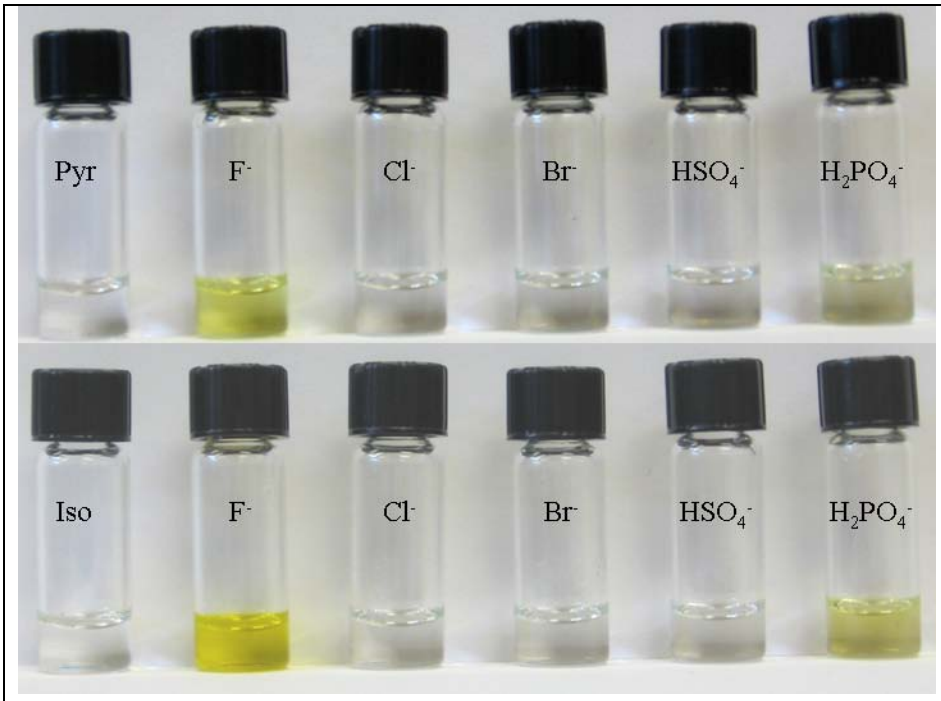

Figure 5. 20. Change in color when adding 1 eq of anion to 1 eq of Host in DMSO. Final [**Host]**=0.5 mM.

Confirmation of host binding to $H_2PO_4^-$ and acetate acid derivatives (di and tri phenyl acetic acids) was obtained by ES-MS experiments similar to those described in detail for the halides. A possible binding mode for acetate ion with the **Iso** host is shown in Figure 5.21.

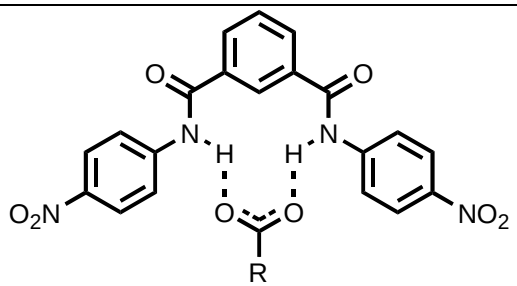

Figure 5. 21 Plausible binding state for Iso with an acetic acid derivative.

Both **Iso** and **Pyr** hosts were titrated separately with DHP (in EtOAc) and the UV-Vis absorption spectra were recorded. 1 mM DMSO solutions of **Pyr** and tetrabutylammonium dihydrogenphosphate were prepared. 0.1 mL of **Pyr** stock solution was added to 2 mL of EtOAc and the resulting mixture was titrated with aliquots of the stock anion solution, added to yield the desired molar ratios. The resulting traces are presented in Figure 5.22 and 5.23.

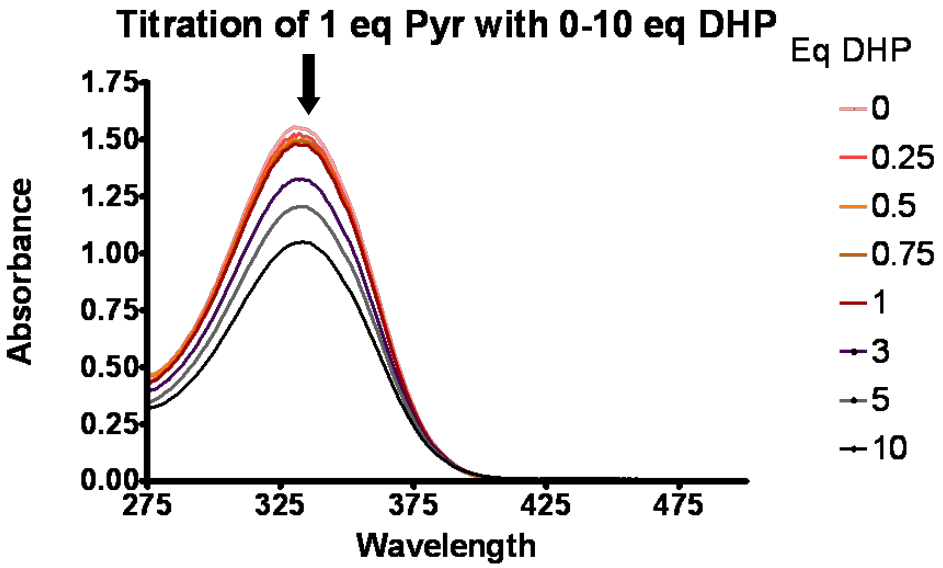

Figure 5. 22 Titration of **Pyr** with 0-10 eq DHP.

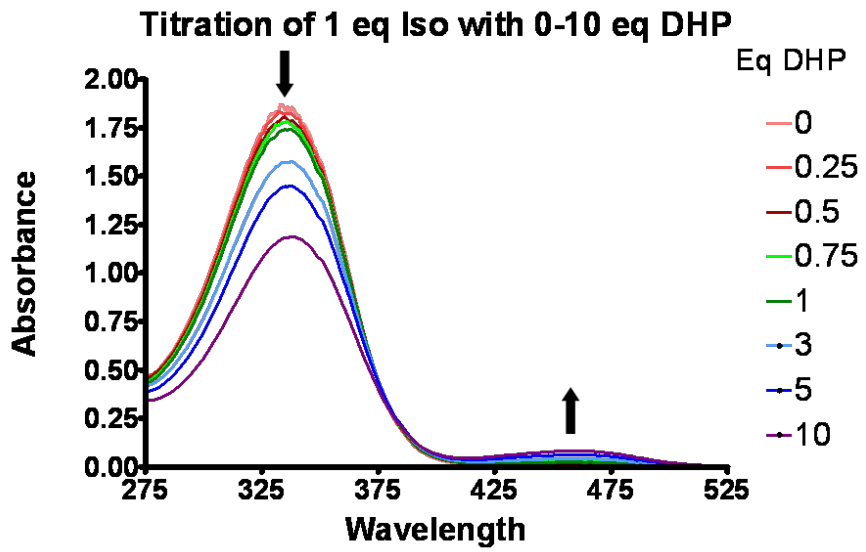

Figure 5. 23 Titration of **Iso** with 0-10 eq DHP

When **Iso** was the host, diminishing intensity for the peak centered at 330nm was noted along with the development of a second peak in the region 400-500 nm (see Figure 5.24). What is even more interesting is that the intensity of the secondary peak is directly proportional with the amount of DHP added. In other words, the secondary peak intensifies as more DHP is added. This behavior, alongside with color change has been reported previously to occur between anions and various ligands featuring amidic hydrogens[24,25,26,27,28,29,30,31] Several authors report that such interactions can be useful for the selective detection of various anions in complex mixtures[32,33,34,35,36]. No effort was made to develop a colorimetric sensor based on these hosts but their structural simplicity suggests that they could be economical scaffolds for this application.

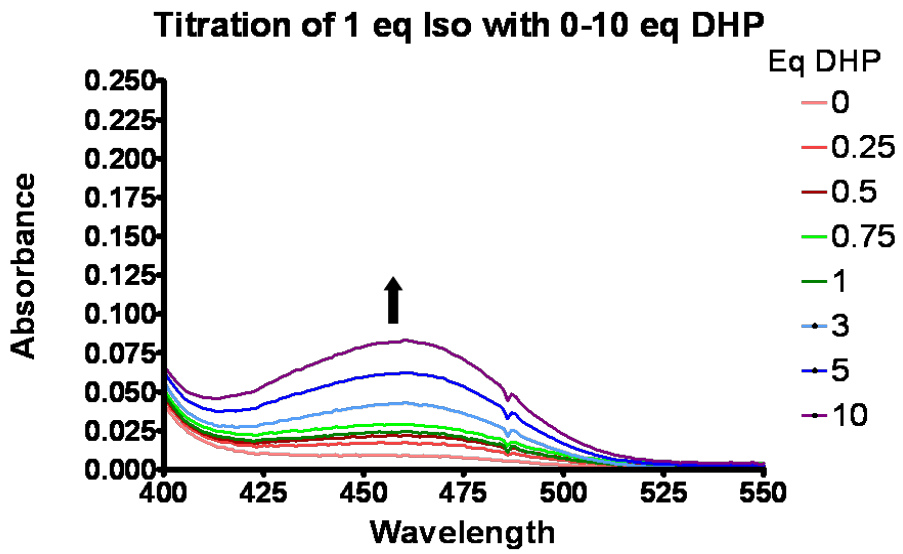

Figure 5. 24 Blow up of the new absorption peak formed upon titrating 1 eq of **Iso** with 0-10 eq DHP

Conclusions

The initial goal of this work was to assess the binding interactions of dipicolinamides and isophthalamides with various halogen anions. We found that **Iso** as well as **Pyr** successfully bind the three halogenated anions studied: F^-, Cl^- and Br^-. Basing our predictions on ionic radii, charge density and the computational studies performed on these hosts and hosts-anion pairs the complexation order should be $F^- > Cl^- > Br^-$. Surprisingly though, competitive ES-MS studies show that in both cases the preferred anion was Cl^- followed by F^- and Br^-. While Br^- was expected to be the least preferred guest due to its higher ionic radius and lower charge density, F^- ranked second mostly because of it's propensity for deprotonation rather than binding. In our ES-MS control experiments we observed that F^- deprotonates the host more than the other anions (Cl^- or Br^-). So even if the host anion binding interaction is expected to be stronger for

F^- than for Cl^- or Br^- which would result in a complexation order of $F^->Cl^->Br^-$ such a selectivity ranking cannot be realistically obtained within our experimental conditions due to the competition from the deprotonation process.

The second finding is that anion binding is always accompanied by host deprotonation and *vice versa*. While there were previous reports documenting fluoride anion's propensity for host deprotonation, we have found proof that deprotonation and binding are present with all the anions, albeit in various ratios.

What differentiates the three anions is the degree to which these two competing processes occur: F^- always favors deprotonation over binding due to its higher basicity and higher charge density, while adduct formation dominates in the case of Cl^- and Br^-.

The two hosts show changes in color when various anions are added to their solutions: F^-, $H_2PO_4^-$, or acetate. This change in color can be useful as a detection method for these anions.

Experimental section

All the solvents used were of HPLC grade as purchased from Sigma Aldrich or Fisher Scientific.

Computational studies

All calculations and visualizations were performed by Dr. Carl Yamnitz using Spartan '06 software from Wavefunction Inc at the DFT level.

In every case, the conformer with the lowest calculated final energy was used for calculation of the complexation energy advantage. This calculation was performed by adding the calculated energies of the host and guest, then subtracting the calculated energy of the complex. The complexation energy is listed as a negative value if the interaction is favorable, the more negative a value the more favorable the interaction.

Competitive chloride binding assayed by electrospray mass spectrometry

The anion tetrabutyl ammonium salts were dissolved in methanol to yield a stock solution of 1 mM while the hosts were dissolved in a mixture of 10% DMSO/MeOH to yield a stock solution of 0.5 mM. In a typical experiment 20 μL of host stock solution and 100 μL of stock anion(s) solution were added to 2 mL of MeOH. The resulted solution was filtered and injected in the ES-MS machine. This protocol ensured that in each experiment competing anions were present in equimolar concentrations (45 μM) and the host was kept at sub-stoichiometric concentrations (4.5 μM). The ratios shown were calculated from the total integration of relevant m/Z peaks for **host**-A^- adducts. Errors

are the calculated standard deviations of ratios from at least three independent experiments.

^{1}H-NMR titrations.

^{1}H-NMR titrations were performed on a 300 MHz Bruckner Advance machine. Solutions of the receptor molecule in DMSO-d_6 were prepared at a concentration of 1 mM. A 1 mL solution thus prepared was transferred to a glass NMR tube and titrated with aliquots from a 1 mM solution containing the titrant anion as the tetrabuthylammonium salt in DMSO-d_6. The chemical shifts of the NH and aromatic protons were monitored as a function of the number of equivalents of anions added.

HPLC experiments

HPLC experiments were conducted on a Xper-Chrom Model 1400 HPLC equipped with a UV-vis detector (λ = 275nm) using a Shodex 5SIL 10E normal phase column. The host and the tetrabutylammonium salts were dissolved in DMSO to yield 1 mM solutions. Aliquots of the host and anion solutions in the desired ratios were mixed separately and the resulting solution was added to 2 mL of EtOAc and then loaded onto the HPLC column. The mobile phase was EtOAc. Experiments were performed at least in triplicate, and traces were recorded using Peak Simple v. 2.08 software.

UV-vis experiments

1 mM DMSO solutions of the host and tetrabutylammonium salts of the anions were prepared. In a typical experiment 0.1 mL of host stock solution was added to 2 mL of EtOAc and the resulting mixture was titrated with aliquots of the stock anion solution, added to yield the desired molar ratios. UV-vis experiments were performed on a Beckman Coulter DU 7400 Spectrophotometer using EtOAc as a solvent. All the traces reported are averages of at least three trials.

References

[1] Gokel, G. W.; Murillo, O. *Acc. Chem. Res.* **1996**, *29*, 425-432.

[2] Fyles, T. M. *Curr. Opin. Chem. Biol.* **1997**, *1*, 497-505.

[3] Gokel, G. W.; Mukhopadhyay, A. *Chem. Soc. Reviews* **2001**, *30*, 274-286.

[4] Gokel, G. W.; Schlesinger, P. H.; Djedovic, N. K.; Ferdani, R.; Harder, E. C.; Hu, J.; Leevy, W. M.; Pajewska, J.; Pajewski, R.; Weber, M. E. *Bioorg. Med. Chem.* **2004**, *12*, 1291-1304.

[5] (a) Sakai, N.; Mareda, J.; Matile, S. *Acc. Chem. Res.* **2005**, *38*, 79-87. (b) Sisson, A. L.; Shah, M. R.; Bhosale, S.; Matile, S. *Chem. Soc. Rev.* **2006**, *35*, 1269-1286.

[6] B. McNally and W. M. Leevy, *Supramol. Chem*., **2007**, *19*, 29–37; (b) B. D. Smith, A. P. Davis and D. Shephard, *Chem. Soc. Rev*., **2007**, *36*, 348–357.

[7] Tabushi, I.; Kuroda, Y.; Yokota, K. *Tetrahedron Lett* **1982**, 4601-4604.

[8] Carmichael, V. E.; Dutton, P. J.; Fyles, T. M.; James, T. D.; Swan, J. A.; Zojaji, M. *J. Am. Chem. Soc.* ***1989***, *111*, 767-769.

[9] Kobuke, Y.; Ueda, K.; Sokabe, M. *J. Am. Chem. Soc.* **1992**, *114*, 7618-7822.

[10] Ghadiri, M. R.; Granja, J. R.; Buehler, L. K. *Nature* **1994**, *369*, 301-304.

[11] C. H. Park and H. E. Simmons, J. Am. Chem. Soc., 1968, 90, 2431;

[12] F. P. Schmidtchen, Angew. Chem., 1977, 89, 751;

[13] E. Graf and J.-M. Lehn, J. Am. Chem. Soc., 1975, 97, 5022

[14] A. Echavarren, A. Galan, J. De Mendoza, A. Salmeron and J.-M. Lehn, Helv. Chim. Acta, 1988, 71, 685

[15] M. Newcomb and M. T. Blanda, Tetrahedron Lett., 1988, 29, 4261

[16] J. L. Sessler, P. A. Gale and W.-S. Cho, Anion Receptor Chemistry, Royal Society of Chemistry, Cambridge, 2006

[17] Anslyn, E. V.; Dougherty, D., A., *Modern Physical Organic Chemistry*, *Third Edition*, University Science, 2005, p24.

[18] Anslyn, E. V.; Dougherty, D., A., *Modern Physical Organic Chemistry, Third Edition*, University Science, 2005, p167.

[19] Yamnitz, C. R.; Negin, S.; Carasel, I. A.; Winter, R. K.; Gokel, G. W. *Chem. Commun.* **2010**, *46*, 2838-2840

[20] Silverstein, R. M.; Webster, F. X.; Kiemle, D. J. John Wiley & Sons, Inc, **2005**, p 7.

[21] Chiu F.C.K., Lo C.M.Y.; *J. Am. Soc. Mass Spectrom.;* **2000,** 1064

[22] Camiolo S.; Gale, P., A.; Hursthouse, M., B.; Light, M., E.; Org. Biomol. Chem, 2003, 741

[23] http://goldbook.iupac.org/I03310.html

[24] Niyaji, H. Sessler, J., L.; *Angew. Chem. Int. Ed*, **2001,** 154

[25] Piatek, P.; Jurczak, J. *Chem. Commun.*, **2002,** 2450

[26] Ali , P.,H. D.; Kruger, P.E.; Gunnlaugsson, T.; *New J. Chem.*, **2008**, 1153

[27] Kumar, V.; Kaushik, M. P.; Srivastava, A., K.; Pratap, A.; Thiruvenkatam, V.; Guru Row, T., N.; *Analytica Chimica Acta*, 2010, 77

[28] Han, M., S.; Kim, D., H.; *Angew. Chem. Int. Ed.* **2002**, 3809

[29] Palacios, M. A.; Nishiyabu, R., Marquez, M.; Anzenbacher Jr, P.; *J. Am. Chem. Soc.* **2007**, 7538

[30] Wang, T.; Ma, L.; Yan, X.-P.; *Org. Biomol. Chem*, **2008**, 1751

[31] Moon, K.S.; Singh, N.; Lee, G.W.; Jang, D.O, *Tetrahedron*, **2007**, 9106

[32] Kumar, V.; Kaushik, M. P.; Srivastava, A., K.; Pratap, A.; Thiruvenkatam, V.; Guru Row, T., N.; *Analytica Chimica Acta*, 2010, 77

[33] Han, M., S.; Kim, D., H.; *Angew. Chem. Int. Ed.* **2002**, 3809

[34] Palacios, M. A.; Nishiyabu, R., Marquez, M.; Anzenbacher Jr, P.; *J. Am. Cem. Soc.* **2007**, 7538

[35] Wang, T.; Ma, L.; Yan, X.-P.; *Org. Biomol. Chem*, **2008**, 1751

[36] Moon, K.S.; Singh, N.; Lee, G.W.; Jang, D.O, *Tetrahedron*, **2007**, 9106

Chapter 6 Future studies

A number of various experiments and techniques have been presented in this dissertation, all of them aimed at investigating and understanding how synthetic ion transporters interact with phospholipid bilayers, bind with and transport ions. While we attempted to exhaust our research, there may remain other avenues yet to be explored. These new directions often come from new developments or fruitful discussions with our peers that refine our thinking about the various projects that we have worked on. Below I will list a few of the ideas that we have about continuing the work presented so far.

Triacsin C analogs

As presented in Chapter 2, Triacsin C is an enzymatic inhibitor that acts on Long Chain Acyl-CoA synthetases[1], preventing them from transforming free fatty acids into CoA esters.

Starting from the reported structure of Triacsin C[2] we designed three new compounds that could potentially act as inhibitors (see Figure 6.1).

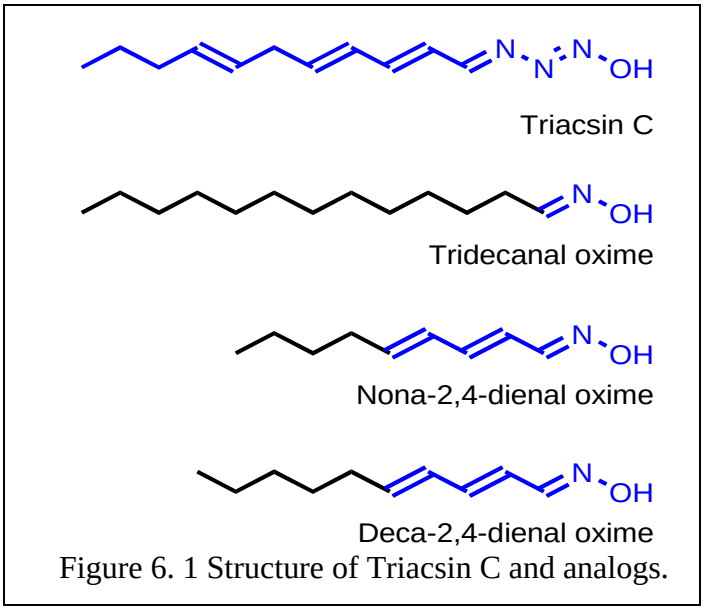

Figure 6. 1 Structure of Triacsin C and analogs.

The structure of these three analogs are designed to mimic either the overall length of the molecule (tridecanal oxime) or the extended unsaturated system present in the natural product (nona- and deca-2,4,-dienal oximes).

Enzymatic inhibitory studies performed on these analogs showed that while they are not as active as Triacsin C, the two unsaturated analogs are significantly more potent than tridecanal oxime.[3]

With these results in mind, a number of alternative structures that can be envisioned that can give us insight into the inhibitory activity of these compounds. The first set of these structures is presented in Figure 6.2.

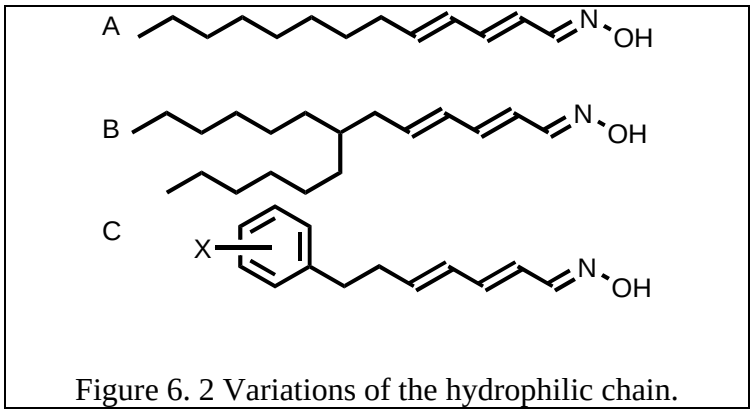

Figure 6. 2 Variations of the hydrophilic chain.

An obvious starting point for the design of new analogs would be the extension of the hydrocarbon chain. We know that Triacsin C has an overall length of 15 atoms, so a structure that will have the same overall length but also possesses a longer system of conjugated double bonds should have an inhibitory activity closer to Triacsin C than tridecanal oxime (structure A).

The active site of the LC Acyl-CoA synthetases is highly conserved among the enzymes in this family.[4] One of the particularities of the active site is the presence of the

"dead end branch", a hydrophobic pocket where the hydrophobic tail of the fatty acid rests during esterification (see Figure 6.3).

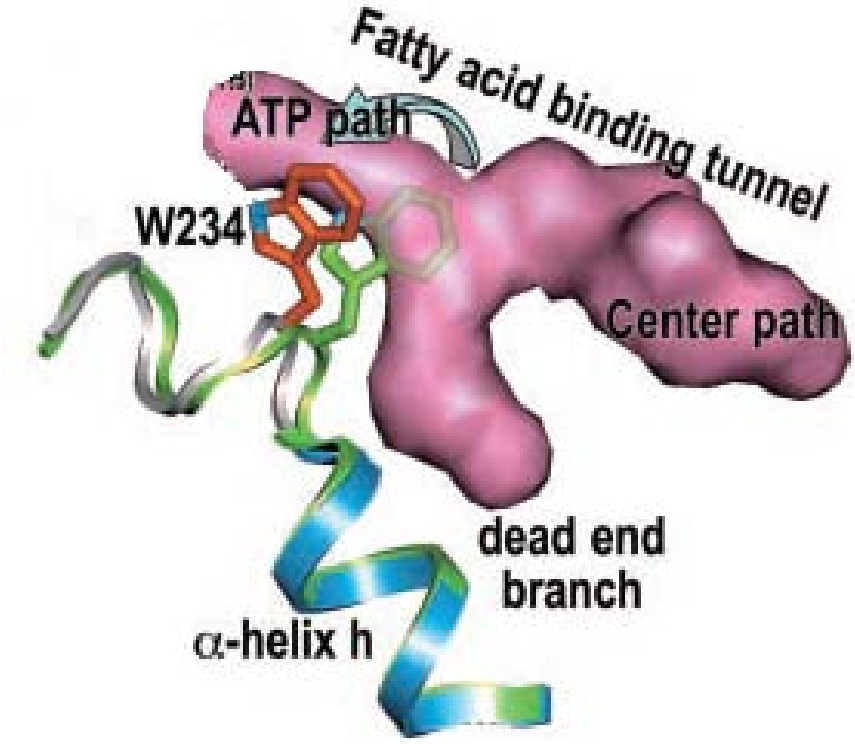

Figure 6. 3 The active site of the LC Acyl-CoA synthetase from Thermus thermophilus (image reproduced from Hisanaga et al[4])

A structure with branched hydrophilic chain can take advantage of this bifurcation and anchor itself better in the active site, blocking the access to both the "dead end branch" and to the central pathway towards the esterification site, thus inhibiting the enzyme more effectively. Structure B builds on this hypothesis with the presence of two *n*-hexyl chains that can rest both in the "dead end branch" and in the center path.

Hydrophobic pockets created inside the enzymes active site are often times comprised of aromatic residues. Structure C tries to take advantage of this fact, having in its structure a substituted aromatic ring. Through the substituent we can modulate the

electron density of the arene and favor arene-arene interactions with the other aromatic residues present in the pocket. If the pocket has electron rich aromatic residues then electron withdrawing substituents (-NO_2, -CN) would yield the best results and *vice-versa* if the aromatic residues are electron poor then electron donating substituents (-CH_3, -OCH_3) would be the better choice. Polysubstitution of the benzene ring is also an option worth considering.

The second set of structures with potentially interesting properties is presented in Figure 6.4.

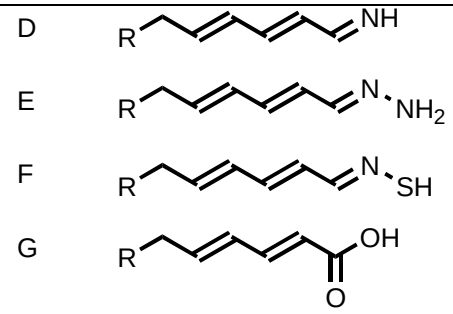

Figure 6. 4 Second set of Triacsin C analogs.

Once the analysis of the hydrocarbon chain analogs has been performed and an optimal chain length/branching pattern has been established we can move on to examine the heteroatoms present in the structure. The original structure has a rather unusual terminal moiety containing three nitrogen atoms and a hydroxyl (=N-N=N-OH). Previous enzymatic studies showed that analogs present inhibitory activity just with an unsaturated oxime thus removing two of the nitrogens from the structure.[3] This begs the question of how important is the terminal hydroxyl and if other functional groups can serve the same purpose. Structures D-G are designed to investigate this. Structure D completely lacks the

hydrogen attached to a sp^3 hybridized heteroatom and while likely inactive, can serve as a useful negative control for future studies. Structures E and F contain different heteroatoms that have the same external shell electronic configuration (NH_2 and SH), while structure G contains a hydroxyl group contained in a carboxyl moiety.

Pyrogallol[4]arenes solution equilibrium

Chapter 3 investigates the solution equilibrium of pyrogallol[4]arenes, whose general structure is shown in Figure 6.5.

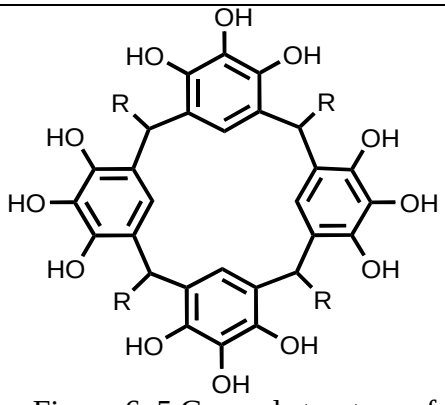

Figure 6. 5 General structure of a pyrogallol[4]arene.

These molecules crystallize in two major conformations: bilayer[5] and hexameric capsule.[6] Aliquots from ethyl acetate solutions containing equal masses of solid samples from these two crystalline motifs, when loaded on an HPLC column have similar profiles. The traces from C_{10} capsule and C_{10} bilayer are shown in Figure 6.6.

Based on the similarities that exist between these traces we assumed an equilibrium state is reached between the capsule and monomer in solution. We tentatively assigned the peaks based on their elution times to monomer (shortest elution time) dimer

and other small oligomers (medium elution time) and capsule and higher oligomers (longer elution times).

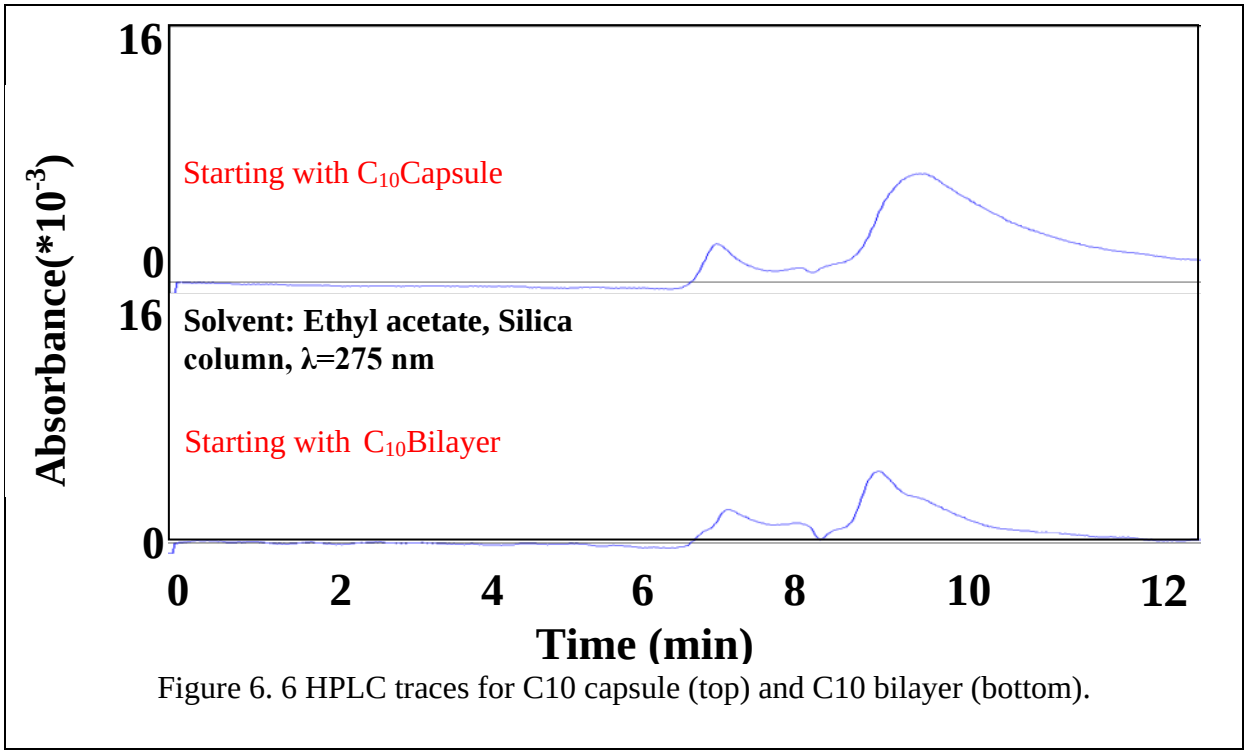

Figure 6. 6 HPLC traces for C10 capsule (top) and C10 bilayer (bottom).

A positive identification of the compounds present in the various peaks could be done using an LC-MS ensemble. While the peaks are eluting they are injected into an electrospray machine and identified based on their M/z ratio.

Another control experiment could be the collection of the fractions corresponding to just one of the peaks (for example, the last one which we believe corresponds to the capsule and higher oligomers) and reinjecting an aliquot from these fractions onto the column. If our hypothesis is correct, after a certain time we should see a trace similar to the ones that we already in hand.

New dipicolinic and isophthalamide dianilides

Chapters 4 and 5 focus on the anion binding and transport abilities of dipicolinamide and isophthalamide derivatives. These compounds have shown remarkable properties as chloride transporters[7] but also to our surprise as possible colorimetric detectors for various anions.

While the anion transport ability of these compounds is proven, the mechanism through which it occurs is still a speculation. We assume a number of these molecules stack and form a pore which allows for ions to pass through the membrane, but the exact number of monomers necessary and the morphology of the pore remains unknown. The insertion and aggregation of the monomers inside the bilayer is most likely the rate limiting step for this process. If two of these monomers would be covalently linked through a flexible tether, the aggregation period should be shortened and the rate of transport improved. Structures such as the one in Figure 6.7 could serve such a purpose.

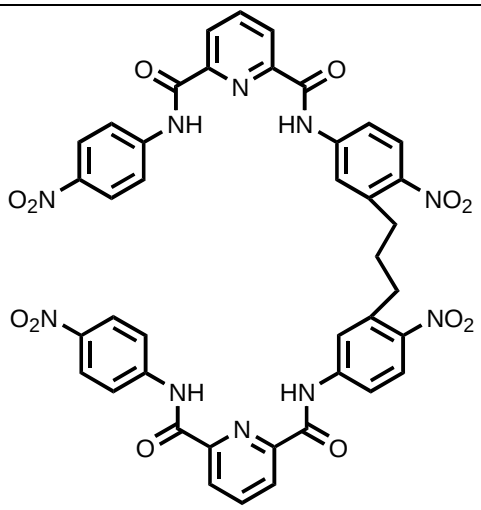

Figure 6. 7 Linked monomers with potential use in the study of the aggregation and transport behavior of **Pyr**.

The color change that solutions of these compounds present upon addition of various anions has been reported previously for structurally related compounds.[8] The interactions leading to the color change are most likely between the amidic protons and the anion, as exemplified in Figure 6.8.

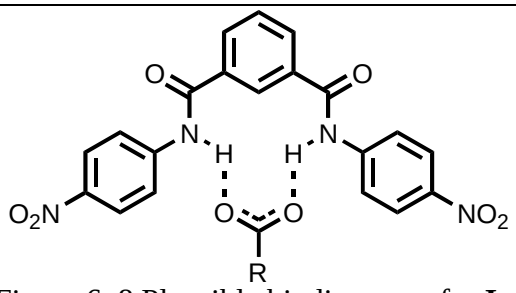

Figure 6. 8 Plausible binding state for **Iso** with an acetic acid derivative.

These interactions can be enhanced by adding extra substituents on the aniline ring: either more electron withdrawing substituents that would increase the acidity of the amidic protons or by adding substituents that can provide additional binding sites. Examples of these kinds of structures are shown in Figure 6.9.

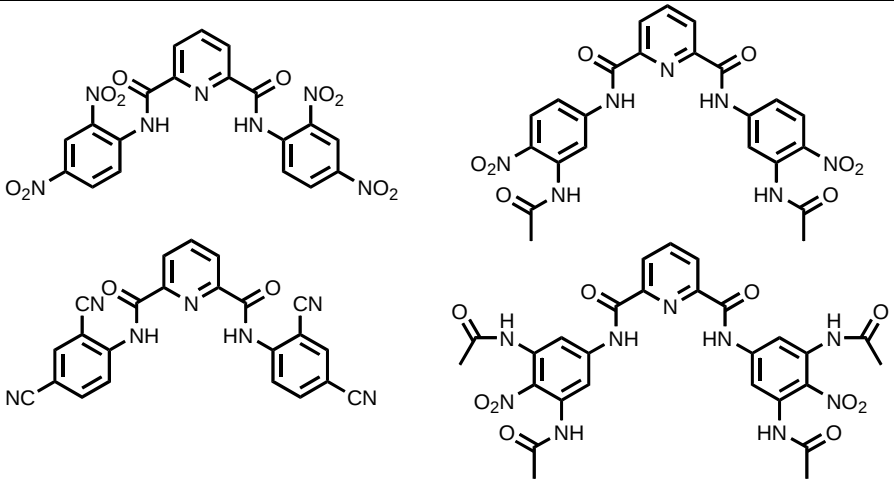

Figure 6. 9 Potential substitution patterns for **Pyr**.

The ideas presented in this chapter show the sizeable amount of work still left to do and the scientific potential of these families of compounds.

References

[1] Omura, S.; Tomoda, H.; Xu, Q.M.; Takahashi, Y.; Iwai, Y; *J. Antibiot.,* **1986**, 39, 1211-1218;

[2] Yoshida, K. M.; Okamoto, K.; Umehara, M.; Iwami, M.; Kohsaka, H.; Aoki H.; *J. Antibiotics*, **1982,** 151;

[3] Knoll, L. J.; Schall, O. F.; Suzuki, I.; Gokel, G.W.; Gordon, J. I.; *J. Biol. Chem*, **1995**, 20090-20097.

[4] Hisanaga, Y., Ago, H., Nakagawa, N., Hamada, K., Ida,K., Yamamoto, M., Hori, T., Arii, Y., Sugahara, M., Kuramitsu, S., Yokoyama, S., Miyano, M. *J. Biol. Chem.* 2004, 31717-31726;

[5] Kulikov, V. O.; Rath, N. P.; Zhou, D.; Carasel, I. A.; Gokel, G. W.; *New Journal of Chemistry*, **2009**, 1563.

[6] G. W. V. Cave, S. J. Dalgarno, J. Antesberger, M. C. Ferrarelli, R. M. McKinlay, J. L. Atwood, *Supramol. Chem*. **2008**, *20*, 157 –159.

[7] Yamnitz, C. R.; Negin, S.; Carasel, I. A.; Winter, R. K.; Gokel, G. W.; *Chem. Commun.* **2010**, *46*, 2838-2840

[8]Kumar, V.; Kaushik, M. P.; Srivastava, A., K.; Pratap, A.; Thiruvenkatam, V.; Guru Row, T., N.; *Analytica Chimica Acta,* 2010, 77

Ionut Alexandru Carasel

CONTACT INFORMATION

Email: alexcarasel@yahoo.com
Address: 825 Leland Avenue Apt 2S
St Louis, MO 63130
Phone: (314) 484-9497

SUMMARY

Ph. D. Candidate in Chemistry with five years of scientific research experience in chemical biology working with multiple projects towards the discovery of novel compounds with potential therapeutic applications.

EDUCATION

2010 **[Expected] Ph.D. Chemistry**, Washington University, St. Louis, MO
2007 **A.M. Chemistry**, Washington University, St. Louis, MO
2005 **B.S. Pharmacy**, University of Medicine and Pharmacy, Cluj-Napoca, Romania

TECHNIQUES AND INSTRUMENTATION

- MS, ES-MS, competitive MS
- Automated peptide synthesis
- HPLC
- NMR: ^{1}H, ^{13}C, 2D, titrations
- Electron microscopy
- UV-Vis spectroscopy
- FT-IR
- Assays of antimicrobial agents
- Organic synthesis / purification
- Molecular modeling / computation
- Fluorescence microscopy
- Crystal growth and X-ray structures

PROFESSIONAL EXPERIENCE

WASHINGTON UNIVERSITY, St. Louis, MO
Graduate Research Associate, Chemistry **2006-Present**

- *Used ES-MS extensively to investigate and understand the binding interactions of synthetic ion transporters with anions and cations. Designed and performed ES-MS competitive experiments using a broad range of compounds and solvent systems. Collaborated closely with MS lab personnel on identifying and solving various experiment and instrument related problems. This work resulted in two publications, one already published (Chem. Commun., **2010**-2838) and the second one ready to be submitted.*
- *Experience with using automated peptide synthesizers and HPLC peptide purification.*
- *Excellent written and oral communication skills resulted from thesis writing, publication of peer reviewed articles, presenting monthly PowerPoint research progress updates and public speaking events.*
- *Independently instructed the research activity of three undergraduate interns.*
- *Proficient with using MS Office and Open Office software suites,Adobe, Scifinder, Chem Draw, Graphpad, Spartan, Mercury, Protein Workshop, Jmol, ImageJ, Spinworks 3 and other instrument specific software.*

WASHINGTON UNIVERSITY, St. Louis, MO
Graduate Teaching Assistant, Chemistry **2005-Present**
Supervised laboratories of up to 20 undergraduate chemistry students, conducted help sections covering lecture material with chemistry students, graded lab reports and exams.

UNIVERSITY OF MEDICINE AND PHARMACY, Cluj-Napoca, Romania
Research Experience for Undergraduates Intern, Chemistry **2001-2005**
Designed, synthesized and characterized novel Cu^{2+} - sulphamide complexes with potential antiviral activity.

PUBLICATIONS AND PRESENTATIONS

Carasel I.A., Yamnitz C.R., Gokel G.W., "Isophthalamides and Dipicolinamides – Halogenated anion selectivity" [Manuscript ready to be submitted]

Yamnitz C.R., Negin S., **Carasel I.A.**, Winter R.K., Gokel GW. "Dianilides of Dipicolinic Acid Function as Synthetic Chloride Channels." *Chemical Communications* **2010**, 2838.

Yamnitz C.R., Negin S., **Carasel I.A.**, Winter R.K., Gokel G.W. "Synthetic Chloride Channels from Small Molecule Dipicolinic Dianilides." Abstracts, Inaugural Symposium of the St. Louis Institute for Nanoscience, February **2010**.

Kulikov O., Rath N.P., Zhou D., **Carasel I. A**., "Guest molecule entrapment by both capsule and hydrocarbon sidechains in self-assembled pyrogallol[4]arenes" *New Journal of Chemistry,* **2009**, 1563

Gokel G.; **Carasel I. A.**; "Biologically active, synthetic ion transporters" *Chemical Society Reviews*, **2007,** 378

Daschbach, Megan M.; Elliott, Elizabeth K.; **Carasel, Ionut A.;** Gokel, George W. "Characterizing the Amphiphilic Behavior of Synthetic Anion Transporters." Abstracts, 42nd Midwest Regional Meeting of the American Chemical Society, Kansas City, MO, United States, November 7-10, 2007

MEMBERSHIP

- The American Chemical Society

LANGUAGE FLUENCIES:

- English (advanced)
- Spanish (advanced)
- Romanian (native)

Professional References

George W. Gokel, Ph. D.
Distinguished Professor of Science, Associate Director, Center for Nanoscience, Department of Chemistry and Biochemistry and Department of Biology,
University of Missouri, St. Louis,
428 Benton Hall
One University Boulevard
St. Louis, MO, 63121 USA
Phone: (314) 516-5312
Email: gokelg@umsl.edu

Rudolph K Winter, Ph.D
Professor of Chemistry, MS Facility supervisor,
Department of Chemistry
University of Missouri, St Louis
315j Benton Hall
One University Boulevard
St. Louis, MO, 63121 USA
Phone: (314) 516-5337
Email: rekwintr@umsl.edu

Kit Mao, Ph. D.
Undergraduate Laboratory Supervisor and Lecturer
Department of Chemistry
Campus Box 1134
One Brookings Drive

Washington University in St. Louis
St. Louis, MO 63130, USA
Phone: (314) 935-6560
Email: mao@wustl.edu